LAWRENCE
LIVERMORE
NATIONAL
LABORATORY

LLNL-TR-403968

Aging and Phase Stability Studies of Alloy 22 FY08 Final Report

S. G. Torres

May 19, 2008

Disclaimer

This work performed under the auspices of the U.S. Department of Energy by Lawrence Livermore National Laboratory under Contract DE-AC52-07NA27344.

TABLE OF CONTENTS

Executive Summary

This report is a compilation of work done over the past ten years in support of phase stability studies of Alloy 22 for the Yucca Mountain Project and contains information previously published, reported, and referenced. Most sections are paraphrased here for the convenience of readers. Evaluation of the fabrication processes involved in the manufacture of waste containers is important as these processes can have an effect on the metallurgical structure of an alloy. Because material properties such as strength, toughness, aging kinetics and corrosion resistance are all dependent on the microstructure, it is important that prototypes be built and evaluated for processing effects on the performance of the material. Of particular importance are welds, which have an as-cast microstructure with chemical segregation and precipitation of complex phases resulting from the welding process. The work summarized in this report contains information on the effects of fabrication processes such as solution annealing, stress mitigation, heat-to-heat variability, and welding on the kinetics of precipitation, mechanical, and corrosion properties.

For a waste package lifetime of thousands of years, it is impossible to test directly in the laboratory the behavior of Alloy 22 under expected repository conditions. The changes that may occur in these materials must be accelerated. For phase stability studies, this is achieved by accelerating the phase transformations by increasing test temperatures above those anticipated in the proposed repository. For these reasons, Alloy 22 characterization specimens were aged at Lawrence Livermore National Laboratory (LLNL) Aging Facilities for times from 1 hour up to 8 years at temperatures ranging from 200 – 750°C. These data as well as the data from specimens aged at 260°C, 343°C, and 427°C for 100,028 hours at Haynes International will be used for performance confirmation and model validation.

1. Introduction

1.1. Background

The current design for nuclear waste packages in the repository at Yucca Mountain consists of an inner container of 316 NG stainless steel for structural integrity and an outer container of a Ni-Cr-Mo alloy, referred to in the Yucca Mountain Project as Alloy 22 (UNS #N06022) on the outside for corrosion resistance. In order to fabricate the containers, welds will be required; the weld process currently being considered is Gas Tungsten Arc Welding (GTAW). Each container would be fabricated by bending or rolling plates into cylinders, using a longitudinal weld to close the seam, and then welding two or more of these cylinders together with a circumferential weld to obtain appropriate lengths. After welding on the bottom lid, the entire container would be solution annealed to eliminate any residual stresses in the material resulting from fabrication processes. The waste packages would be filled, and final closure welds would weld Alloy 22 lids onto the container. These closure welds cannot be heat treated because the waste cannot be taken to the temperatures required to solution anneal the Alloy 22. Because stress corrosion cracking is now considered one of the most likely failure mechanisms for the waste package, it is currently proposed to mitigate the residual stresses in the Alloy 22 closure weld by burnishing or laser shock peening the weld to put the residual stresses into compression.

The waste packages are required to maintain integrity without substantial leakage for a long duration. This long lifetime combined with a somewhat elevated temperature from the heat generated by radioactive decay of the waste (approximately 180°C peak temperature), makes characterization of the materials involved essential. For most engineering applications, these temperatures are low; however, the times involved are very long. Consequently, one area of concern is phase stability of the outer container materials since the precipitation of deleterious phases over such long times can affect the corrosion resistance and/or the mechanical properties of the Alloy 22 welds as well as the base metal.

Previous work shows that above approximately 600°C up to at least 760°C, Tetrahedrally Close-Packed (TCP) phases [1] (primarily the Mo-rich μ and P phases) form. Because Mo provides the Ni-Cr-Mo alloys with resistance to localized corrosion, segregation of the Mo to the TCP phases can cause a depletion of Mo in the matrix and lead to localized corrosion. Below approximately 600°C, $Ni_2(Cr,Mo)$, which has an ordered structure, forms [2,3,4-6]. This long-range ordering (LRO) has been linked to an increased susceptibility to stress corrosion cracking and hydrogen embrittlement [2]. Cieslak et al. [7] and Ogborn et al. [8] investigated the microstructures of Alloy 22 welds and found segregation of Mo (and also, to some extent, W) in the interdendritic regions of the weld. This enrichment of Mo and W causes TCP phase precipitation to occur during the welding of Alloy 22, with predominantly μ and P phases (and sometimes σ phase) forming in the fusion zone. This segregated structure tends to increase the corrosion rate somewhat over the rate of base metal [9,10] and reduces ductility [11]. In order to predict long-term behavior of the welds, it is important to know whether these precipitates present in the as-welded condition are thermodynamically stable at the low repository temperatures and, if so, how fast they grow and what effect they have on the properties of the weld.

1.2. Thermal Aging Facilities

The Aging Facilities allowed Lawrence Livermore National Laboratory (LLNL) to provide information and insight on how prototypes could best be manufactured with respect to heat treatment parameters and to perform the evaluations of processing effects on material performance. Evaluation of fabrication processes is important because fabrication can have an effect on the metallurgical structure of an alloy and on the condition of the surface.

It can't be known ahead of time exactly when precipitation reactions will start. Extra sets of characterization specimens were introduced in the furnaces at various time intervals in case (after analyzing specimens removed at scheduled times) it was decided that an additional longer aging time was needed. The extra sets outside the furnace are reserved in case, it is discovered that shorter times should have been investigated. Staggered specimens were introduced so that some time exists for analyzing scheduled specimens before a decision on when to pull the staggered specimens has to be made.

Experimental data acquired from specimens aged in the Aging Facilities will provide enhanced confidence in model predictions. The objective of the Aging/Phase Stability (APS) model is to provide a quantitative model which can be used to predict the amount of any phases forming as a function of both time and temperature. The APS model is currently used to provide predictive insight into the long-term metallurgical stability of Alloy 22 base metal under repository conditions. Experimental data acquired from welds will also be available when the APS model is expanded to include welds.

Figure 1.2.1 shows the high temperature Aging/Salt Bath Facilities at LLNL. Base metal polarization disks, characterization, charpy, and tensile blanks were aged at temperatures between 400 and 650°C since 2000, and Alloy 22 thick (1.25") weld characterization and tensile blanks were added in 2005. The Salt Bath Furnace is capable of heating specimens to high temperatures within seconds, thereby eliminating the lag time of waiting for a furnace to reach its test temperature. This was used to determine the onset of precipitation by using various salts that were designed to obtain a certain temperature range. Figure 1.2.2 shows the low temperature Aging Facility where base metal characterization and tensile blanks, and Alloy 22 thick (1.25") welds, were aged at 200°C and 300°C since 2004. Both facilities were shut down and decommissioned in December 2007, and the removed specimens are being stored so they can resume aging or be used for future analyses (Appendix A).

Figure 1.2.1. High Temperature Aging and Salt Bath Facilities used for heat treating base metal and welds.

Figure 1.2.2. Low Temperature Aging Facility used for long term aging of Alloy 22 base metal and welds at 200°C and 300°C.

1.3. Experimental Techniques

This section details the methods applied in the metallurgical characterization of specimens studied. Image Analysis was used primarily for determining secondary phase volume fractions, and Electron Backscatter Diffraction (EBSD) was used to identify secondary (TCP) phases or to map the evolution of recrystallization/grain growth. Both characterization techniques require a polished specimen surface. All specimens evaluated were metallurgically prepared by successively grinding the surface with silicon carbide paper (from 400 up to 1200 grit), followed by successive polishing to 0.02 μm colloidal silica. Note: Several methods were tried in order to prepare the samples for SEM examination. Early metallographic preparation techniques involved etchants of oxalic acid, sodium metabisulfate, and sodium hydroxide. The use of a TiO coating was also tried to obtain contrast between the precipitates and the matrix to determine if they could be observed using an optical microscope. The optimum technique was found to be in the as polished condition using the backscatter detector on a scanning electron microscope (SEM). In the as polished condition, sample preparation variability due to etching was eliminated as well as the question of whether precipitates were being dissolved during electropolishing.

1.3.1. Image Analysis

This technique is composed of two distinct steps. The first involved imaging the specimen to acquire enough micrographs that were statistically representative of the secondary phases present (if any) in a specimen. Because the primary focus was the determination of the amount of precipitation of TCP phases, differences in the chemical composition between the matrix and the secondary phases can be imaged by using a backscatter electron detector in the SEM. Because the amount of electrons backscattered in a volume of material is directly proportional to the atomic number (Z), of the material, the TCP phases show up with a higher intensity (white) than the matrix (black).

By applying a grayscale threshhold to the captured micrographs, all pixels in the image corresponding to the matrix are effectively eliminated. From the resulting image, the TCP phase content of the imaged area can be determined as the ratio of remaining pixels to the total number of pixels in the area. Image analysis software output consists of an area fraction of the remaining pixels. Figure 1.3.1.1 is an example of the thresholding procedure for a micrograph obtained from

the fusion zone of a weld. This procedure was also used to determine the volume fraction of TCP phases in bulk base metal.

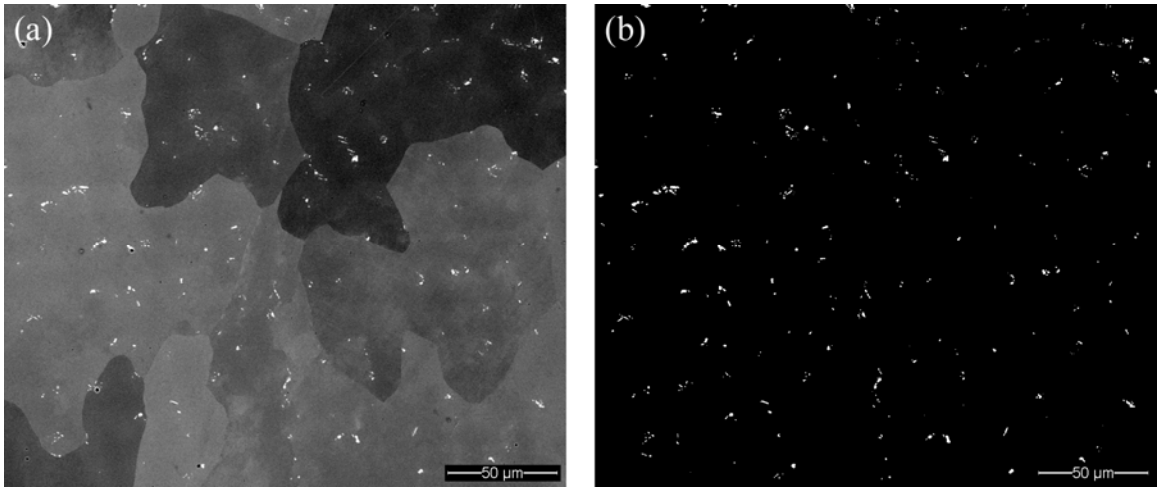

Figure 1.3.1.1. (a) Backscattered electron SEM micrograph captured in the fusion zone of an as-welded specimen. Due to compositional differences the TCP phases appear white. (b) Thresholded image of Figure 1.3.1.1 (a). (Source: DTN LL050303712251.029)

While this technique is highly effective in measuring the TCP phase content, it was not utilized to estimate the volume fraction of long range ordering (LRO). LRO precipitates show up as bright objects in a Transmission Electron Microscope (TEM). However, because LRO micrographs are acquired in a TEM, the micrographs represent the projection of a three dimensional volume (versus a section plane), and the thickness of the observed section needs to be taken into account. Because the volume fraction within a given region varies appreciably between the six crystallographically related variants, and because within a given variant, the volume fraction varies from region to region on a scale of ~ 0.2 - 0.4 μm, principles of stereology need to be applied to account for overlapping ordered precipitates. Collaboration with individuals at SNL-Livermore on the development of this method was not completed; therefore, no results are presented regarding quantification of LRO by use of TEM. Instead microhardness measurements were used to predict the start/finish of LRO. Because LRO occurs as a very fine distribution of precipitates, it has a dramatic effect on the hardness of Alloy 22, particularly in the early stages of transformation. Although the amount of LRO cannot be quantified with a great deal of accuracy using microhardness measurements, hardness gives a very good indication of when this transformation begins.

1.3.2. Electron Backscatter Diffraction

Electron Backscatter Diffraction (EBSD) is a technique in which a focused beam of electrons coincides with the crystalline surface of the specimen at a shallow angle (typically 20°), causing electrons to backscatter. The shallow angle restricts the backscattered electrons that escape to those that can pass without interference to the atoms lying in the crystalline planes of the material. Due to this limitation, the electrons that escape do so in a conical pattern.

A phosphor screen in the path of the escaping electrons allows the observation of part of this cone, in the form of a band. Because multiple crystal planes cause diffraction, multiple bands can be seen and form a diffraction pattern. This pattern is then imaged using a CCD camera, and software can be used to obtain information from the pattern. Figure 1.3.2.1 shows an example of a diffraction pattern for tungsten. Because the width and geometric relationship of these bands is

material and phase dependent, the observed diffraction pattern can be used to determine the local crystal orientation as well as identify the source phase of the diffraction. Specimens were tilted to 70^{o} in the SEM chamber and an accelerating voltage of 30kV with a beam current of 98 μA was used in spot mode.

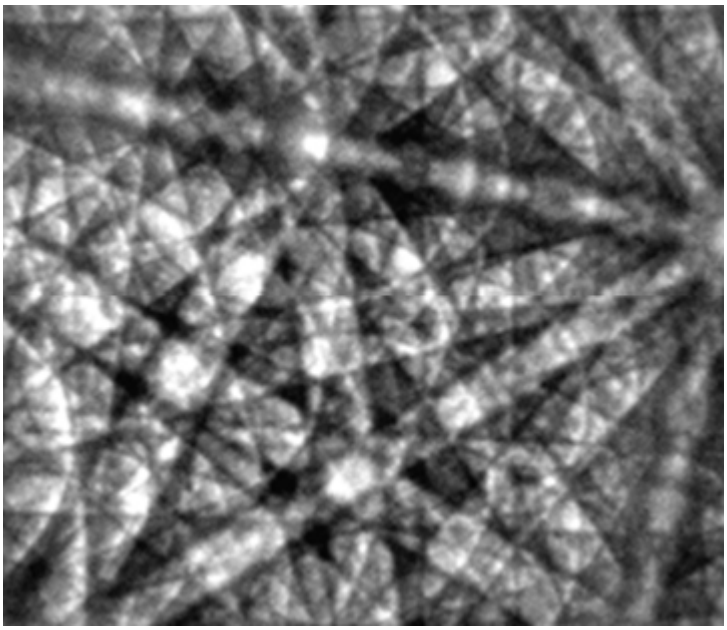

Figure 1.3.2.1. An example of a diffraction pattern for tungsten showing the multiple bands associated with multiple crystal planes.

1.3.3. Wavelength Dispersive Spectroscopy

Wavelength Dispersive Spectroscopy (WDS) is a technique used for the determination of the chemical composition of materials. A focused electron beam is used, which during the interaction with the material being analyzed produces characteristic X-rays that are analyzed by a specially designed detector. Because each element produces X-rays with a characteristic wavelength, these X-rays are effectively the signature of the elements within the material. All X-rays of all wavelengths (within the detector range) are counted, and the relative intensities (counts) of the elements in question are used to determine the chemical composition of the material. The advantage of WDS versus the more commonly used Energy Dispersive Spectroscopy (EDS) is the discriminatory ability of WDS in detecting the wavelength of emitted X-rays.

1.3.4. Electron Microprobe Analysis

Electron Microprobe Analysis (EMPA) is also a technique used for determining the chemical composition of materials used by the analysis of X-rays produced from electron beam interactions with the material. In EMPA, the high-energy of the electron beam used allows the generation of X-rays characteristic of the elements within specimen volumes as small as 3 μm across. These resulting X-rays are diffracted by analyzing crystals and are counted using gas-flow and sealed proportional detectors. Chemical composition is determined by comparing the intensity of X-rays from standards of a known composition with those from unknown materials and correcting for the effects of absorption and fluorescence in the specimen. The major difference between EMPA and other methods is the intensity of the electron beam used, which allows for a more accurate and sensitive analysis.

1.3.5. Transmission Electron Microscopy

Transmission Electron Microscopy (TEM) is a technique used to image materials where a beam of electrons is transmitted through an ultra thin specimen. The beam interacts with the specimen as it passes through it due to differences in density or chemistry. The beam that is transmitted through the specimen contains information about these differences, and this information in the beam of electrons is used to form an image of the specimen.

Specimens for TEM were mechanically thinned to 175 - 200 μm followed by jet polishing in a 5% perchloric - acetic acid solution at room temperature and 40 - 60 V. Additional specimens without preferential etching of second phases were prepared by dimpling (dimple grinding) and ion milling. Identification of LRO was performed in 1999 - 2000 by Summers/Shen [12-14] using a Philips CM300 FEG TEM equipped with a Link/Oxford energy dispersive x-ray (EDX) detector and operated at 300kV with a beam spot size ranging from 1.0 to 3.2 nm (a JEOL JEM-200CX TEM operated at 200 kV was also used). Work performed by Sandia National Laboratories (SNL-Livermore) was done on a Philips CM30 TEM at 300 kV.

2. Phase Stability/Kinetics of Alloy 22

Because of the extremely long times involved and because the phases that form in Alloy 22 and other similar Ni-base alloys are known to have a detrimental effect on their mechanical (Matthews [11], Tawancy [15]) and corrosion properties (Leonard [16], Hodge [17], Hodge and Kirchner [18]), phase stability of Alloy 22 is of concern.

In the fully annealed condition, Alloy 22 is a metastable face-centered cubic (fcc) solid solution that can precipitate one or more of several phases under certain conditions. To determine whether the solid solution will be stable for tens of thousands of years requires that the kinetics of precipitation be studied. Further, phases forming at high temperatures where the rate of formation is not prohibitively long must be studied and the results extrapolated to the lower temperatures expected in the potential repository. Although the phases forming and their effect on the properties have been studied extensively, very little work has been done on the kinetics of precipitation. Hodge [17] measured volume fraction of precipitation in C-276, a Ni-Cr-Mo alloy similar to Alloy 22 with nominally 16% Cr, 16% Mo, 4% W, and 5% Fe; and found the activation energy to be 260 kJ/mol (62 kcal/mol). Heubner et al. [10] looked at aged Alloy 22 specimens optically and produced a Time-Temperature-Transformation (TTT) diagram, but it was not within the scope of that paper to extrapolate the kinetics of precipitation to lower temperatures. The results summarized in this report are an attempt at measuring the kinetics of intermetallic precipitation in Alloy 22.

2.1. Tetrahedrally Close-Packed Phases

In the mill annealed (MA) condition, Alloy 22 is a metastable gamma (γ) phase; that is, when the alloy is exposed to high temperatures, precipitation of second phases will occur. The formation of these second phases can be divided in two distinctive regimes according to the temperature range at which this precipitation occurs.

At temperatures above approximately 600°C up to at least 760°C, Tetrahedrally Close-Packed or TCP phases [1] (primarily the Mo-rich μ and P phases) form [2-6,16,17,19]. Because Mo provides the Ni-Cr-Mo alloys with resistance to localized corrosion, segregation of the Mo to the TCP phases can cause a depletion of Mo in the matrix and lead to localized corrosion [2,3,16,17]. Of the two intermetallics that form, μ and P phases are similar both chemically and crystallographically (Leonard [16], Raghavan et al. [19], Cieslak et al. [7]). Table 2.1.1 shows the structure type, crystal structure, and lattice parameters for the TCP phases [20]. A small amount of σ phase has been observed in Alloy 22 base metal aged at 760°C (Summers et al. [21]) and in Alloy 22 welds (Cieslak et al. [7]). Also at the higher temperatures, carbides have been observed (Hodge [17] and Tawancy et al. [2]) and are generally believed to be Mo-rich M_6C or $M_{12}C$ type carbides. In the higher temperature range, as the aging time increases, precipitation first develops preferentially at grain boundaries and later starts to form at twin boundaries and finally within the grains. However, not all grain boundaries are equally susceptible to second phase precipitation.

Table 2.1.1. Structure type, crystal structure, and lattice parameters for TCP phases

Phase	Structure Type	Crystal Structure
μ	Fe_7W_6	Rhombohedral a=0.904, α=30.5°
P	$Cr_9Mo_{21}Ni_{20}$	Orthorhombic a=1.698, b=0.475, c=0.907
σ	CrFe	Tetragonal a=0.880, c=0.454

2.2. Long Range Ordering

Below approximately 600°C, $Ni_2(Cr,Mo)$ forms [2,3,4-6]. This long-range ordering (LRO) has been linked to an increased susceptibility to stress corrosion cracking and hydrogen embrittlement [2]. The ordered phase that forms in Alloy 22 is $Ni_2(Cr,Mo)$, which has an orthorhombic Pt_2-Mo type superlattice as illustrated in Figure 2.2.1 [13]. In relationship to the disordered fcc Ni-rich matrix, the unit cell of the superlattice has the lattice parameters $\boldsymbol{a} = \mathbf{a_0}/\sqrt{2}$, $\boldsymbol{b} = 3\mathbf{a_0}/\sqrt{2}$ and $\boldsymbol{c} = \mathbf{a_0}$ where $\mathbf{a_0}$ is the lattice constant of the disordered fcc unit cell.

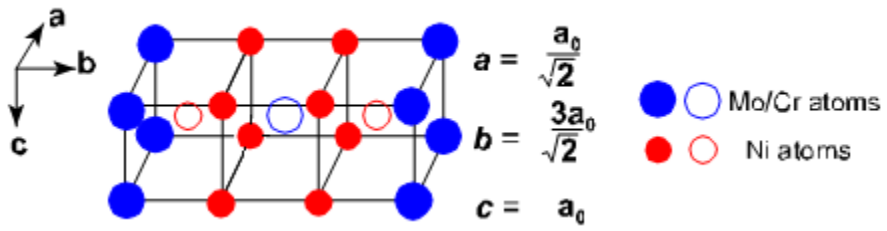

Figure 2.2.1. Orthorhombic unit cell of the LRO phase [13].

The kinetics of LRO are treated in a manner similar to TCP phase precipitation. However, very little kinetic data exists for LRO in Alloy 22. Table 2.2.1 summarizes the observations made on selected specimens of various aging times and temperatures, using TEM to identify the presence of LRO and using SEM to determine whether or not TCP phases were present in Alloy 22 base metal [13,22]. LRO was observed in Alloy 22 base metal aged at 593°C for 16,000 hours and at 538 and 593°C for 1,000 hours. LRO was also observed in the specimens aged at 427°C for 30,000 and 40,000 hours. The volume fraction of the ordered phase has not been measured in these specimens. Alloy 22 base metal specimens aged for 40,000 hours at 260 and 343°C and for 1,000 hours at 482°C were also examined in TEM, but no LRO was observed. These data indicate that ordering most likely does not occur below 343°C in Alloy 22 base metal for times less than 40,000 hours.

Table 2.2.1. Phases Observed in Alloy 22 using TEM [13]

Aging Condition	Phases Observed to Form in Alloy 22
260°C for 40,000 hours	No LRO No signs of grain boundary precipitation in base metal
343°C for 40,000 hours	No LRO No signs of grain boundary precipitation in base metal
427°C for 30,000 hours	LRO No signs of grain boundary precipitation in base metal
427°C for 40,000 hours	LRO No signs of grain boundary precipitation in base metal
482°C for 1000 hours	No LRO No signs of grain boundary precipitation in base metal
538°C for 1000 hours	LRO No signs of grain boundary precipitation in base metal
593°C for 1000 hours	LRO Grain boundary films of P phase
593°C for 16,000 hours	LRO Grain boundary films of P phase Carbide precipitates at grain boundaries
649°C for 16,000 hours	No LRO Precipitation of P and μ phases mainly at grain boundaries
704°C for 16,000 hours	No LRO Precipitation of P and μ phases at grain boundaries and within the grains Carbide and σ precipitation at grain boundaries
760°C for 16,000 hours	No LRO Precipitation of P and μ phases at grain boundaries and within the grains σ precipitation at grain boundaries

Unlike TCP phase precipitates, LRO results in very small and finely dispersed precipitates. As a result, SEM image analysis is not well suited to determine the extent of LRO kinetics. However, due to the uniformly and finely dispersed nature of LRO, microhardness measurements can be used to determine LRO trends. Figure 2.2.2 summarizes the analyses of microhardness measurements made on aged Alloy 22 base metal [22]. Trend lines have been included for the results at 500 and 550°C. The microhardness of "as-received" material was 217 Hv.

The microhardness measurements indicate that LRO has occurred at temperatures in approximately the 500 to 550°C range up to 40,000 hours. In addition, for results up to 40,000 hours, no LRO is evident for temperatures below 400°C, and little LRO is seen at temperatures around 600°C. The decrease in LRO kinetics near 600°C corroborates well with a critical order-disorder temperature of about 620°C calculated in the computational model [22]. The calculated isothermal Time-Temperature-Transformation (TTT) diagrams associated with the ordered phase (oP6) transformation of a ternary Ni-Cr-Mo surrogate for Alloy 22 are displayed for 2, 10, and 15% transformation rates. The microhardness measurements add confidence to the observation from the computational TTT diagrams that forming the ordered phase from the fcc-solid solution at less than 300°C within tens of thousands of years is unlikely. However, once the presence of LRO has been detected from microhardness measurements, TEM analysis should be performed and the volume fraction of the oP6 phase measured, to experimentally validate the computational TTT diagrams.

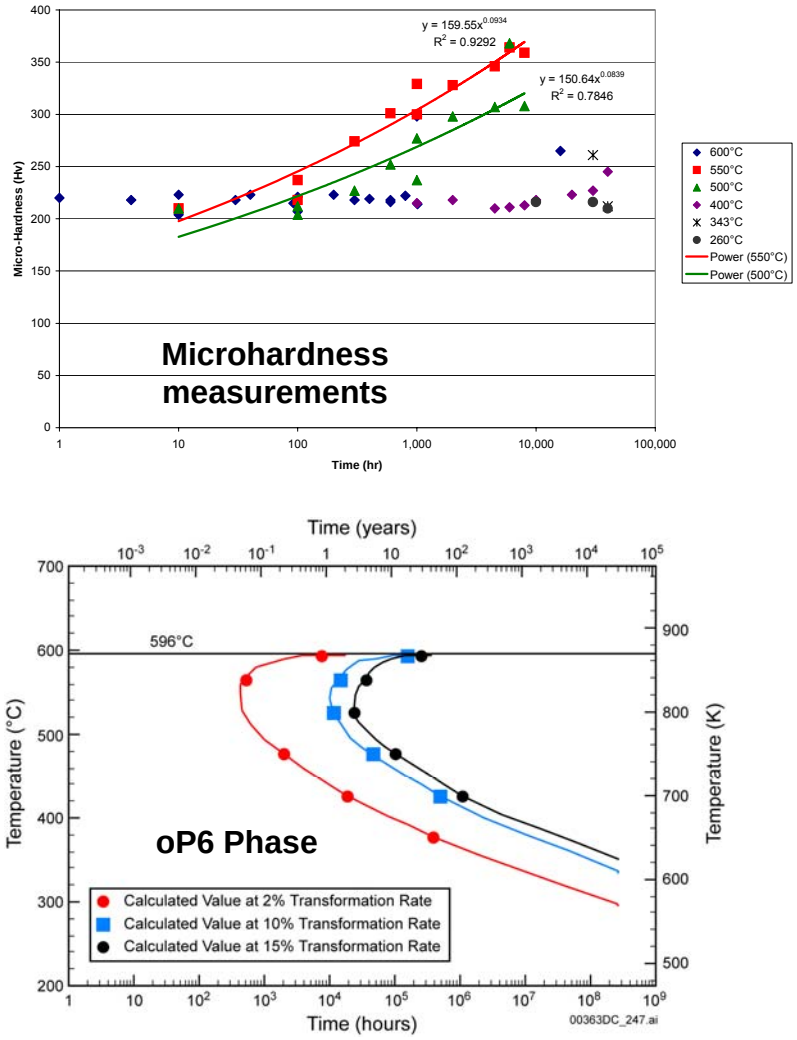

Figure 2.2.2. **The top graph shows micohardness measurements as a function of aging time, and the bottom graph shows the theoretical Dictra predictions for the ordered phase (oP6) [22].**

3. Aging and Phase Stability Model

3.1. Introduction

The goal of the Aging and Phase Stability (APS) model was to determine whether the single-phase solid solution is stable under repository conditions, and if not, how fast phases may precipitate. Precipitation kinetics in the annealed base metal, as well as in the annealed and stress-mitigated welds, must be modeled. The APS model, which is based on fundamental thermodynamic and kinetic concepts and principles, will be used to provide predictive insight into the long-term metallurgical stability of Alloy 22 under relevant repository conditions. Thus, there are no direct inputs from the APS model to total system performance assessment (TSPA).

The time required for these precipitation reactions to occur increases as the temperature decreases. At the expected repository temperatures, the kinetics of these precipitation reactions are too slow to measure experimentally. For this reason, the rates at which they occur are measured at temperatures that are high in comparison to expected repository temperatures and then extrapolated to lower temperatures. Extrapolation from the relatively short laboratory time frame (tens of years) to the long repository time frame (tens of thousands of years) must be performed over durations spanning orders of magnitude. Because of the extended time period over which the extrapolation is performed, small changes in the short-term data can have a large effect on the predicted results. Theoretical calculations are used to establish confidence in such extended extrapolations.

Computations using the APS model were conducted in four general steps [25]: (1) validation of the Thermo-Calc results for the alloy systems and components of interest, (2) determination of the property diagrams for the nickel-based alloys of interest, (3) determination of the kinetic properties (TTT diagrams) of the nickel-based alloys of interest, (4) validation of the computational phase kinetic results with measured data [22]. Experimental results were measured in three areas: (1) volume fraction measurements in aged Alloy 22 base metal, including grain boundaries, (2) volume fraction measurements in aged Alloy 22 weld metal (0.5” and 1.25” plate), and (3) microhardness measurements in aged Alloy 22 base metal, indicative of LRO.

3.2. Thermo-Calc and DICTRA

Thermo-Calc and DICTRA are based on the so-called CALPHAD (CALculation of PhAse Diagrams) approach (Saunders et al. [23]; Spencer [24]), introduced in the 1970s by Larry Kaufman, that involves the coupling of phase diagram calculations for multicomponent alloy systems with other forms of thermo-chemical inputs to determine phase formation, proportions, and transformations.

Even in binary alloy systems, difficulties often occur in determining phase formation characteristics solely by reference to an experimentally determined phase diagram. These difficulties arise from kinetic limitations on reaching equilibrium at low temperatures and from inherent limitations on the accuracy of some of the available experimental techniques. One of the major steps in the Thermo-Calc application is a full characterization of a phase diagram that includes all available thermodynamic information. This, in turn, offers a reliable overall assessment that also allows the calculation of ancillary properties from the same database. In analyzing higher-order multicomponent alloys, the Thermo-Calc application avoids thermodynamic inconsistencies with built-in safeguards, which ensure that phase boundaries are developed in accordance with the fundamental rules of classical thermodynamics.

DICTRA fulfills the need to provide critical modeling and analysis of data by solving the diffusion equations, calculating thermodynamic equilibrium (with Thermo-Calc), solving the flux-balance equations, and finally predicting the displacement of phase-interface positions. This

application is used to analyze the kinetics of phase evolution in alloys selected for the barriers of the waste package by predicting TTT diagrams for relevant phases forming as functions of time.

This application will help determine the solidification path and the effect of welding, and eventually post-annealing, on the stability and long-term aging of alloys selected for the waste package. Kinetics studies are focusing on the time-dependent formation of complex Frank–Kasper phases (such as P and σ phases), and the long-range ordering in terms of phase evolution from the fcc matrix for times extending tens of thousands of years. The DICTRA application was applied to the study of grain boundary formation of carbides, silicides, and TCP phases, and the study of phase evolution under non-isothermal conditions.

Starting with the thermo-chemical database provided by the SGTE (Scientific Group Thermodata Europe) data group, a detailed analysis of the stability of the binary alloys Ni–Cr, Ni–Mo, and Mo–Cr, and of the ternary Ni–Cr–Mo alloys was undertaken. The study then focused on the role of additional solutes such as Si, C, Co, Nb, Ta, and W on stability, ordering, and precipitation in Ni–Cr–Mo-based alloys. Finally, kinetic and thermodynamic modeling was combined and applied to the study of diffusion-controlled transformations with the use of the DICTRA software linked to Thermo-Calc [22,26].

3.3. Surrogate Ternary Alloys

Calculations were performed to test the validity of the thermo-chemical database, and compared with the re-assessed database for the same section of the ternary phase diagram with all the phases considered except the P phase which was suppressed. The calculated phase diagram compared favorably with the experimental counterpart, as far as the boundary of the γ-solid solution was concerned. A two-phase region (fcc + σ) was also predicted by Karmazin [27] in the temperature range 620 - 1370^{o}C at lower Ni content. However, because Karmazin did not report on the structural characterization of these phases at high temperature in this stability region, the predicted two-phase region could not be confirmed.

Simplified Ni-Cr-Mo alloys were made and aged to: (1) determine ordering tendency, (2) test the validity of the predictions, and (3) ascertain whether the “suspension” of the P phase during the calculation of the phase diagram was equivalent to assuming that the kinetics of P-phase formation was much slower than the one associated with the formation of the σ phase. Additionally, a Ni-Cr-Mo-W alloy was made to determine the effect of tungsten on ordering (see Table 3.3.1). Figure 3.3.1 is a summary of the results of isothermal TTT diagram calculations for a) a binary Ni-Cr alloy with 10% transformation of the fcc matrix in the oP6-ordered phase of Ni_2Cr-type, and b) a fcc-based matrix of a ternary surrogate of Alloy 22 transforming into the P phase, with transformation rates ranging from 1 to 20%. Analyses of these aged surrogate alloys should be performed and compared to the TTT curves shown in Figure 3.3.1.

Table 3.3.1. Chemical Compositions in wt.% for Ternary/Quaternary Alloys

Element	Alloy (ST184)	Alloy (ST185)	Alloy (ST186)
Molybdenum	9.0	13.5	13.5
Chromium	28.0	21.5	21.5
Tungsten	---	---	3.0
Nickel	remainder	remainder	remainder

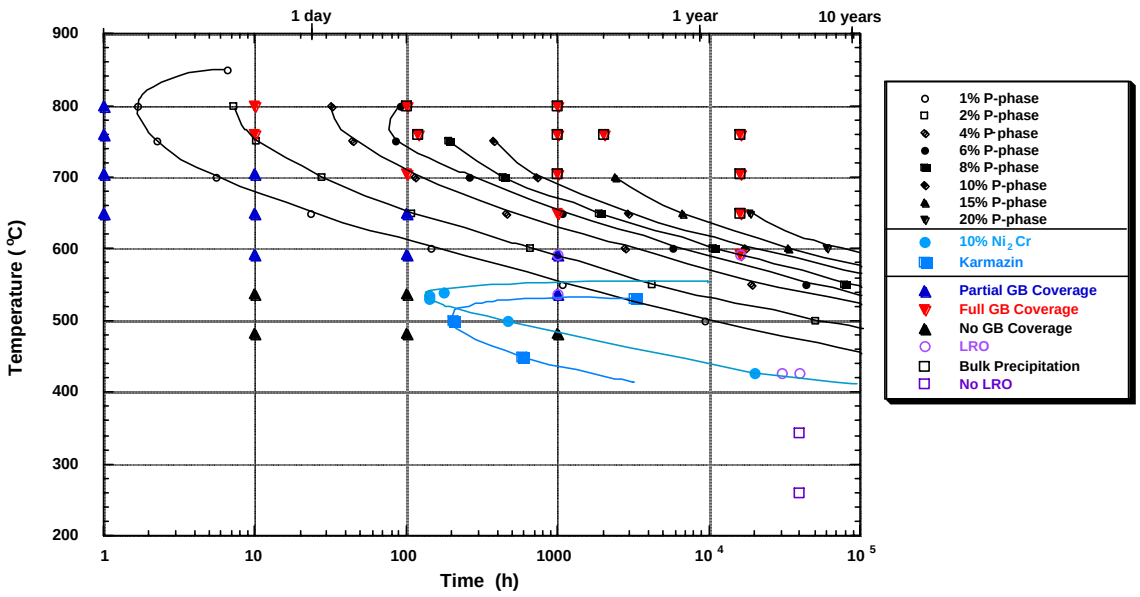

Figure 3.3.1. Summary of the results of isothermal TTT diagram calculations for a) a binary Ni-Cr alloy with 10% transformation of the fcc matrix in the oP6-ordered phase of Ni_2Cr-type (lower curves describing the prediction and the results extracted from the work of Karmazin [27]), and b) an fcc-based matrix of a ternary alloy (surrogate of Alloy 22, with 55.7 Ni, 21.1 Cr, and 13.5 Mo, in wt.%) transforming into the P phase, with transformation rates ranging from 1 to 20%.

3.4. Conclusions

In contrast to the formation from the fcc-matrix of the oP6 ordered phase that is rather slow, the incipient formation of the P phase is quite fast (a few hours in the bulk). However, as was concluded previously, the extrapolation of these TTT curves to lower temperatures clearly indicates the impossibility of forming the P phase out of the fcc-solid solution at less than 300°C for as long as tens of thousands of years [22,26].

The CALPHAD (CALculation of PHAse Diagrams) approach has been applied to the study of thermodynamics (stability) and kinetics (aging) of phase evolution in nickel-based alloys, to determine whether the single-phase solid solution is stable under repository conditions and, if not, how fast other phases may precipitate. The model predicts that alloys annealed at appropriate temperatures and quenched should not display any deleterious phase at relevant repository conditions due to the high temperatures required for measurable kinetics.

Note also, that in these calculations, grain boundary formation is not considered; that is, the results only apply to bulk formation and homogeneous phase evolution in Alloy 22 base metal. Similar predictions and calculations still need to be considered for welds. There are not enough experimental data to complete a TTT curve for Alloy 22 base metal and welds because specimens aged for longer times still need to be analyzed. Volume fraction measurements for TCP phases completed to date have been summarized in tables throughout this report. Volume fraction measurements of specimens aged at temperatures where LRO may be present have not been performed and should be considered if LRO becomes a performance confirmation issue.

4. Effects of Fabrication Processes

Evaluation of fabrication processes is important because fabrication can have an effect on the metallurgical structure of an alloy and on the condition of the surface. Virtually all material properties including strength, toughness, aging kinetics and corrosion resistance depend to some extent on the microstructure of the material. A weld has an as-cast microstructure with chemical segregation as well as precipitation of complex phases. The rate of cooling after a solution annealing heat treatment can cause precipitation in Alloy 22. The heat treatment itself causes an oxide to form that is thicker than, and may be chemically and structurally different from, the passive film that gives Alloy 22 its corrosion resistance. Stress mitigation processes introduce cold work into the material, which is known to accelerate precipitation reactions. Cold work may also affect corrosion resistance. For these reasons, it is important that full-scale prototypes be built and evaluated for processing effects on performance.

4.1. Heat-to-heat Variability

During the manufacturing of alloys, there can be variability in the chemical composition from heat-to-heat that still meets a particular specification range. In order to further understand the effects (if any) that varying weight percents of elements may have on the performance of Alloy 22, several different base metal and weld heats were made by ATI-Allegheny Ludlum Company (ALC) [28]. Variations were created from the proposed nominal composition and threshold limits based on the elemental compositional ranges specified for Alloy 22 in ASTM B-575 [29]. The five elements that were varied, Cr, Mo, Fe, W, and Ni, were chosen because they represent the major constituents of Alloy 22 and are the key elements that can have an effect on the formation of secondary phases such as mu, P, and sigma. Variations in the ranges of the minor constitutive elements of Alloy 22 were not considered. Table 4.1.1 shows the compositions of base metal and weld filler material that was received from ALC. Additional details regarding the manufacturing and analyses of these heats by ALC is published elsewhere [28].

No aging or analyses were performed by LLNL in support of aging and phase stability studies on these specimens. They are mentioned here for informational purposes in the event that specimens from various heats may need to be analyzed in the future to support performance confirmation.

Table 4.1.1. Base metal and weld wire compositions for heat-to-heat studies manufactured by ALC [28] (1.05" x 4.5" bars were fabricated from heats)

Heat Number	Type	Al	C	Cr	Cu	Fe	Mg	Mo	Ni	O	P	S	V	W
HC70	Wire	0.15	0.004	19.34	0.01	<.02	0.0023	15.10	61.94	0.0015	<.003	<.0003	<.01	3.16
HC71	Wire	0.16	0.005	19.79	0.01	0.42	0.0032	15.75	60.35	0.0011	0.006	<.0003	<.01	3.47
HC72	Wire	0.17	0.002	20.50	0.01	0.39	0.0017	16.25	58.84	0.0010	0.007	<.0003	<.01	3.74
HC73	Wire	0.18	0.001	21.58	0.01	0.28	0.0018	16.25	57.84	0.0013	0.008	<.0003	<.01	3.79
HC74	Wire	0.16	0.001	22.29	0.01	0.35	0.0016	16.28	56.79	0.0011	0.008	<.0003	<.01	4.04
HC75	Wire	0.16	0.002	22.86	0.01	0.14	0.0027	16.82	55.59	0.0012	0.01	<.0003	<.01	4.33
HD15	Wire	0.16	0.005	20.59	0.43	4.03	0.0017	16.26	53.58	<.0006	<.003	<.0004	0.11	3.82
HC76	Plate	0.17	0.003	20.31	0.01	2.51	0.0011	12.71	61.60	0.0015	0.003	<.0003	<.01	2.64
HC77	Plate	0.19	0.004	20.22	0.01	2.50	0.0023	12.63	61.57	<.00065	0.003	<.0003	<.01	2.66
HC78	Plate	0.17	0.005	20.78	<.01	3.00	0.002	13.28	59.67	0.0014	0.004	<.0003	<.01	3.00
HC79	Plate	0.14	0.004	20.81	0.01	3.02	0.0017	13.31	59.59	0.0013	0.004	<.0003	<.01	3.01
HC80	Plate	0.18	0.006	21.22	<.01	3.99	0.0018	13.11	58.39	0.0012	0.004	<.0003	<.01	3.01
HC81	Plate	0.16	0.005	21.03	<.01	3.98	0.0018	13.13	58.64	0.0014	<.003	<.0003	<.01	2.98
HC82	Plate	0.19	0.008	21.60	<.01	4.97	0.0021	13.73	56.37	0.0012	0.006	<.0006	0.01	3.00
HC83	Plate	0.15	0.010	21.60	<.01	5.07	0.0023	13.71	56.33	0.0010	0.006	<.0003	0.01	2.99
HC86	Plate	0.21	0.006	22.36	<.01	5.74	0.0015	14.23	53.95	0.0008	0.006	<.0003	0.01	3.39
HC87	Plate	0.18	0.007	22.39	<.01	5.78	0.0015	14.23	53.90	0.0011	0.006	<.0003	0.01	3.36
HD16	Remake	0.16	0.006	21.22	0.04	3.02	0.0014	13.51	56.03	0.0013	<.003	<.0003	0.25	3.00
HD17	Remake	0.15	0.005	21.31	0.01	2.98	0.0016	13.60	56.00	0.0008	<.003	<.0003	0.25	2.99
B575 Spec.	N06022 (Plate)	-	0.015 max	20.0-22.5	-	2.0-6.0	0.5 max	12.5-14.5	balance		0.02 max	0.02 max	0.35 max	2.5-3.5
	N06686 (Wire)		0.01 max	19.0-23.0		2.0 max		15.0-17.0	balance		0.04 max	0.02 max		3.0-4.4

Table 4.1.2 compares the mechanical properties measured by ALC of 1.05" x 4.5" bars taken from the heats produced, and compared to the standards in ASME SB-575. The properties were acceptable, with the exception of the elongation data of HC86 and HC87 which had high strengths and low elongations. ALC reported that examination of these as-received bars revealed that the grain size of these heats was much finer than that of the other heats, and that the grain boundaries were decorated with second phase particles. Their conclusion was that for this very highly alloyed composition, it appeared that the standard commercial anneal that was applied (1121°C for 30 minutes) was not sufficient [28]. Although the results were below the minimum requirements, all the data were reproduced here to demonstrate the impact of chemical composition on the mechanical properties.

Table 4.1.2. Comparison of Mechanical Properties of Experimental Heats with Requirements of ASME SB-575 (UNS N06022) for 1.05" x 4.5" Bars, 1121°C/30mins/Air Cooled [28]

Heat No	Chemistry Set	Yield Strength (ksi)	UTS (ksi)	Elong. (percent)	RA (percent)
HC76	A	45.6	111.2	73.5	79.4
HC77	A	44.9	112.0	73.3	79.3
HC77	A	46.6	114.0	72.5	78.5
HC77	A	45.0	111.0	75.2	81.1
HC78	B	46.3	110.6	74.6	80.1
HC79	B	47.7	113.1	72.8	79.9
HC80	C	45.4	110.3	71.9	79.5
HC81	C	45.4	110.7	72.8	80.1
HC82	E	50.5	121.9	58.5	63.5
HC83	E	51.6	122.2	57.6	61.2
HC84	F	48.6	114.2	70.7	75.6
HC85	F	52.9	122.4	64.2	65.8
HC86	G	64.5	136.2	41	39.3
HC86	G	63.7	135.6	40	35.9
HC86	G	64.4	136.8	40.8	39.5
HC87	G	63.8	135.3	39.4	32.0
HC87	G	62.6	133.3	36.9	32.6
HC87	G	63.1	134.5	33.7	30.1
HD16	H	47.3	112.3	74.5	81.0
HD17	H	46.6	111.2	76.7	82.2
ASME SB-575 (UNS N06022)		45.0	100.0	45	NR

In 2004 - 2005 a computational modeling study was performed by Hu, Turchi, and Wong [30] to determine which compositions manufactured by ALC may optimize phase stability, to assist in deciding the most effective annealing temperature and to validate the computational modeling predictions (CALPHAD). A total of eight variations of Alloy 22 chemical compositions and the nominal composition were evaluated [Table 4.1.3].

Table 4.1.3 Chemical Compositions (wt.%) Assessed by Hu et al. [30] for Alloy 22

Element	Nominal	1	2	3	4	5	6	7	8
Cr	21.2	21.2	20.0	20.5	20.9	21.2	21.6	22.0	22.5
Mo	13.5	13.5	12.5	12.8	13.1	13.4	13.7	14.0	14.5
Fe	4.0	4.0	2.0	2.7	3.4	4.1	4.8	5.5	6.0
W	3.0	3.0	2.5	2.65	2.75	2.85	2.95	3.25	3.5
Co	2.0	2.0	2.0	2.0	2.0	2.0	2.0	2.0	2.5
C	0.01	0.01	0.01	0.01	0.01	0.01	0.01	0.01	.015
Si	0.08	0.08	0.08	0.08	0.08	0.08	0.08	0.08	0.08
Mn	0.5	0.5	0.05	0.05	0.5	0.5	0.5	0.5	0.5
V	0.3	0.3	0.3	0.03	0.3	0.3	0.3	0.3	0.035
P	-	-	-	-	-	-	-	-	0.02
S	-	-	-	-	-	-	-	-	0.02
Ni	55.7	55.7	60.11	58.46	56.96	55.56	54.06	52.36	50.015

Based on the computational analyses of the eight chemical compositions for Alloy 22, the following behaviors regarding phase formation and stability were observed by Hu et al. [30]:

1. With a total concentration of Cr and Mo of approximately less than 34 wt%, the formation of σ-phase may be avoided. Sigma phase is expected to be particularly detrimental to mechanical properties.

2. With the concentration of Fe as low as possible, the fcc phase may be more stable, because as Fe concentration increases, the fcc phase becomes less stable with decreasing temperature.

3. The presence of W appears to enhance the stability of the fcc phase.

4. At low Mo content, σ-phase does not form, and there is an enhanced stability of the oP6 phase (LRO) at low temperatures.

5. At the nominal composition of Alloy 22, σ-phase begins to appear at approximately 950°C. The emerging σ-phase begins to compete with the fcc phase. The amount of oP6 phase decreases gradually as the Mo content increases.

6. As Mo composition increases further, σ-phase becomes more stable and starts to form at higher temperatures (~ 1100°C). The growth of σ-phase begins to deplete the matrix of Mo and Cr. The temperature where σ-phase first forms is critical in determining the effective annealing temperature for Alloy 22. The amount of oP6 phase decreases further as the Mo content increases.

Conclusions

Without considering corrosion property data for the various compositions, it was determined from the computational analyses that compositions 2 and 8 should initially be fabricated and studied [30]. The two heats whose compositions are most similar to compositions 2 and 8 are HC76 and HC87, respectively. Hu et al. [30] demonstrated that as the concentrations of Mo and Cr are increased, many changes can take place within the microstructure of Alloy 22. However, while it is advantageous to predict the behavior of materials through computational modeling, it is crucial to validate these predictions with experimental data. Unless additional testing is completed to demonstrate that changing Cr and Mo levels will provide adequate corrosion resistance while better optimizing high temperature phase stability, it is recommended that the current compositional limits for Alloy 22 continue to be used by the Yucca Mountain Project (YMP).

4.2. LLNL Heats

Several different heats of Alloy 22 base metal and weld metal have been used in studies at LLNL over the course of the past ten years (see Appendix B). All heats were within the specified composition and threshold limits based on the elemental compositional ranges specified for Alloy 22 in ASTM B-575 [29]. A few of the heats are listed here for comparative purposes with the ALC compositions shown in Section 4.1. Table 4.2.1 lists some of the Alloy 22 heats used in base metal and weld specimen aging studies, and their respective chemical compositions are listed in Table 4.2.2 [31]. Specimens used in aging and phase stability studies were purchased from Metal Samples and Haynes International.

Table 4.2.1. Alloy 22 Heats Used in Base Metal and Weld Specimen Aging Studies [31]

Base Metal	Weld Metal	Aging Conditions	Properties Measured
2277-3-3223	–	Mill annealed* (MA) and aged 593 to 760°C	Mechanical, Volume Fraction
2277-0-3195	–	MA + aged 593 to 760°C (2000 and 16,000 hours only)	Mechanical
2277-7-3173	–	Aged 427°C	Mechanical and Corrosion
2277-6-3181	–	Aged 482 to 760°C	Corrosion, Volume Fraction
2277-9-3201	2277-8-3281	As-welded + aged 593 to 704°C	Mechanical, Volume Fraction
2277-9-3201	2277-8-3277	Aged 760°C	Mechanical, Volume Fraction
2277-6-3171	2277-7-3181	As-welded	Mechanical
2277-7-3173	2277-3-7281	Aged 427°C	Mechanical
2277-9-3237	2277-8-3277	Aged 482 to 760°C	Corrosion
2277-6-3181	2277-7-3173	Aged 427°C	Corrosion

**The mill anneal is done at 1020-1135°C for 20-30 minutes.*

Table 4.2.2. Chemical Composition (wt. %) of Alloy 22 Heats used in Aging Studies [31]

Heat*	Al	C	Co	Cr	Fe	Mg	Mn	Mo	N	Ni	Si	V	W
3-3223	0.25	0.002	1.56	21.60	4.3	0.017	0.24	13.50	0.04	55.33	0.037	0.15	3.00
0-3195	0.29	0.003	1.74	21.10	4.7	0.010	0.21	13.50	0.02	55.67	0.023	0.12	2.90
6-3171	0.31	0.002	0.70	21.97	4.42	0.036	0.23	13.31	0.03	56.2	0.032	0.15	2.86
7-3173	0.26	0.003	1.13	21.64	3.77	0.020	0.24	13.46	0.04	55.78	0.027	0.14	3.01
9-3201	0.36	0.003	0.65	21.07	3.67	0.025	0.25	13.76	0.04	55.20	0.025	0.16	2.90
6-3181	0.32	0.004	1.11	21.59	3.90	0.023	0.28	13.64	0.03	55.93	0.024	0.17	3.03
9-3237	0.34	0.004	0.90	21.26	3.97	0.036	0.25	13.15	0.02	55.97	0.027	0.21	2.90
8-3281	0.32	0.002	1.47	21.58	3.97	0.031	0.32	13.49	0.04	55.33	0.025	0.14	2.96
8-3277	0.33	0.006	1.10	21.58	4.17	0.023	0.25	13.29	0.03	55.5	0.022	0.18	3.18
7-3181	0.29	0.003	1.47	21.32	4.29	0.023	0.25	13.25	0.03	55.24	0.027	0.15	3.03
3-7281	0.21	0.003	0.21	21.49	3.13	–	0.18	13.38	0.04	57.97	0.060	0.15	3.00

**All heats were Alloy 22 (designated as 2277 in heat number). See Table 4.3.1 for the heats used for base metal and those used for weld metal.*

4.3. Solution Annealing Studies of Alloy 22 Thick Welds (1.25")

In October 2003, the Center for Nuclear Waste Regulatory Analyses (CNWRA) showed that solution annealing of Alloy 22 welds decreased the repassivation potential for crevice corrosion when compared to as-welded material [32]. It is important to understand this effect so that it can be determined how much, if any, solution annealing decreases the repassivation potential of Alloy 22 welds. Tests were designed to show the effect on precipitate volume fraction of solution annealing at a short time (20 minutes). Longer times were also included so that it could be clearly demonstrated whether the precipitates, which are known to be present in the as-welded condition, were dissolving or growing (or precipitating). If one of the three types of phases present grew at the expense of the others, the phase was identified. Volume fractions of phases present were measured, and microprobe traces were done across the dendrites in the welds in order to indicate the extent of homogenization.

Specimens were aged for 20 minutes at four temperatures for corrosion testing. The specimens were tested in two environments with three replicates for a total of 24 tests. It is important to test these specimens where differences in the susceptibility can be detected. If the test environment is too aggressive, then the attack will be severe and little difference will be detected even if there is a difference in susceptibility. The same is true for test environments that are too benign. Based on previous critical potential tests, the lower nitrate and intermediate temperature NaCl-KNO_3 environments are most likely to be sensitive to material susceptibility. Results from the corrosion testing are detailed in Torres et al. [33] and are summarized in this report.

4.3.1. TCP Phase Quantification and Mapping

Backscatter electron imaging was used to identify the presence of TCP phases in polished specimens. Due to weld symmetry, only half of the weld (*i.e.* one "U") was studied for each of the specimens (see Figure 4.3.1.1.). This imaging technique was used to:

1. Determine the volume fraction of TCP phases present in the weld, and
2. Map the fusion zones of the as-welded and solution annealed specimens.

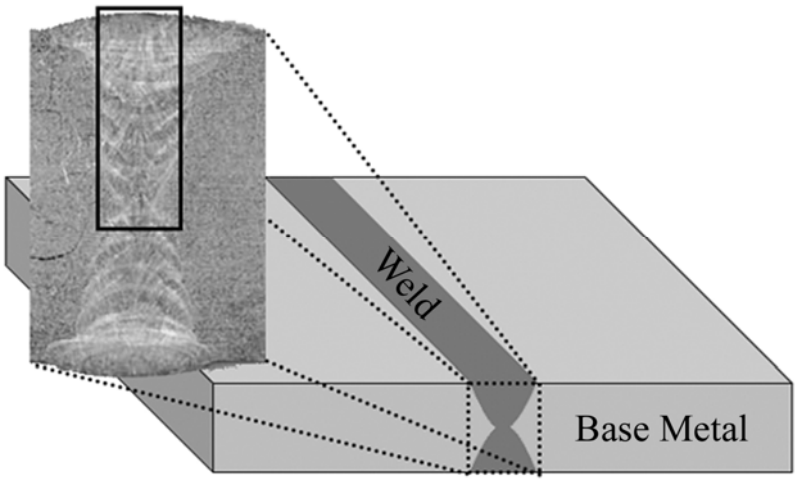

Figure 4.3.1.1. Schematic of weld cross-section showing the region of weld examined (black box) [33].

For TCP phase quantification, approximately 40 micrographs were collected at a magnification of 1500X within the top 4 mm of the weld, at regular intervals for each specimen. Imaging was restricted to this weld region because it is the most pertinent to material performance from a corrosion point of view. It is also likely to contain the greatest amount of solute. Image analysis was then performed, yielding an area fraction for the TCP phase (white) portion of each image. The average area fraction of TCP phases in each specimen can be determined from all micrographs measured. Since the images were obtained on a regularly spaced grid, the volume fraction of TCP phases is equal to the measured area fraction.

The fusion zones were mapped for the as-welded specimen and the specimen that was solution annealed at 1121°C for 20 minutes. This was performed by collecting 880 micrographs (for each specimen) and stitching them together to form a collage [33]. The collage layout consisted of 44 rows and 20 columns, with the first row at the top of the weld (last weld pass), and the last row near the center of the weld (first weld pass). The individual micrographs were imaged at 500X, which yielded a field of view of approximately 511 μm x 441 μm for each micrograph. To eliminate the chance of overlap, neighboring images were separated by a stage translation of 520 μm and 450 μm in the x and y directions, respectively. The total area covered during the imaging of both specimens was 10.4 mm by 19.8 mm.

For each of the two specimens imaged in this manner, two collages were generated. The first was of the micrographs as captured (which allowed the visualization of the complete fusion zone microstructure) while the second was of the micrographs after a grayscale threshold had been applied, yielding a map detailing the locations of the TCP phases within the weld fusion zone.

4.3.2. Crystallographic Orientation Mapping

EBSD was used in scanning each specimen to map the microstructure and determine the crystallographic texture of the fusion zones after solution annealing. Due to the size of the area of interest, a combination of beam and stage translations were used during the scans. Data were collected on a square grid, with grid step sizes of 12 μm to 30 μm (depending on the specimen's grain size) and typically covered an area of approximately 9 mm x 20 mm. In order to align the EBSD scans with the micrograph collages for the as-welded specimen (and the specimen annealed at 1121°C for 20 minutes) two fiducial marks (one at either end of the weld fusion zone) were used.

4.3.3 Results and Discussion

The results of the TCP volume fraction measurements and observed microstructure for each solution annealing condition are listed in Table 4.3.3.1. TCP phases are present in only three of the seventeen specimens, the as-welded specimen and the specimens solution annealed for 20 minutes at 1075°C and 1121°C. Because the volume fractions measured were < 1% and the TCP phases were inhomogeneously dispersed, the relative error associated with the values is high. Therefore, the values determined should only be used as an indication of the presence of TCP phases. It is important to note that for the specimens with zero volume fractions, the lack of TCP phase observations does not fully eliminate the possibility of their existence, rather it indicates that if any are present, they are significantly smaller than 0.25 μm (the resolution of the SEM).

It was apparent that the location of the TCP phases follows the weld pass geometry and that while the TCP phase distribution is spatially homogeneous (at the apparent length scale) near the top of the weld, there was a distinct banding structure in the first few weld passes. It was also observed that while the specimens treated at 1075°C and 1121°C were still in the process of recrystallization, the specimen treated at 1200°C appeared fully recrystallized while the specimen treated at 1300°C possessed coarsened grains. Figure 4.3.3.1 shows the effect of solution annealing temperature on grain size for welds annealed for 20 minutes. It should be noted that at 1200°C, the grain size distribution is more uniform than at 1075°C, 1121°C, and 1300°C. The

recrystallization behavior in the 1075°C and 1121°C specimens closely resembled the weld pass geometry.

Full recrystallization (> 95%) of the columnar dendrites in the fusion zone was observed in the specimens annealed for 168 hours at 1075°C, 24 hours at 1121°C, and 20 minutes at 1200°C. In the specimen aged at 1300°C, full recrystallization must have occurred well before 20 minutes because rapid grain growth and coarsening behavior were observed at the 20 minute mark. Also observed was significant grain coarsening near the fusion zone boundary of the specimens annealed at 1075°C for 168 hours, 1121°C for durations of 72 hours and greater, 1200°C for durations of 24 hours and greater, and for all the specimens annealed at 1300°C.

Table 4.3.3.1. TCP Phase Volume Fractions and Recrystallization Behavior of Solution Annealed Alloy 22 Welds [33]

Annealing Temperature	Annealing Duration	Volume Fraction (%)	Recrystallization Behavior
None	None	0.11 ± 0.09	Not Applicable
1075°C	20 minutes	0.53 ± 0.42	Small amount near weld toe
1075°C	24 hours	0	Banding at weld pass interfaces; grain growth at root pass region
1075°C	72 hours	0	Grain coarsening near weld toe; recrystallization throughout weld, except near weld top
1075°C	168 hours	0	Fully recrystallized; abnormal grain growth in root pass region and near fusion zone boundary
1121°C	20 minutes	0.24 ± 0.15	Recrystallization at root pass region and banding at weld pass interfaces
1121°C	24 hours	0	Fully recrystallized; large grains at root pass region and near base metal
1121°C	72 hours	0	Grain growth in fusion zone; abnormal grain growth near fusion zone boundary
1121°C	168 hours	0	Grain coarsening in fusion zone; abnormal grain growth near fusion zone boundary
1200°C	20 minutes	0	Fully recrystallized; homogeneous grain sizes observed throughout
1200°C	24 hours	0	Grain growth in fusion zone; abnormal grain growth near fusion zone boundary
1200°C	72 hours	0	Coarsened grains throughout
1200°C	168 hours	0	Coarsened grains throughout
1300°C	20 minutes	0	Abnormal grain growth in fusion zone
1300°C	24 hours	0	Coarsened grains throughout
1300°C	72 hours	0	Coarsened grains throughout
1300°C	168 hours	0	Coarsened grains throughout

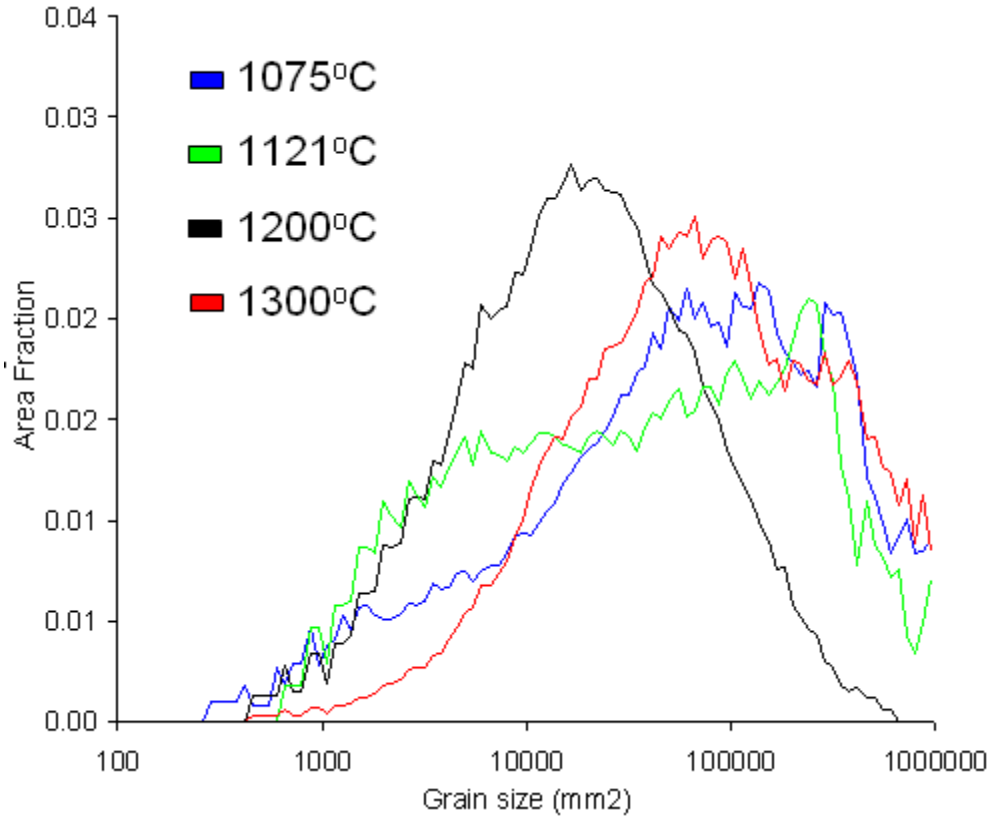

Figure 4.3.3.1. Area fraction vs. grain size for welds annealed for 20 minutes at 1075°C, 1121°C, 1200°C, and 1300°C, showing the effect of solution annealing temperature on the grain size [33].

4.3.4. Summary

Because the primary focus of the solution annealing treatment from a microstructural point of view is the dissolution of TCP phases and homogenization of the microstructure, two aspects of the results need to be considered; the extent of TCP phase dissolution and the extent of fusion zone recrystallization. The former is important from a corrosion aspect, because the presence of TCP phases indicates chemical segregation and local depletion of Cr and Mo, and hence a potential decrease of corrosion performance. Based on the results, it was observed that solution annealing at higher temperatures (1200°C and 1300°C), or longer durations at lower temperatures (1075°C and 1121°C), are required to dissolve TCP phases. Because it would be unrealistic to hold the waste container for multiple days at these elevated temperatures during fabrication, solution annealing at either 1075°C or 1121°C does not provide a viable solution. This leaves solution annealing for 20 minutes at either 1200°C or 1300°C. Considering the coarsening observed in the 1300°C specimen, and the relatively homogeneous nature of the grain structure in the 1200°C specimen, the choice of solution annealing at 1200°C for 20 minutes appears to be the most appropriate treatment to perform from a microstructural point of view.

Similar studies and observations were made by the Center for Nuclear Waste Regulatory Analyses (CNWRA) [32]; however, they noted that there was a high-volume fraction of precipitates in solution-annealed Alloy 22 welds, indicating that solution annealing promoted precipitation of secondary phases. In the LLNL study, secondary phases were only observed for three conditions (as-welded, and solution annealed at 1075°C and 1121°C for 20 minutes); there were no signs of precipitation for all other solution annealing times and temperatures as

summarized in Table 4.3.3.1. The resolution of the SEM used in this study is about 0.5 microns, so any precipitates smaller than this that may be present could not be measured or observed.

The observed differences in microstructure between LLNL and the CNWRA data could be due to the sample preparation techniques utilized where etching was done prior to imaging versus observation of the samples in an as-polished condition. Previous volume fraction measurements made by the CNWRA on aged welds were etched, and measurements were made down the centerline of the weld (the depth was not reported).

Corrosion Summary

Repassivation potentials (E_{r1} and E_{rco}) showed a tendency to rise with increasing annealing temperature in 1 M NaCl at 90°C, except the E_{r1} values at 1300°C where one specimen had a much lower E_{r1} value than the other two, causing the average to be low. The same trend is observed in the 6 m NaCl + 0.9 m KNO_3 at 100°C tests, except that the specimens annealed at 1200 and 1300°C show a greater ability to repassivate crevice corrosion that has initiated. In both cases, the trend of increasing repassivation potentials indicates that samples annealed at higher temperatures are able to repassivate more easily. Repassivation potentials, open circuit potentials, and corrosion rates all improve with increasing annealing temperatures.

Optical microscopy examination indicates less localized corrosion degradation with increasing annealing temperatures in both the 1 M NaCl and 6 m NaCl + 0.9 m KNO_3 environments [33]. However, the residual surface oxide from the annealing process may have obscured the quantification of the localized corrosion susceptibility from the cyclic potentiodynamic polarization curves.

4.4. Weld Stability Studies

While there have been many studies of Alloy 22 base metal phase stability, relatively little is known about the stability of Alloy 22 weld structures. Welding produces a cast microstructure with chemical segregation regardless of the alloy used. Cieslak et al. [7] and Ogborn et al. [8] investigated the microstructures of Alloy 22 and other similar alloy welds. They found segregation of primarily Mo but also to some extent W in the interdendritic regions of the weld. This enrichment of Mo and W causes TCP phases to form during welding of Alloy 22; μ, P, and σ phases were seen in Alloy 22 welds. This segregated structure tends to increase the corrosion rate somewhat over the base metal [9,10] and reduces ductility [11]. The growth of TCP phases in Alloy 22 welds due to thermal aging causes a further reduction of the corrosion resistance and mechanical properties of the weld.

In order to predict long-term behavior of welds, it is important to know whether these precipitates present in the as-welded condition are thermodynamically stable at the low repository temperatures and, if so, how fast they grow and what effect they have on the properties of the weld. The kinetics of the reactions that occur in the weld may be different than for the base metal because the precipitates are already nucleated in the weld and there is chemical segregation. Conclusions will remain uncertain until theoretical calculations that take into consideration the numerous phases involved, their compositions, and segregation in the weld are performed and experimentally validated.

Some limited testing of C-4 welds was done by Matthews [11] who found that weld metal was less ductile than base metal and both showed decreased ductility after aging 8000 hours at 649°C. Rebak and Koon [9] found that Alloy 22 welds had a higher corrosion rate than base metal when tested using the ASTM G 28 B procedure, but that the corrosion rate decreased after aging between 10,000 and 40,000 hours at 427°C.

As observed by Cieslak et al. [7], TCP phases are present in the interdentritic regions of the as-welded structure. After aging, the amount and size of TCP precipitates increases with both time and temperature up to 760°C. Nucleation of precipitation was also observed to form along grain boundaries in some areas of these specimens. The volume fraction of second phase precipitates in 0.5" Gas Tungsten Arc Welded (GTAW) welds is shown as a function of time in Figure 4.4.1 [22]. Each of the data points in Figure 4.4.1 represents the average of 20–40 measurements. In the as-welded condition, there is approximately 0.2 volume % TCP phase. It has been shown that area-fraction measurements are mathematically equivalent to volume-fraction measurements [34]. Therefore, the area-fraction measurements presented in this report are equivalent to the volume-fraction values in Alloy 22 as a function of time and temperature. Extrapolations of these data do not indicate that precipitate nucleation and growth in the welds will occur to a significant extent at temperatures below approximately 300°C.

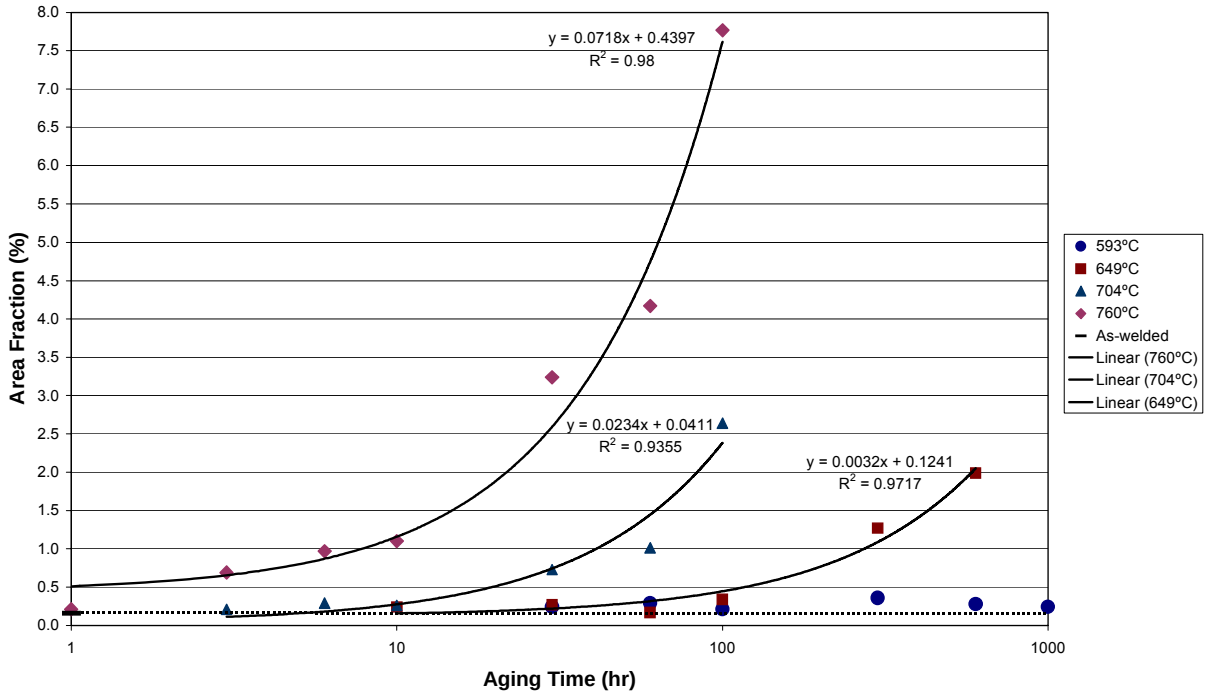

Figure 4.4.1. TCP phase precipitation kinetics in Alloy 22 GTAW 0.5" welds as a function of temperature and time [22].

4.5. Evaluation of Weld Stability in Prototypical Thick Welds

The prediction of phase stability in Alloy 22 welds was based on data (an empirical model) taken from 0.5" welds produced and aged at Haynes International, Inc. The heat input for thicker 1.25" welds would be greater and may alter the initial state of precipitation in the welds and therefore the stability of the weld microstructure. This concern was raised by the Nuclear Regulatory Commission (NRC).

Therefore, thick prototypical (1.25") welds were cut into specimen blanks and introduced to the aging studies. Specimen blanks were 1.25" thick x 0.6" wide and approximately 4" long cut perpendicular to the weld. These specimens were used primarily for metallurgical characterization (phase identification and volume fraction measurement).

4.5.1. Methods

Analyses of six of the seventeen Alloy 22 thick (~1.25") weld specimens that were aged from 200 to 750°C were conducted. The specimens analyzed to date are those aged at 650°C for 20 and 100 hours and the remaining four at 700°C and 750°C for 10 and 100 hours. Characterization requires a polished specimen surface, and all specimens evaluated were metallurgically prepared as described in Section 1.3.

Backscatter electron imaging was used to identify the presence of TCP phases in all six specimens. The method used is described in Section 1.3.1. For each specimen, between 50 and 60 micrographs were captured at 1500X and analyzed.

4.5.2. Results and Discussion

Analysis of the micrographs, as tabulated in Table 4.5.2.1 shows that the kinetics at 650°C for precipitation are slow, with virtually no difference in the TCP phase volume fraction between 20 and 100 hours of aging. A marginal increase in TCP phase volume fraction can be seen between the specimens aged at 700°C, with the specimen aged for 100 hours containing approximately 5 times the volume fraction as the specimen aged for 10 hours. A more significant increase is seen at 750°C however, with over a 20-fold increase in the TCP phase volume fraction between the 10 and 100 hour specimens.

Table 4.5.2.1. Effect of Aging Time and Temperature on TCP Phase Content of Alloy 22 Thick 1.25" Welds [33]

Description	Volume Fraction (%)	Standard Deviation
Alloy 22 Thick Weld Aged at 650°C - 20 hours	0.16	0.12
Alloy 22 Thick Weld Aged at 650°C - 100 hours	0.10	0.11
Alloy 22 Thick Weld Aged at 700°C - 10 hours	0.14	0.12
Alloy 22 Thick Weld Aged at 700°C - 100 hours	0.78	0.83
Alloy 22 Thick Weld Aged at 750°C - 10 hours	0.21	0.18
Alloy 22 Thick Weld Aged at 750°C - 100 hours	5.75	1.95

Figure 4.5.2.1 illustrates the reason for the differences in volume fraction. It can be seen that the difference is minimal between the TCP phase morphology and density for the 650°C and 700°C specimens as well as the 10 hour 750°C specimen. The specimen aged at 750°C for 100 hours shows significant precipitation of small TCP phase particles in both the primary and secondary interdendritic regions. These features can be clearly seen in Figure 4.5.2.2. *Note: The lighter shaded interdentritic regions in Figures 4.5.2.1(a) through (e) are due to solute segregation and are not TCP phases. Only the brightest white regions are TCP phases.*

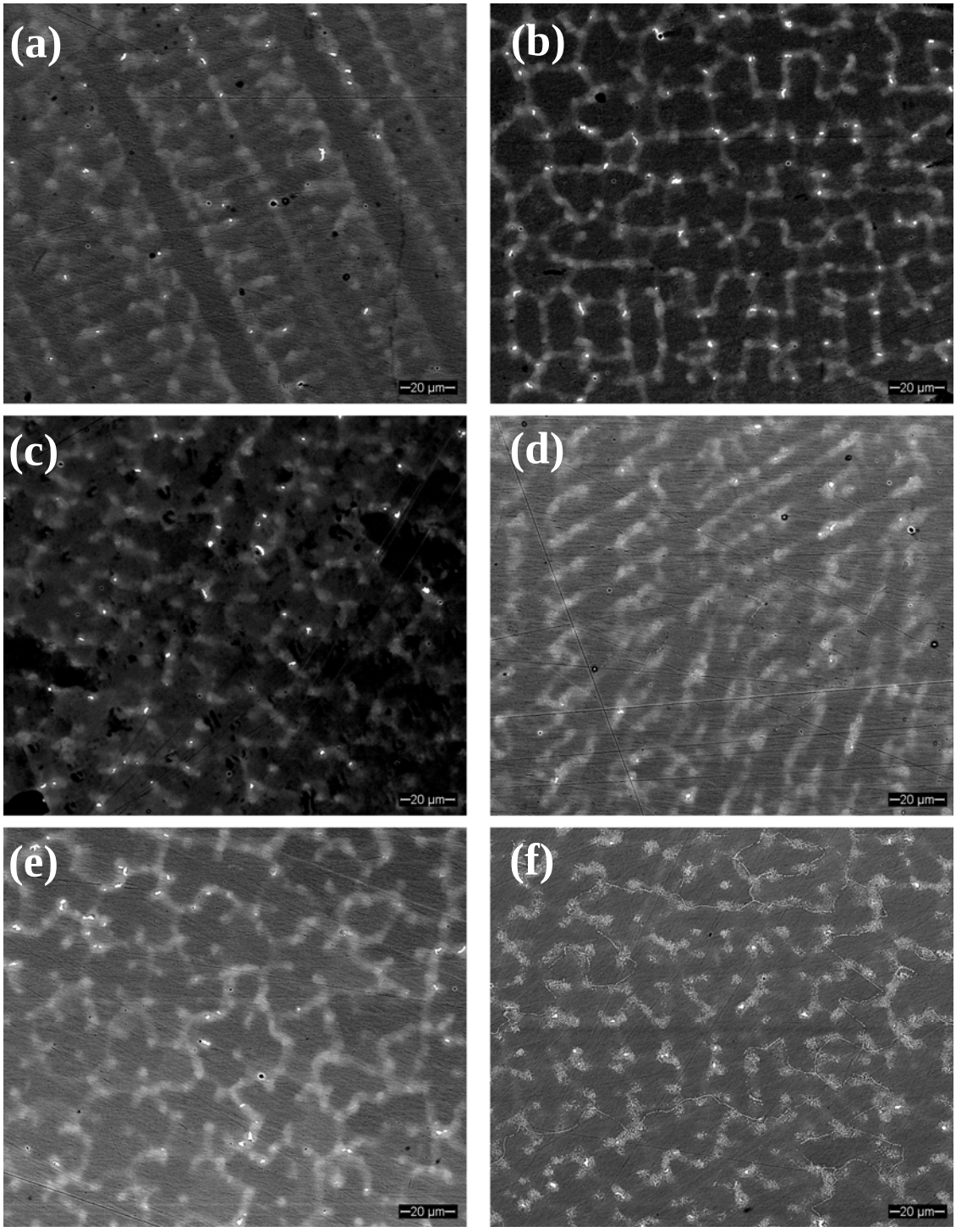

Figure 4.5.2.1. Backscattered Electron SEM Micrographs of specimens aged for (a) 20 hours at 650°C, (b) 100 hours at 650°C, (c) 10 hours at 700°C, (d) 100 hours at 700°C, (e) 10 hours at 750°C, and (f) 100 hours at 750°C [33].

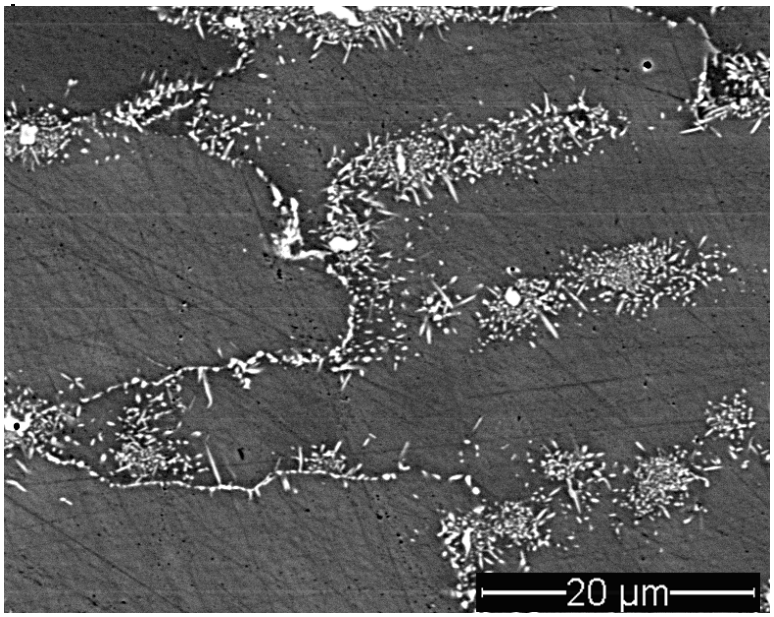

Figure 4.5.2.2. High magnification image of an Alloy 22 weld aged for 100 hours at 750°C. The formation of TCP phases can be seen on the dendritic structure and grain boundaries.

Comparison of the results obtained for the 1.25” thick welds with those previously obtained for 0.5” welds aged at Haynes, International is shown graphically in Figure 4.5.2.3 [33]. The results for the aged 1.25” thick welds are superimposed on those obtained for the Haynes 0.5” welds aged at 649°C, 704°C, and 760°C for similar times. It can be seen that for all specimens investigated in this work, the amount of TCP phases observed is comparable or less than that observed in the 0.5” welds aged by Haynes, International. While many differences in welding parameters may exist between the 0.5” and 1.25” welds, it can be preliminarily concluded that at these times and temperatures, thick welds do not show a significant increase in TCP phase precipitation.

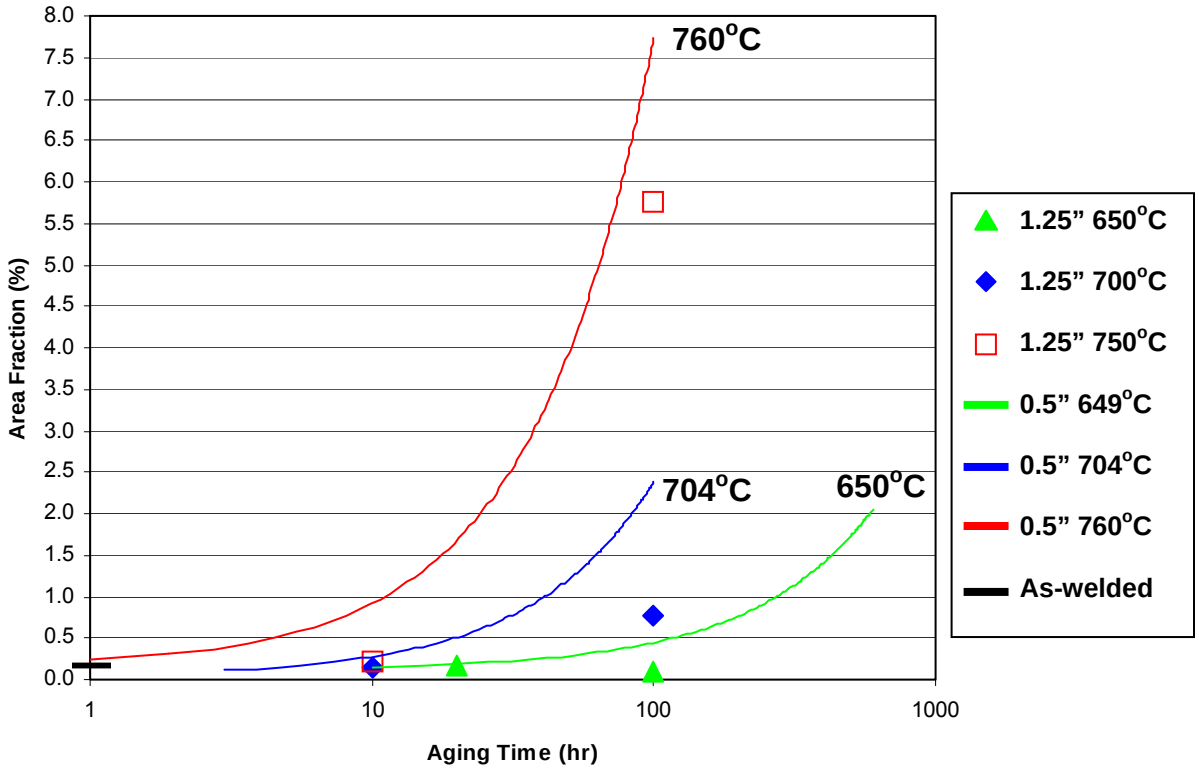

Figure 4.5.2.3. Plot comparing results for 1.25" welds aged at 650°C, 700°C, and 750°C to previous work on 0.5" welds. 1.25" weld data are represented by points, while previous data are shown as curves fit to the data [33].

4.5.3. Summary

Analyses of six of the seventeen Alloy 22 thick (~1.25") weld specimens that were aged at 200 to 750°C were conducted. The specimens analyzed to date were those aged at 650°C for 20 and 100 hours and the remaining four at 700°C and 750°C for 10 and 100 hours. The TCP phase kinetics are fastest at 750°C, resulting in an increase in volume fraction of TCP phases to approximately 6%. While many differences in welding parameters may exist between the 0.5" and 1.25" welds, it can be preliminarily concluded that at these times and temperatures, thick welds do not show a significant increase in TCP phase precipitation. The TCP phase formation in an as-welded specimen and specimens aged for longer durations at these and other temperatures still need to be investigated.

4.6. The Heat Affected Zone

The heat affected zone (HAZ) of a weld is the region of the base metal near the weld that is subjected to a significant thermal pulse during the welding process. TCP precipitation kinetics in the HAZ will be similar to those in the base metal, but the actual rates of precipitation may be different. The high temperatures, approaching the melting point, seen in the HAZ of welds may trigger nucleation of TCP and/or carbide precipitates. If nuclei are already present, precipitation will proceed much faster than in the base metal where they are not present.

Very few precipitates have been observed in the HAZ of weld specimens thus far, however only two weld specimens have been examined: one in the as-welded condition and one after aging at 427°C for 40,000 hours. The precipitates observed may simply be carbides that were present in the mill-annealed (i.e., as-received) condition. Carbides are known to be present in Ni–base alloys similar to Alloy 22, but they are usually within the grains and are generally called primary carbides to distinguish them from other secondary phases that form, often on grain boundaries, after an aging treatment (Tawancy et al. [2]).

During the welding process, melting of the alloy occurs, and an as-cast structure develops upon cooling. As an Alloy 22 weld solidifies, Mo and Cr are rejected from the solid phase, causing their concentration to increase in the liquid. Therefore, the interdendritic regions, which are the last solids to form in a weld, tend to have high concentrations of these elements relative to typical values for Alloy 22 (Cieslak et al. [7]). Because formation of the TCP phases, which are also enriched in Mo and/or Cr, is favored by higher Mo and Cr concentrations, these phases are present in the interdendritic regions of Alloy 22 welds. P phase is primarily seen in the as-welded condition of Alloy 22 welds, but σ and μ phases were also seen (Cieslak et al. [7]).

Because precipitates are present in Alloy 22 welds in the as-welded condition, kinetics of precipitation is not an issue as it is in the base metal and HAZ. Instead, it must be verified that the weld's mechanical and corrosion properties are not degraded by this precipitation. Whether these precipitates are stable and grow, or unstable and dissolve with aging, at repository-relevant temperatures must still be determined.

4.7. Haynes 11.4 year (100,028 hours) Aged Welds

The characterization of welds aged by Haynes International at 260, 343, and 427°C for approximately 100,028 hours was performed by Sandia National Laboratories (SNL), Livermore, CA. It should be noted that the aged plates were only 0.5" thick, and because there is not sufficient material to acquire corrosion/mechanical property data, the results presented are a limited metallurgical evaluation. In previous TEM analyses of an Alloy 22 weld aged at 427°C for 40,000 hours performed at LLNL [16], LRO was observed, and for this reason the welded specimen aged for 11.4 years at 427°C was prepared first for TEM study to determine the precipitation kinetics of the LRO phase.

4.7.1. Results and Discussion

Figure 4.7.1 illustrates the locations (white box) where SEM micrographs were taken to document the presence of TCP phases for 0.5" welded specimens aged at 260 and 343°C for 11.4 years. The microstructure of both sides of the weld can be seen as well as the heat affected zone (HAZ) and adjacent base metal.

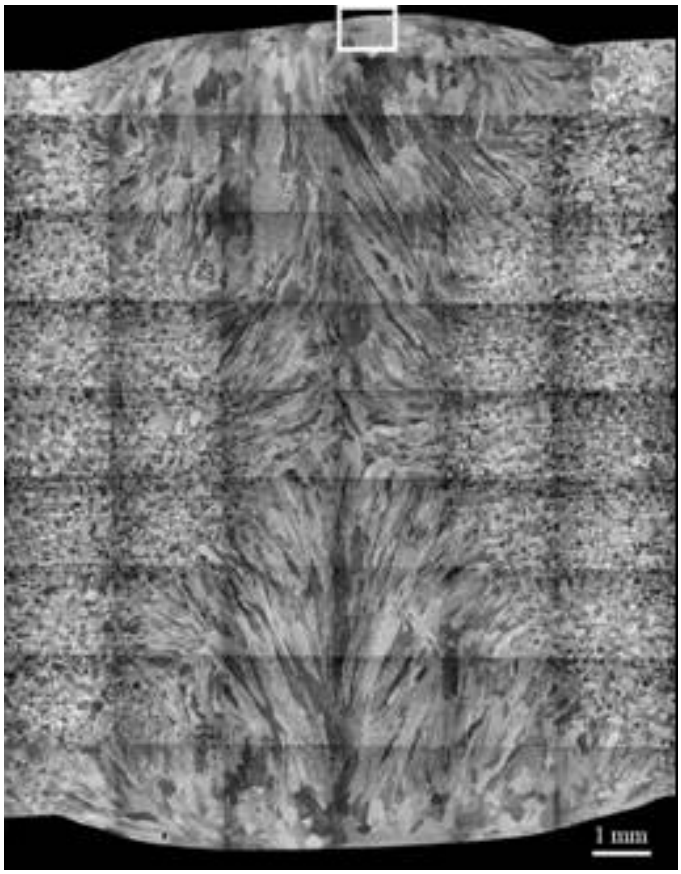

Figure 4.7.1. Overview micrograph collage illustrating the weld region (white box) examined for 0.5" welded specimens aged at 260 and 343°C for 11.4 years [33].

Figure 4.7.2 (a) shows a micrograph of an as-welded, non-aged Alloy 22 specimen indicating the presence of TCP phases (bright white areas) resulting from the welding process. In the same figure, (b) and (c) show micrographs of the 0.5" welded specimens aged at 260 and 343°C, respectively for 11.4 years, also indicating the presence of TCP phases. TEM analyses performed by SNL confirmed that both sigma and P phases were present in the welds aged at 260°C and 343°C; however, volume fraction measurements were not feasible.

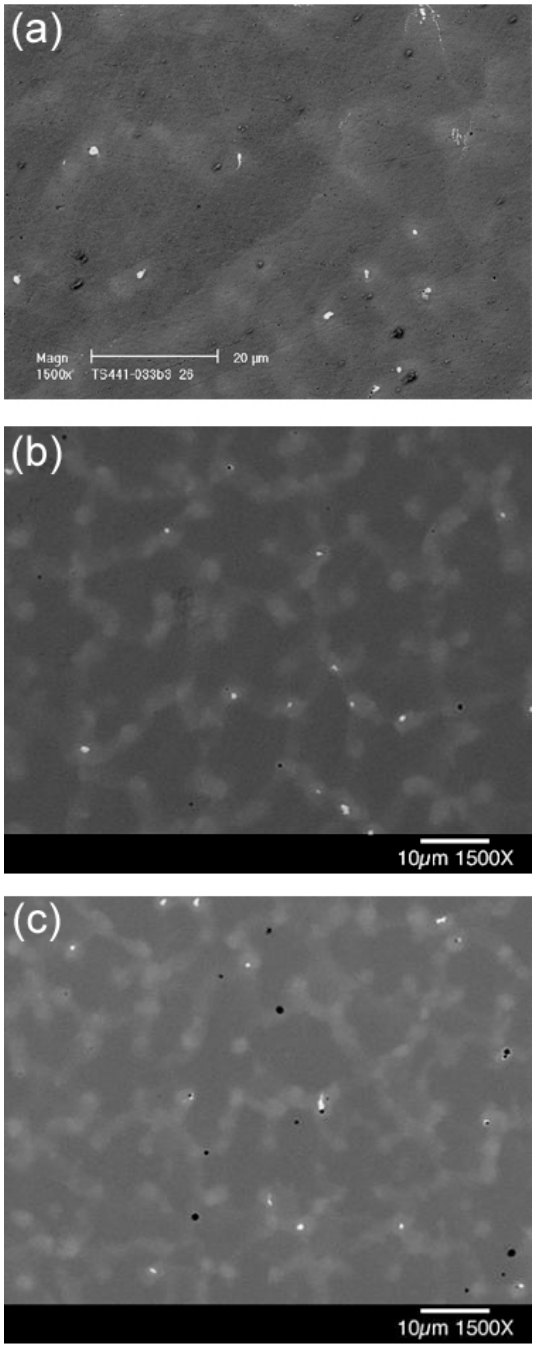

Figure 4.7.2. 1500X backscattered electron micrographs illustrating the TCP phase sizes and morphologies in 0.5" welds for an (a) as-welded specimen, (b) specimen aged at 260°C for 100,028 hours, and (c) specimen aged at 343°C for 100,028 hours [33].

There is virtually no observable difference in the TCP phase size and morphology between the 11.4 year aged specimens (b and c) and the TCP phases created during the initial welding process in the as-welded specimen (a). P and sigma were the only TCP phases observed in the welds after aging at 260, 343, and 427°C for 100,028 hours.

The evolution of LRO at the aging temperature of 427°C as a function of time is illustrated in Figure 4.7.3. Previous TEM analyses by LLNL for an Alloy 22 welded specimen aged at 427°C for 40,000 hours had shown the formation of LRO with a very fine particle size that was uniformly distributed (a). In comparison, the welded specimen aged at 427°C for 100,028 hours shows a significant increase in the LRO phase size, as observed in Figure 4.7.3 (b). It is important to note that the precipitates in this welded aged specimen were not uniformly distributed, with some regions growing coarser precipitates (Figure 4.7.3 (b)) and other regions growing denser areas of smaller precipitates (Figure 4.7.3 (c)). This is just one example of the difficulty involved in trying to develop a method to accurately determine values for the volume fraction of LRO in aged weld specimens. The LRO phase sizes analyzed by SNL were coarser than those observed by LLNL for an Alloy 22 welded specimen aged at 427°C for 40,000 hours.

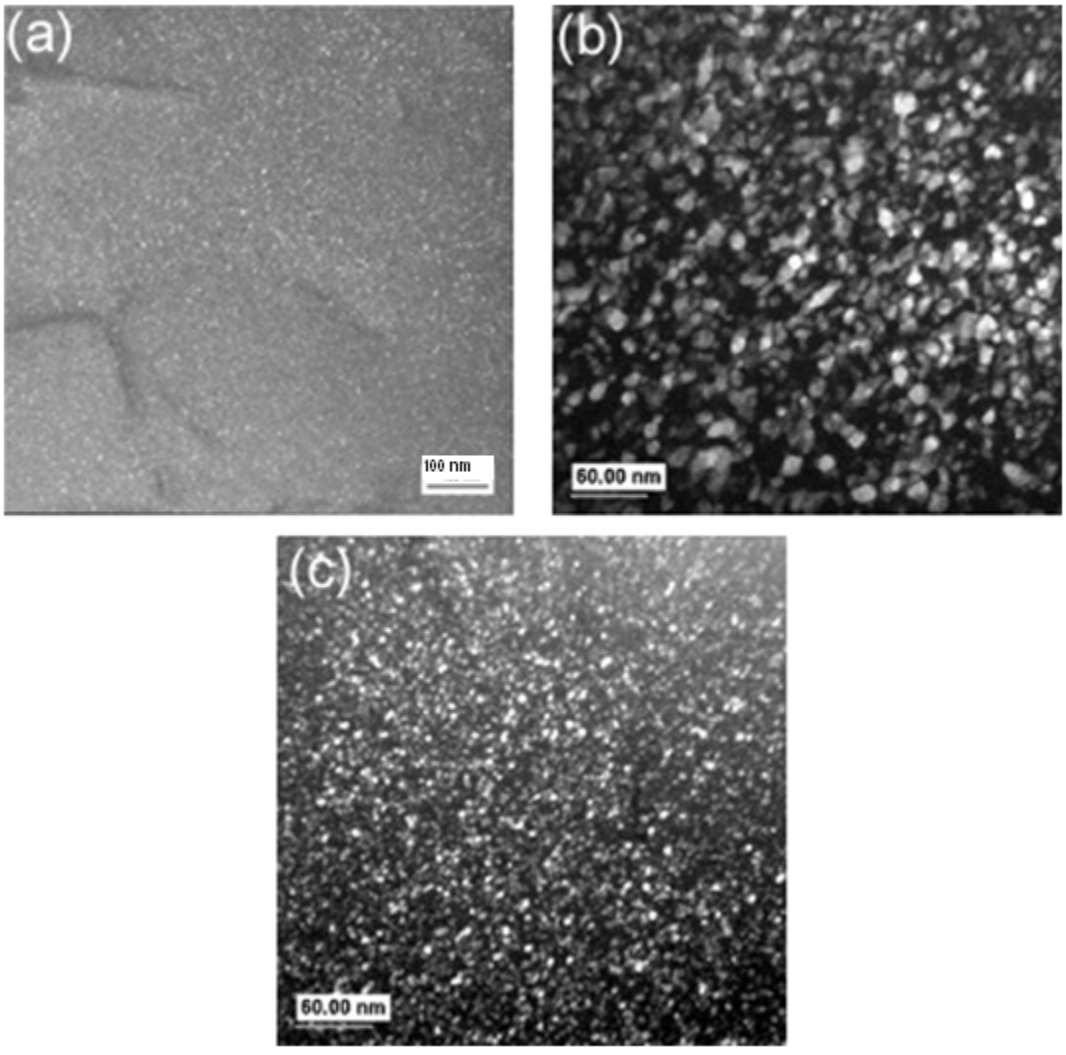

Figure 4.7.3. Transmission electron micrographs illustrating the differences in LRO phase sizes and morphologies in 0.5" Alloy 22 aged specimens for (a) welded specimen aged for 40,000 hours at 427°C, (b) welded specimen aged for 100,028 hours at 427°C, (c) another area for the same welded specimen aged for 100,028 hours at 427°C [22,33].

4.7.2. Summary

Comparison of a non-aged, as-welded specimen to specimens aged at 260°C and 343°C for 100,028 hours showed no differences in the TCP phase morphology and size. However, for the specimen aged at 427°C for 100,028 hours, the net amount of long range ordering appeared to increase, along with a substantial increase in the typical size of the LRO precipitate observed. TEM analyses of both base metal and weld metal aged at 260 and 343°C showed no LRO. TEM analyses performed at SNL of the welded specimen aged at 427°C for 11.4 years did qualitatively show the presence of LRO. P and sigma were the only TCP phases observed in the welds after aging at 260, 343, and 427°C for 100,028 hours. No volume fraction measurements were made.

5. Effect of Stress Mitigation Processes on Secondary Phase Precipitation

Stress Corrosion Cracking (SCC) is a potential degradation mode that can result in penetration of the waste package outer barrier (Alloy 22). SCC of materials may occur when an appropriate combination of material susceptibility, tensile stress, and environment is present. The phase stability of Alloy 22 (N06022) is important because the precipitation of tetrahedrally close-packed (TCP) phases over time has been known to adversely affect corrosion and mechanical properties. Prior observations have shown that these phases precipitate during the welding process. After welding, residual stresses due to solidification and cooling remain. When the weld cannot be stress-relieved by solution annealing, the application of commercially available stress-mitigation processes such as low plasticity burnishing (LPB) and laser shock peening (LSP) may be used to produce near-surface compressive stresses. Mitigation processes which result in compressive stresses on the surface delay the onset of SCC. These post-weld processes are designed to mitigate tensile residual stresses and generate compressive stresses at the surface down to a significant depth. Laser peening and low plasticity burnishing have been proposed to mitigate stresses in the closure weld region of the Alloy 22 waste package outer barrier.

These studies involved examination of cross-sectional samples of aged 1.25” welds of Alloy 22 plates using electron backscatter diffraction (EBSD) for TCP identification, and micrograph analysis for TCP quantification. Precipitation in the LSP treated weld was observed primarily in inter-dendritic regions, similar to that in the as-welded material. Precipitation in the LPB treated weld was observed in both inter-dendritic and intra-dendritic regions.

5.1. Low Plasticity Burnishing

Low plasticity burnishing (LPB) is a method of Computer-Numerically Controlled (CNC) burnishing that originated as a means of producing a layer of compressive residual stress of high magnitude and depth with minimal cold work [35-37]. The process is characterized by a single pass of a smooth free rolling spherical ball under a normal force and can be held in any CNC machine or robotic positioning apparatus. The force is sufficient to deform the surface of the material in tension, creating a compressive layer of residual stress. A schematic diagram of the burnishing set-up is shown in Figure 5.1.1 [38]. The ball is supported in a fluid bearing with sufficient pressure to lift the ball off of the surface of the retaining spherical socket. The ball is in mechanical contact only with the surface to be burnished and free to roll on the surface of the work piece. The tool path and normal pressure applied are designed to create a chosen distribution of compressive residual stress [35].

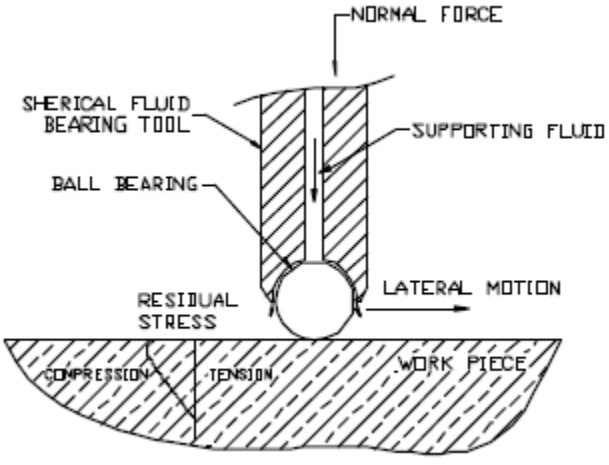

Figure 5.1.1. Low Plasticity Burnishing (LPB) schematic [38].

5.2. Laser Shock Peening

Laser shock peening (LSP) produces only shallow cold work in treated parts, and there is evidence that the stress induced by laser shock peening has a very low thermal relaxation rate and remains effective at high temperature operating conditions.

During LSP, a system fires a laser pulse that is focused at the surface of a metal coated with dark paint and a thin overlay of transparent material, like water. Figure 5.2.1 is a schematic of laser shock peening. The laser light passes through the water and is absorbed by the dark paint. The interaction creates a pressure shock wave that in turn creates a deep compressive stress layer directly underneath the focused pulse [39]. (The water layer acts like a lid on a pot to help contain the shock.)

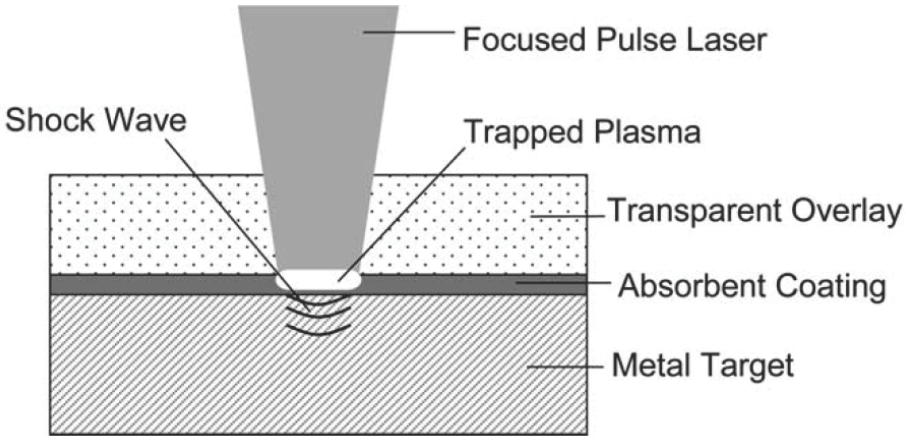

Figure 5.2.1. Laser Shock Peening (LSP) schematic (drawn by B. El-Dasher).

5.3. Methods

The effect of stress mitigation on TCP phases was investigated by LLNL on eight specimens that were prepared for SEM analyses. One specimen from each plate was characterized in the as-welded condition to use as a comparison for the specimens that would be aged. The specimens aged at 700°C were aimed at determining the precipitation rate of TCP phases. The specimens aged at 550°C were aimed at precipitating the ordered phase (since LRO occurs below 600°C).

Two of the specimens were as-welded (no stress mitigation), three were burnished, and three were laser peened. One specimen from each set was aged at 700°C for 50 hours, and another set of three specimens were aged at 700°C for 500 hours. These eight specimens were studied for TCP phase content and type.

Characterization of the effect of stress mitigation on LRO was performed by Sandia National Laboratories (SNL), Livermore, CA for three weld specimens aged at 550°C for 1000 hours and one as-fabricated (non-aged/treated) weld. Of the aged specimens, one was as-welded (untreated), the second a burnished weld, and the third a laser shock peened weld. These specimens were prepared for and studied using a Transmission Electron Microscope (TEM) as described in section 1.3.5.

5.3.1. TCP Phase Quantification

Backscatter electron imaging was used to identify the presence of TCP phases in six of the specimens aged at 700°C and one each of the as-welded specimens from the burnished and peened plates. The method used is outlined in Section 1.3.1. For each specimen, approximately 40 micrographs were captured at 1500X.

5.3.2. TCP Phase Identification

The method described in Section 1.3.2 was also employed to identify the TCP phases. Due to the small size of the TCP phases present in the fusion zone of the weld, automated EBSD scans could not be performed. A manual method of acquiring the phase identifications was developed where multiple areas of a specimen were randomly imaged at a high magnification (12,000X) and diffraction patterns would be collected from all the phases present in the field of view of any given image. The phases that yielded poor or no diffraction would be considered “unidentified”.

This manual process was carried out on the six aged specimens, with up to 30 diffraction patterns collected and identified (indexed) per specimen. Once all the TCP phase information was collected, a relative volume fraction consisting of four components (σ, μ, P, and unidentified) was calculated based on the relative area fractions of the identified and unidentified TCP phases imaged.

5.3.3. LRO Phase Characterization

The determination of the ordered phase content in the specimens aged at 550°C was conducted using TEM analyses by SNL. Multiple regions of each of the three specimens were imaged in dark-field mode to elucidate the presence of the ordered phase regions, with 6 variants imaged for each area in order to allow for statistical accuracy in determining the amount of LRO present. For comparison, a specimen in the as-welded condition was also prepared and imaged.

5.4. Results and Discussion

5.4.1. Phase Stability

It was observed that the microstructure of the specimens aged at 700°C for 50 hours were very similar to the as-welded (non-aged) specimens. This is reflected in the volume fractions shown in Table 5.4.1.1 [33]. However, after aging at 700°C for 500 hours, the TCP phase volume fraction grew substantially.

Table 5.4.1.1. Effect of Stress Mitigation and Aging at 700°C on TCP Phase Volume Fraction

Aging Times	As-received		50 Hours at 700°C			500 Hours at 700°C		
Mitigation Condition	Burnished	Peened	Untreated	Burnished	Peened	Untreated	Burnished	Peened
Volume Fraction (%)	0.09	0.11	0.08	0.14	0.13	1.89	6.53	1.89
Standard Deviation	0.06	0.06	0.07	0.08	0.09	1.25	2.69	0.97

Figure 5.4.1.1 shows a comparison of the untreated, burnished, and peened specimens. All three specimens contained small particles of precipitates that decorate the interdendritic region between the secondary dendrites.

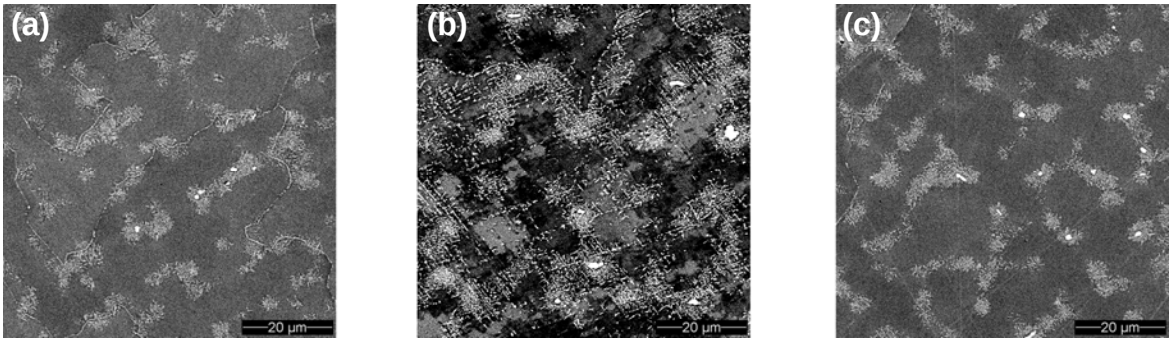

Figure 5.4.1.1. Cross-sectional backscattered electron micrographs of (a) untreated, (b) low plasticity burnished, and (c) laser shock peened Alloy 22 welds aged at 700°C for 500 hours [33].

The burnished specimen shows additional TCP phase formation around the dendrite boundaries and on straight lines within the dendrites, perhaps on crystallographic slip plane traces. These features can be clearly seen in Figure 5.4.1.2. It should be noted that these features were more prevalent in the top 1 mm of the weld where deformation from the burnishing process was greatest.

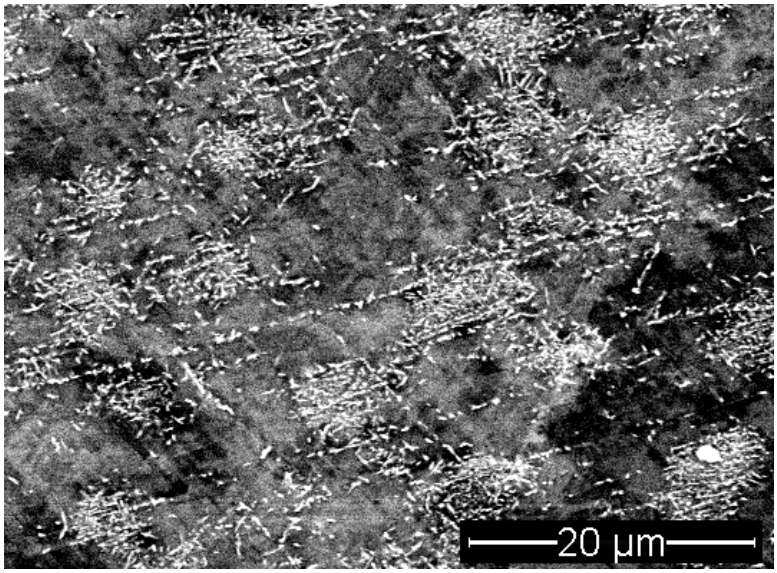

Figure 5.4.1.2. High magnification image of the low plasticity burnished Alloy 22 weld aged for 500 hours at 700°C. The micrograph was obtained within 1 mm of the top of the weld [33].

Results of the relative volume fractions for all six specimens are shown in Table 5.4.1.2 [33]. Of the TCP phases identified, the dominant phase is P, and the specimens aged at 700°C for 500 hours have a higher degree of unidentifiable TCP phases.

Table 5.4.1.2. Effect of Stress Mitigation and Aging at 700°C on observed TCP phase types

Stress Mitigation Treatment	Aging Time @ 700°C (hours)	TCP Phase Volume Fraction (%)			
		P	μ	σ	Unidentified
None	50	49.3	22.8	0.0	27.9
None	500	37.7	27.0	0.0	35.3
Burnished	50	51.5	17.1	0.0	31.3
Burnished	500	47.8	1.7	0.0	50.5
Peened	50	59.5	9.9	0.0	30.6
Peened	500	51.4	8.5	0.0	40.0

Characterization of the TCP phase types present showed that the majority of those identifiable are P phase, with the remainder being μ phase. The fact that no sigma phases were observed does not fully preclude them from existing at these temperatures, but indicates that if they are present, they are not sufficiently stable to coarsen to an extent that would render them identifiable. The observation that P phase appears to be stable supports the predictions of the Aging and Phase Stability (APS) Model at this temperature [22].

5.4.2. Long Range Ordering Characterization

Characterization of the as-welded specimen showed no signs of LRO. This is clearly seen in Figure 5.4.2.1 where the presence of dislocations can be seen, and the selected area electron diffraction (SAED) pattern shows the absence of any superlattice reflections (indicating no ordered phase).

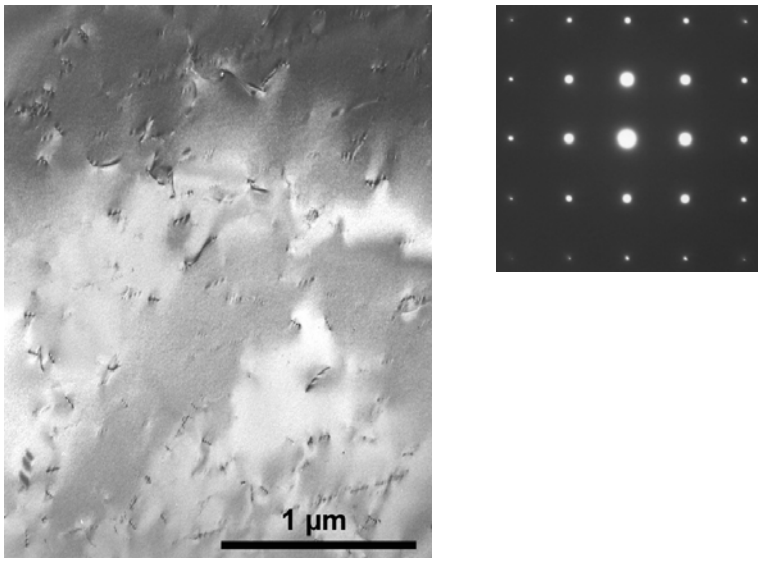

Figure 5.4.2.1. As-welded specimen (untreated). Bright-field image of matrix (~1.3 mm from the top of the weld) showing dislocations (left) and [001] SAED pattern showing no superlattice reflections indicating no LRO precipitates (right) [33].

In contrast, the as-welded specimen aged at 550°C for 1000 hours contains both dislocations and the ordered phase (Figure 5.4.2.2). The ordered phase precipitates were verified by the presence of the superlattice reflection pattern in the SAED and is also shown in the dark field image. The superlattice reflections are uniform in intensity indicating that there are random orientations. *Note: The TEM specimens were taken 1.45 mm from the top of the weld.*

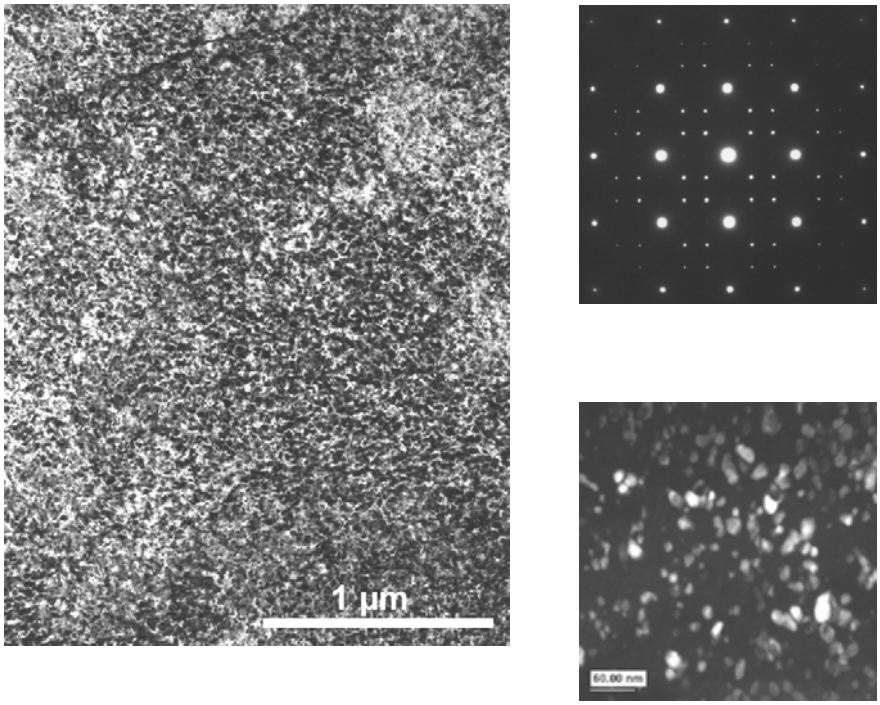

Figure 5.4.2.2. As-welded specimen aged at 550°C for 1000 hours. Bright field image of matrix shows the fine complex features of precipitates/dislocations (left). [001] SAED pattern with LRO superlattice reflections (upper right). Dark field image of LRO phase, one variant, the LRO ~10 - 30 nm (lower right) [33].

In Figure 5.4.2.3 the images acquired from the laser peened specimen aged at 550°C for 1,000 hours are shown. The SAED pattern shows two “brighter” diagonal spots in the superlattice reflections, indicating possible preferred orientation compared to the SAED pattern in Figure 5.4.2.2 for the as-welded aged specimen. Similar diagonal bright spots can be seen in the SAED of the burnished specimen aged at 550°C for 1,000 hours in Figure 5.4.2.4. This specimen also contains a non-uniform fine microstructure as well as a large number of twins (most likely deformation twins).

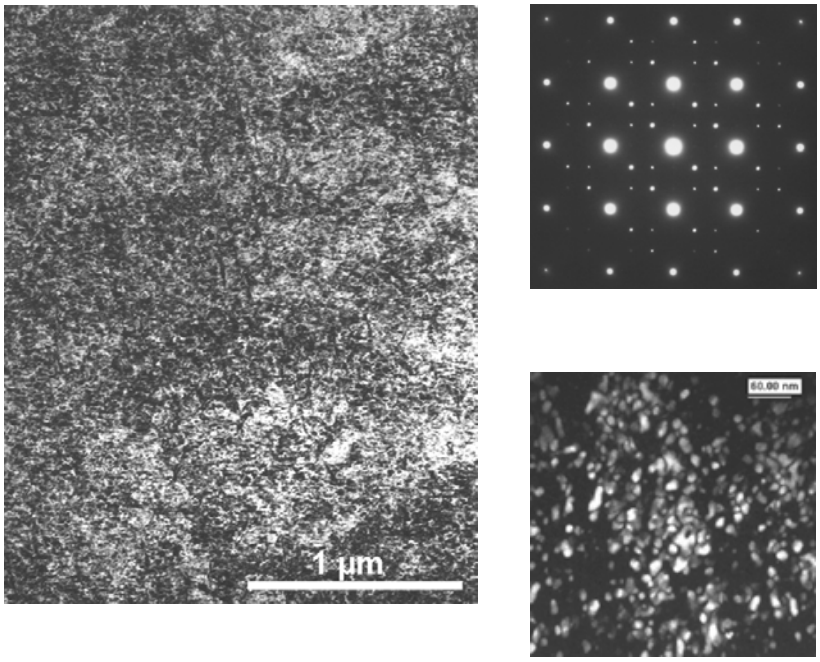

Figure 5.4.2.3. Laser peened specimen aged at 550°C for 1000 hours. Bright field image (left), [001] SAED pattern showing LRO superlattice reflections (upper right). Dark field image of LRO phase, one variant (lower right) [33].

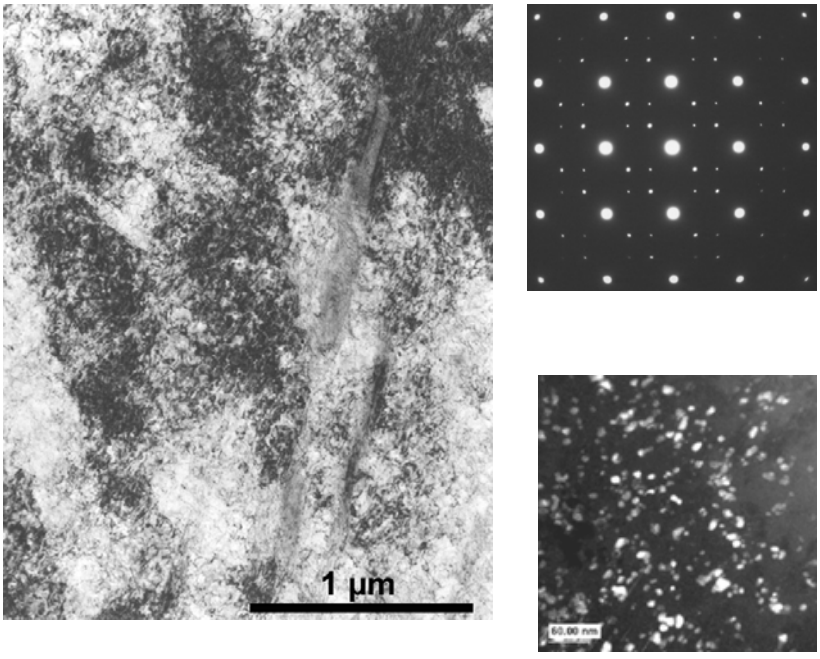

Figure 5.4.2.4. Burnished specimen aged at 550°C for 1000 hours. Bright field image (left). [001] SAED pattern showing LRO superlattice reflections (upper right). Dark field image of LRO phase, one variant (lower right) [33].

5.5. Summary

Alloy 22 weld specimens subjected to the stress mitigation techniques of low plasticity burnishing and laser shock peening were studied by LLNL for TCP phase stability by aging at 700°C for 50 and 500 hours. In comparison to non-aged specimens, aging for 50 hours provided little change in the observable TCP phase content, with total volume fraction values near 0.1%. Aging for 500 hours increased the amount of TCP phases, which primarily precipitated between the secondary dendrites of the weld fusion zone. A noticeable difference was observed for the burnished specimen aged at 700°C for 500 hours; increased precipitation resulted in a total volume fraction approximately three times that of the untreated or laser peened specimens aged for the same duration.

Alloy 22 weld specimens subjected to the same stress mitigation techniques were characterized by SNL for the presence of LRO by aging them at 550°C for 1000 hours. Characterization of the as-fabricated welded specimen showed no signs of LRO. All the aged specimens contained a fine microstructure which consisted of a mix of dislocations and the ordered phase. The burnished specimen also contained a high density of twins.

Due to the difficult nature of quantification of objects in TEM micrographs, values for the volume fraction of LRO in the aged specimens were not measured. However, based on the TEM micrographs obtained from each of the aged specimens, it is apparent that they all contain a high fraction of the ordered phase. It was observed that the precipitation rate of the LPB treated weld is significantly higher than the LSP treated weld.

6. Mock-up Waste Package Studies

A total of 43 machined cylindrical specimens (~ 51 mm x 25 - 51 mm) and the solution annealed quarter-length, full-diameter prototype waste package were received in April 2004 from the American Tank and Fabricating Company. The specimens listed in Table 6.0.1 were received from the various areas of the waste package with no post solution anneal oxide film. Visual examination of the waste package indicated that the film had been removed.

Table 6.0.1. Description of Hockey Pucks Received from American Tank and Fabricating Company

Location on Prototype	No. of Specimens
Bottom Lid	15
Top Lid	15
Longitudinal Weld	7
Trunnion	4
Vent Hole	2

Of the specimens cut from the quarter-length, full-diameter prototype waste package, only the base metal beneath the trunnion (the region to cool the slowest following solution annealing) was examined metallographically.

6.1. Methods

Two “hockey puck” specimens were examined. One specimen was obtained from the longitudinal seam weld as close to the trunnion as possible, and the second from the longitudinal seam weld underneath the trunnion. The sections examined are illustrated schematically in Figure 6.1.1. (section A represents the longitudinal seam weld specimen, and section B represents the trunnion weld specimen).

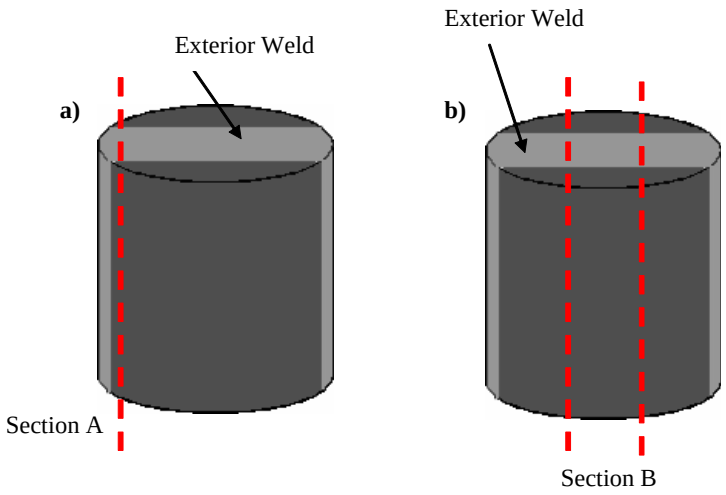

Figure 6.1.1. Schematic illustrating hockey puck sections observed for a) the hockey puck obtained from the longitudinal seam weld region near the trunnion and b) the hockey puck obtained from the longitudinal seam weld beneath the trunnion [33].

6.1.2. TCP Phase Quantification

Backscatter electron imaging was used as described in Section 1.3.1 to document the presence of TCP phases in both specimens. To obtain an estimate of total volume fraction of TCP phases in each specimen, the top of the weld regions across the entire width (~ 30 mm for the trunnion weld and 21 mm for the seam weld by a 4 mm depth) of both specimens were imaged and analyzed. A total of 223 images were captured, 144 images for the longitudinal seam weld and 79 images for the trunnion weld.

6.1.3. Phase Identification

Because the three possible TCP phases are crystallographically different (tetragonal for σ, rhombohedral for μ, and orthorhombic for P), EBSD patterns from each of the phases are unique to that phase. The technique described in Section 1.3.2 was utilized in an automated scan across the area near the top of the weld on the trunnion specimen, where regions of secondary phases were observed that were not seen in the longitudinal seam weld specimen. Further characterization was limited to only the trunnion specimen because no similar regions of secondary phases were observed. Automated scanning was possible in this region because the particle sizes were large (~2 – 5 μm).

6.1.4. TCP Phase Chemical Composition

Wavelength Dispersive Spectroscopy (WDS), described in Section 1.3.3, was used to determine the compositional chemical variations of the TCP phases and adjacent matrix regions observed near the top of the trunnion longitudinal seam weld specimen.

6.2. Results and Discussion

6.2.1. TCP Phase Stability

Using the preliminary automated method of analysis, it was observed that although both the trunnion and seam welds have an extremely small volume fraction of precipitates (see Table 6.2.1.1), the trunnion weld had about twice the amount of secondary phase content than the longitudinal seam weld (both were less than 0.1%). Both specimens contained weld porosity (which was not measured) formed by gas entrapment during solidification from the welding process.

.

Table 6.2.1.1. TCP Volume Fraction for the Seam and Trunnion Welds [33]

Specimen Description	TCP Vol. Fraction (%)
Trunnion Weld	< 0.05
Seam Weld	< 0.05

Comparison to the data presented in Section 4.3.3 for the specimen solution annealed at 1121°C for 20 minutes shows that the dissolution of TCP phases in the weld region of the mockup package was more extensive, with almost two orders of magnitude less TCP phase volume fraction.

Although the overall TCP volume fraction was less than 0.05% in both specimens, for the trunnion weld, the majority of the precipitate volume fraction was observed at the exterior of the weld surface as shown in Figure 6.2.1.1. The region shown in Figure 6.2.1.1 is of interest as it is

representative of the surface that could be most susceptible to corrosion, and therefore the identification of the type of phase(s) present in this region is important.

While the reason for the presence of this localized secondary phase is not definitively known, it is likely in part due to the presence of the trunnion, which prevented the surfaces beneath to cool at the same rate as the "exposed" waste container surfaces during solution annealing. Another reason for the location of these phases is the presence of a free surface, which can make phase transformations occur easier as lattice mismatches between the phases and the matrix do not yield the same amount of stress.

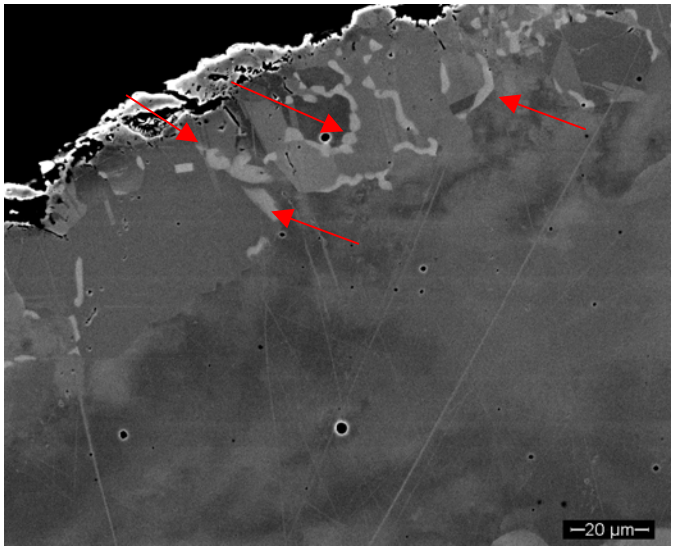

Figure 6.2.1.1. Micrograph of the top cross-sectional area of the trunnion longitudinal seam weld specimen, illustrating the presence of a secondary phase at the weld surface (indicated by red arrows) [33].

6.2.2. TCP Phase Identification

The region near the surface of the trunnion weld (shown in Figure 6.2.1.1) was scanned using EBSD to identify the phase(s). The results showed that virtually all of the secondary phases observed are σ phase. While it is known that σ can be stable at high temperatures [7], none was observed in the solution annealing study for specimens annealed for durations < 24 hours. Therefore another driving force for this transformation must exist. A possible driving force may be excessive Cr or Mo segregation, perhaps due to slow cooling of the weld pool during fabrication or solution annealing (because σ is more stable at higher Cr and Mo content).

6.2.3. TCP Phase Chemical Composition

Figure 6.2.3.1 shows a micrograph indicating the areas of the hockey puck trunnion longitudinal seam weld specimen where WDS was used to determine the variation in chemical composition. Locations 1 - 3 are measurements made directly on the TCP phase determined by EBSD to be σ, and locations 4 - 6 are measurements directly adjacent to the TCP phases. Locations 7-9 are within "lighter" areas (indicating compositional differences compared to the matrix), and locations 10 - 12 are of the matrix far away from any observed secondary phases.

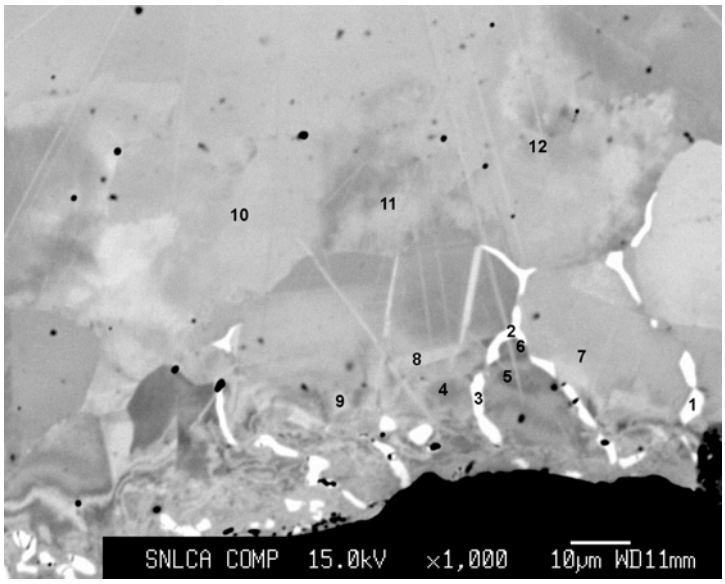

Figure 6.2.3.1. Micrograph showing numbered regions of the trunnion longitudinal seam weld specimen analyzed for chemical segregation using WDS [33].

The elemental weight percent values measured at each of the numbered points are listed in Table 6.2.3.1. The results obtained from the σ phases (locations 1 - 3) show a very high Cr and Mo content, while the regions adjacent to the phases possess Cr and Mo weight percent approximately 2% lower than that measured in the matrix. The excess Cr and Mo in the phases combined with the Cr and Mo depleted zone surrounding the phases indicate that a large amount of segregation is the reason for the formation of the σ phases observed.

Considering the elemental weight percent values published by Cieslak et al. [7] for the three TCP phases (σ, μ, and P) seen in the weld fusion zone (Table 6.2.3.2), it is clear that σ contains the most Cr, indicating that it is the most stable of the three with high Cr content. This is also verified in examination of the phase diagrams [7]. The higher Cr content not only played a part in the formation of the σ phase, but it also may have prevented it from transforming into μ or P during cooling.

Table 6.2.3.1. WDS Results in weight percent (wt.%) for Chromium, Molybdenum, Nickel, and Tungsten as Measured in the Hockey Puck Trunnion Longitudinal Seam Weld Specimen [33]

Location	Elemental Weight Percent (%)				
	Cr	Mo	Ni	W	Total
1	29.2	29.7	33.3	4.7	96.9
2	27.9	28.4	34.5	4.5	95.3
3	28.2	29.0	34.5	4.6	96.3
4	20.9	13.4	60.4	2.8	97.6
5	20.2	12.6	62.0	2.8	97.5
6	20.0	12.1	62.9	2.4	97.4
7	21.3	13.5	60.7	2.7	98.2
8	21.4	14.0	60.0	3.0	98.4
9	20.9	13.9	60.6	3.0	98.5
10	21.6	14.4	60.3	3.3	99.6
11	21.8	14.1	60.3	2.9	99.1
12	21.4	14.1	59.8	2.9	98.2

Note: The weight percentages shown in Table 6.2.3.1 do not total 100% because they were not normalized.

Table 6.2.3.2. Chemical Composition (wt. %) of TCP Phases (Cieslak et al. [7])

Phase	Cr	Mo	Ni	W
σ	23	35	34	4.2
P	21	37	33	5.0
μ	20	39	33	6.3

Figure 6.2.3.2 shows a graphical representation of a WDS trace collected across the region containing the σ phase. The trace indicates that as chromium, molybdenum, and tungsten increase, there is a depletion of nickel in the matrix at the dendrite boundaries due to the formation of σ.

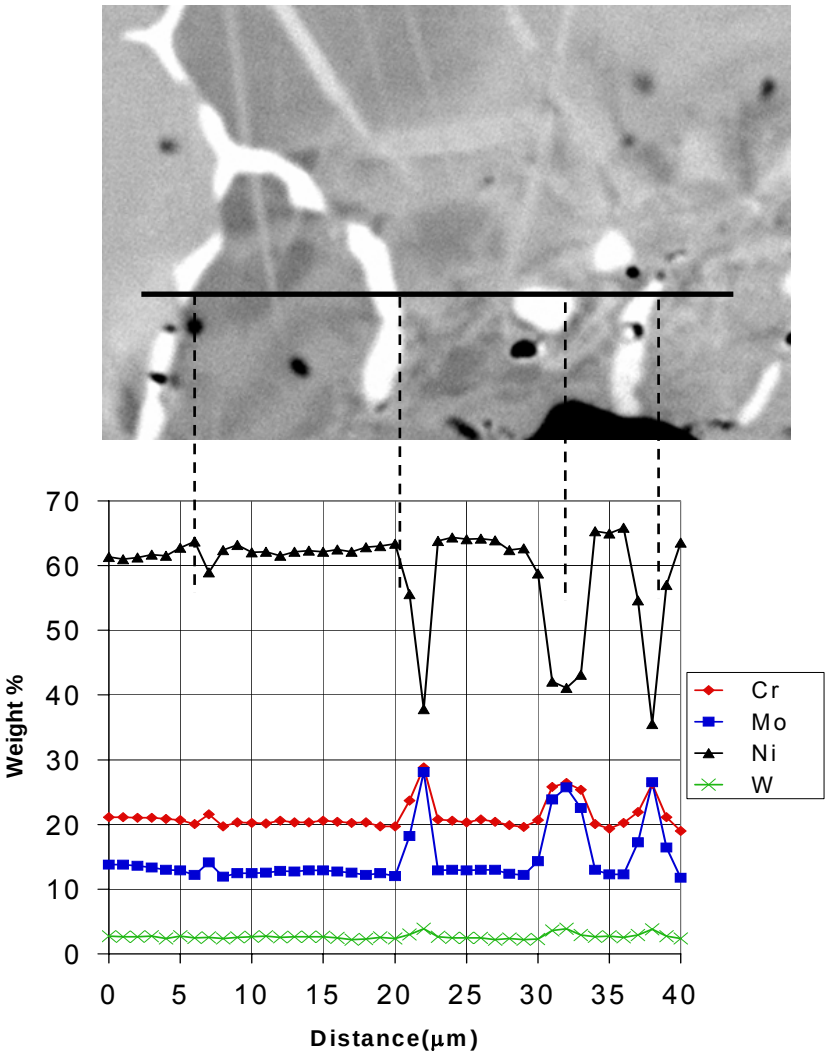

Figure 6.2.3.2. WDS traces with corresponding micrograph showing compositional variations across and adjacent to TCP phases in the hockey puck trunnion longitudinal seam weld specimen [33].

6.3. Summary

Solution annealing of the mock-up waste container appears to decrease the total concentrations of TCP phases in the fusion zone of the weld. The weld region beneath the trunnion showed an increase in the amount of secondary phases at the top of the weld, in contrast with the longitudinal seam weld region not covered by the trunnion.

This secondary phase was determined to be σ which was rich in Cr. The source of this phase is increased segregation of Cr to the interdendritic region either during the welding of the seam or as a result of the heat input from welding the trunnion to the container. The high Cr content may have allowed the σ phase to remain stable during the cooling of the container after quenching.

7. Other Alloys Aged by Haynes International and LLNL

In February 2003, sixty two samples (base metal and welded plates) consisting of five various alloys were purchased from Haynes International (Kokomo, Indiana) because they were shutting down their aging facilities after 11 years. These samples were purchased for potential future phase stability/corrosion studies. These samples are invaluable since they can be used to study the phase stability of five different alloys aged for up to 11.4 years. A listing of these alloys and their aging times/temperatures are in Appendix C. Table 7.0.1 shows the nominal compositions of alloys aged by Haynes International and LLNL [40].

The C-4, 22, 276, G-30, and Ultimet alloys are from the Haynes International Hastelloy family of corrosion-resistant alloys. Alloy 59 is a Krupp VDM corrosion-wear resistant Co-Cr-Ni-Mo alloy.

Table 7.0.1. Nominal Chemical Compositions of Alloys (in wt.%) [40]

Alloy	Ni**	Cr	Mo	Fe	W	Mn	C	Co	Si	Other
C-4	65	14 - 18	14 - 17	3.0 *	-	1.0*	0.01*	2.0	0.08*	Ti 0.7*; P0.025*; S 0.010*
C-22	56	22	13	3	3	0.5*	0.010*	2.5 *	0.08*	V 0.35 *
C-276	57	16	16	5	4	1.0*	0.01*	2.5	0.08*	V 0.35*
G-30	43	28 - 31.5	4.0 - 6.0	13 -17	1.5 - 4.0	1.5 *	0.03*	5.0 *	0.8*	Cb + Ta = 0.3 - 1.5; Cu 1.0 - 2.4
Ultimet	9	26	5	3	2	0.8	0.06	54	0.30	N 0.08
59	59	22 -24	15 - 16.5	1.0*	-	0.5	0.01*			Al 0.1 - 0.4

Note: All samples were purchased as "Q" per the YMP procedures with the exception of the Ultimet alloy samples which did not meet all the requirements of the Quality Assurance (QA) Surveillance and are therefore non-Q.

* *Maximum*

** *Balance*

8. Future Recommendations

Future analyses should be designed to support performance confirmation issues which may arise due to manufacturing processes and to ensure that the integrity of the waste package remains unchanged over tens of thousands of years. A comprehensive assessment methodology should be developed that shows how the full-scale waste package manufacturing processes (e.g. rolling, solution annealing, welding, stress mitigation, etc.) affect the corrosion and metallurgical performance of Alloy 22 over extremely long times. Past studies were performed on specimens of base metal and welds from plate manufactured on much smaller scales (under essentially "ideal" conditions).

8.1. Weld Stability Studies

Weld Stability studies of 1.25" welds from thick prototypical plate were introduced into the Aging Facility to be aged by LLNL (rather than the manufacturer) in March 2005, 10,000 hour specimens were removed in May 2006, and all remaining specimens were removed in December 2007 when the Aging Facility was decommissioned. Analyses of specimens aged at 400°C should begin after approximately 20,000 hours, and the time at which specimens are pulled for analyses decreases as the aging temperature increases. These thick welds can provide a more realistic benchmark for determining the effects on phase stability, segregation, and mechanical properties resulting from manufacturing processes such as rolling, additional heat input and number of weld passes, until specimens from full-scale prototypes can be analyzed.

Although the Haynes 100,028 hour (11.4 years) aged welds are available and have been studied as previously mentioned, these data will be limited since there is not sufficient material to acquire corrosion/mechanical property data, samples are only 0.5" thick (not prototypical), and specimens were aged at lower temperatures (260, 343, and 427ºC) where the kinetics are very slow.

Future analyses should include measurement of precipitate volume fraction, microprobe traces for quantifying segregation in the welds, tensile tests (strength), and Charpy impact toughness tests in the as-welded, as-annealed weld, and aged specimens. These measurements should be expanded to include analyses of dendrite kinetics and dendrite orientation and growth. A coordinated effort between variability in weld microstructure/morphology and the effect it has on corrosion performance should also be implemented. Specimens that have been cold-worked (deformed) by rolling, bending, or forming should also be evaluated to determine the effect of cold work on the diffusion rates of phase precipitation. However, evaluation of specimens from full-scale waste package prototypes should be evaluated and will provide more representative data.

It is suggested that one of each 1.25" as-welded specimen, aged at 550 and 650°C for ~ 24,000 hours, be evaluated for TCP phases and LRO. The effects of aging temperature and welding processes on the chemical segregation in the HAZ (ie. grain morphology, void analyses) should also be evaluated concurrently, in addition to the grain size as a function of temperature and aging time. Grain size can affect the mechanical properties of a material. Further evaluation of other 1.25" welds/HAZ aged at similar times and lower temperatures can be selected and continued aging studies resumed (as needed), or analyses performed based on the data acquired from the 550 and 650°C specimens. Aged tensile specimen blanks can then be selected and mechanical properties measured to determine if the material still meets required specifications.

8.2. Full-scale Waste Package Analyses

Metallurgical specimens sampled from different areas of a full-scale waste package prototype that have been fabricated following the present-day waste package manufacturing strategy should be measured for the presence of TCP phases and LRO. Continued assessment needs to be performed on specimens from full-scale waste package prototypes to provide information and insight on how the prototypes could best be manufactured with respect to heat-to-heat variability, heat treatments, and welding. To date, metallurgical characterization was done only on longitudinal welds for two hockey puck samples from a ¼ scale length full diameter waste package (at LLNL).

It is suggested that specimens/material of rolled plate prior to forming, after forming, after welding, and after solution annealing of full-size Alloy 22 waste packages be obtained from the manufacturer(s). Characterization of the effects of the entire fabrication sequence on the microstructure and corrosion resistance is necessary to assess performance of the waste package specifically: (1) the extent of chemical segregation (Mo, Cr, P, and S) in the base metal, weld metal and heat affected zone from various locations of a full-scale waste package prototype and (2) the manufacturing processes (thermo-mechanical processing, and heat treatment) on grain size and mechanical properties.

8.3. Heat-to-heat Variability Studies

As discussed in Section 4.1. the specimens of Alloy 22 with compositions shown in Table 8.3.1 (HC76 and 87) should be annealed, aged and tested to determine if the σ-phase does form at temperatures as low as 700°C and as high as 1100°C [30]. Although the microstructure of composition 8 was predicted to weaken with such high concentrations of Cr and Mo, corrosion performance should be improved with higher Mo content. The experimental data would clarify both hypotheses, and also whether the critical annealing temperature of Alloy 22 would need to be re-evaluated. For composition 2, the corrosion properties need to be verified due to lower concentrations of Cr and Mo.

Since heats HC76 and HC87 have already been manufactured and are the closest chemical compositions to composition 2 and 8, respectively, it is suggested that these alloys be annealed, aged and evaluated for TCP phases, corrosion and mechanical properties.

Table 8.3.1. Chemical Compositions Proposed by Hu et al. [30] Compared to Similar ALC Heats for Alloy 22

Element (wt. %)	Composition 2	HC 76	Composition 8	HC 87
Cr	20.0	20.31	22.5	22.39
Mo	12.5	12.71	14.5	14.23
Fe	2.0	2.51	6.0	5.78
W	2.5	2.64	3.5	3.36
Co	2.0	-	2.5	-
C	0.01	0.003	0.015	0.007
Si	0.08	-	0.08	-
Mn	0.05	-	0.5	-
V	0.30	<.01	0.035	0.01
P	-	0.003	0.02	0.006
S	-	<.0003	0.02	<.0003
Ni	60.11	61.60	50.02	53.90

8.4. Model Validation/Input to Modeling

The objective of the Aging/Phase Stability (APS) model is to provide a quantitative model which can be used to predict the amount of any phases forming as a function of both time and temperature. The APS model will continue to be used to provide predictive insight into the long-term metallurgical stability of Alloy 22 under relevant repository conditions. However, current modeling can only predict transformations in bulk base metal (based on a simplified ternary composition) and not welds. Therefore, kinetics of precipitation on grain boundaries and in welds are measured experimentally and compared to the theoretical predictions in bulk base metal. Given the short-term nature of these data, conclusions will remain uncertain until theoretical calculations that take into consideration the numerous phases involved, their compositions, and segregation in the weld are performed and experimentally validated.

Enhanced confidence in model predictions can be achieved through the extension of modeling to multicomponent systems, precipitation on grain boundaries, and aging behavior of welds. The current model does not separate out the different phases that form in Alloy 22 due to lack of experimental data on the separate growth kinetics. Kinetics of growth of one particular phase could be faster than that modeled using the overall kinetics of all the phases forming. Periodic measurements should be made to confirm/validate the model if a difference is seen in the kinetics of the individual phases. Once the thermodynamic and kinetics modeling has been extended to multicomponent systems, it will be better able to handle modeling of transformations in welds. The model can currently handle modeling of solidification (such as that experienced by welds). Experimental input, temperature profiles and the resulting segregation are needed for further advances.

It is proposed that volume fraction measurements be made on the base metal specimens aged for ~ 51,000 hours at 650 and 600ºC. After these samples have been analyzed for the presence of TCP phases, one of the base metal specimens aged for ~ 67,000 hours at 550ºC should be analyzed for TCP and LRO. Once the volume fraction/presence of LRO has been established, it can be determined whether additional base metal samples (if any) should be analyzed at 500 and 400ºC. If additional data are needed at temperatures below 400ºC, the specimens aged by Haynes up to 100,028 hours for longer times and lower temperatures should be used, due to the sluggish nature of the kinetics. Base metal specimens aged below 600ºC would be analyzed for the presence of long range ordering using microhardness measurements. A method to measure volume fraction of the ordered phase still needs to be developed.

It needs to be demonstrated that the APS Model is still valid by re-running with base metal data acquired from Haynes 100,028 hour samples and any additional data from volume fraction measurements not previously modeled. Volume fraction data of bulk and grain boundary measurements acquired to date for Alloy 22 base metal are reported and discussed in detail in [22]. Analyses of ternary alloys discussed in Section 3.3 that have been aged up to 37,000 hours should be performed (as needed) and the model adjusted as necessary.

Once all values acquired to date have been modeled, additional determinations can be made for analyses of previously aged specimens based on model predictions to complete the Time-Temperature-Transition (TTT) curve. This information would also be valuable in determining the cooling/heating rates required to avoid the formation/growth of deleterious phases that can cause stress corrosion cracking and hydrogen embrittlement. After the experimental conditions that control welding are finalized (composition of the filler, thermal history and temperature gradient), the DICTRA application should be used to address issues on phase formation and evolution under non-isothermal conditions in Alloy 22.

9. Conclusions

Transformation diagrams predicted for Alloy 22, and validated with experimental data, indicate no significant phase instabilities (long-range ordering and tetrahedrally close packed phase precipitation) even if the temperature were held for several thousand years. Even for potential temperatures below 300°C, the diagrams do not indicate significant phase instabilities in the longer times of interest. Plastic deformation due to cold work such as that planned for stress mitigation, however, is known to accelerate phase transformations. While it is not likely that the kinetics will be accelerated to an extent that would degrade waste package performance, this has not been quantified. Also, the current understanding of phase transformations in welds has been obtained experimentally from thin welds and very limited data from thick welds. Enhanced confidence in model predictions may be obtained through extension of the modeling effort to welds and through continued experimental study of thick prototypical welds and the HAZ.

Continued evaluation of fabrication processes is important because fabrication can have an effect on the metallurgical structure of an alloy and on the condition of the surface. Additionally, aged specimens from full-scale prototypes can continue to provide information on the performance of the material (kinetics, phase stability, corrosion etc.) of actual waste packages over time in the repository.

10. Acknowledgements

The author appreciates the efforts and previously published works of Tammy S. Gdowski for technical discussions and encouragement during the various phases of this work. The work of and collaborations with Bassem El-Dasher, Frank Wong, Tien Shen, and Nancy Yang is also appreciated. The author is grateful for the funding and support provided by Jim Blink, Mark Sutton and the Yucca Mountain Project. Part of this work was performed under the auspices of the U.S. Department of Energy by Lawrence Livermore National Laboratory in part under Contract W-7405-Eng-48 and in part under Contract DE-AC52-07NA27344.

11. References

1. "Icosahedral Coordination in Metallic Crystals," Introduction to Quasicrystals, ed. M.V. Jaric (New York, New York: Academic, 1988), 1-7.
2. H.M. Tawancy, R.B. Herchenroeder, and A.I. Asphahani, “High-Performance Ni-Cr-Mo-W Alloys,” Journal of Metals, 35 (1983), 37-43.
3. H.M. Tawancy, “Precipitation Characteristics of μ-phase in Wrought Nickel-base Alloys and its Effect on the Properties,” Journal of Material Science, 31 (1996); 3929-3936
4. “Phase Stability and Mechanical Properties of Alloy 22 Aged in the Temperature Range 590 to 760°C for 16,000 Hours,” in Scientific Basis for Nuclear Waste Management XXII, Materials Research Society Symposium Proceedings Volume 556, ed. D.J. Wronkiewicz and J.H. Lee, (Warrendale, PA: Materials Research Society, 1999), 919-926.
5. R.B. Rebak, T.S.E. Summers, and R.M. Carranza, “Mechanical Properties, Microstructure and Corrosion Performance of Alloy 22 Aged at 260°C to 800°C,” (Paper presented at the 1999 Fall meeting of the Material Research Society, Boston, Massachusetts, 29 November 1999).
6. R.B. Rebak,, N.E. Koon, J.R. Dillman, P. Crook, and T.S.E. Summers, “Influence of Aging on Microstructure, Mechanical Properties, and Corrosion Resistance of a Ni-22Cr-13Mo-3W Alloy.” (Paper presented at the NACE International Corrosion 2000 Conference, Orlando, FL, March 2000).
7. M.J. Cieslak, T.J. Headley, and A.D. Romig, Jr., “The Welding Metallurgy of Hastalloy Alloys C-4, ALLOY 22, and C-276,” Metallurgical Transactions A, 17A (1986), 2035-2047.
8. J.S. Ogborn, D.L. Olson, and M.J. Cieslak, "Influence of Solidification on the Microstructure Evolution of Nickel Base Weld Metal," Material Science and Engineering A, 203 (1995), 134-139.
9. R.B. Rebak and N.E. Koon, “Localized Corrosion Resistance of High Nickel Alloys as Candidate Materials for Nuclear Waste Repository. Effect of Alloy and Weldment Aging at 427°C for up to 40,000 H." (Paper presented at the NACE Corrosion 98 Conference, San Diego, CA, March 1998).
10. U.L. Heubner, E. Altpeter, M.B. Rockel, and E. Wallis, "Electrochemical Behavior and its Relation to Composition and Sensitization of Ni-Cr-Mo Alloys in ASTM G-28 Solution," Corrosion, 45 (1989), 249-259.
11. S.J. Matthews, “Thermal Stability of Solid Solution Strengthened High Performance Alloys,” in Superalloys: Metallurgy and Manufacture, Proceedings of the Third International Symposium, B.H. Kear, D.R. Muzyka, J.K. Tien, and S.T. Wlodek, eds. (Baton Rouge, Louisiana: Claitor’s Publishing Div., 1976), 215-226.
12. T.H. Shen, “Phase Identification of Long Term Aged C-22 Alloy”, LLNL Technical Memorandum (April 4, 1999).
13. T. H. Shen, “TEM Observation of Ordering in Alloy 22”, LLNL Technical Memorandum (September 30, 1999).
14. T. H. Shen “X-ray Microanalysis of Precipitates in Alloy 22”, LLNL Technical Memorandum (March 20, 2000).
15. Tawancy, H.M., “Order-Strengthening in a Nickel-Base Superalloy (Hastelloy Alloy S)”, Metallurgical Transactions A, 11A (1980), 1764–1765.

16. R.B. Leonard, “Thermal Stability of Hastelloy Alloy C-276,” Corrosion**,** 25 (1969), 222-228.
17. F.G. Hodge, “Effect of Aging on the Anodic Behavior of Ni-Cr-Mo Alloys,” Corrosion, 29 (1973), 375-383.
18. Hodge, F.G., and Kirchner, R.W., 1976, An Improved Ni-Cr-Mo Alloy for Corrosion Service. Corrosion **32**: 332–336.
19. M. Raghavan, B.J. Berkowitz, and J.C. Scanlon, “Electron Microscopic Analysis of Heterogeneous Precipitates in Hastelloy C-276,” Metallurgical Transactions A, 13A (1982), 979-984.
20. P. Villars and L.C. Calvert, *Pearson's Handbook of Crystallographic Data for Intermetallic Phases*, Vol.1 (ASM, Metals Park, Ohio, 1985).
21. Summers, T.S.E., Wall, M.A., Kumar, M., Matthews, S.J., and Rebak, R.B., 1998, Phase Stability and Mechanical Properties of C-22 Alloy Aged in the Temperature Range 590 to 760°C for 16,000 Hours. Presented at the MRS Annual Meeting, Symposium QQ, Boston.
22. “Aging and Phase Stability of Waste Package Outer Barrier”, ANL-EBS-MD-000002 REV 01 ICN 0. Las Vegas, Nevada (June 2003).
23. Saunders, N. and Miodownik, A.P. 1998. *CALPHAD, Calculation of Phase Diagrams: A Comprehensive Guide.* New York, New York: Pergamon Press.
24. Spencer, P.J. 1999. "Computer Simulations from Thermodynamic Data: Materials Production and Development." *MRS Bulletin, 24,* (4), 18-19. Warrendale, Pennsylvania: Materials Research Society.
25. BSC (Bechtel SAIC Company) 2003a. “Aging and Phase Stability of Waste Package Outer Barrier”. ANL-EBS-MD-000002 REV 01 ICN 00. Las Vegas, Nevada: Bechtel SAIC Company.
26. Turchi, P.E.A., Kaufman, L. and Liu, Zi-Kui, Modeling of Stability and Aging of Candidate Ni-Cr-Mo Based Alloys for the Yucca Mountain Project, LLNL Report No. UCRL-MI-153055 (April 2003).
27. L. Karmazin, “Lattice Parameter Studies of Structure Change of Ni-Cr Alloys in the Region of Ni_2Cr”, Mater. Sci. and Eng., **54**, 247-256 (1982).
28. Report Nickel-Based Alloy Weld filler Material and Base Metal Composition Test Program, Volume #1, Final Technical Report, May 2004 by Allegheny Technologies, Albany, OR.
29. ASTM B 575-99a, “Standard Specification for Low-Carbon Nickel-Molybdenum-Chromium,Low-Carbon Nickel-Chromium-Molybdenum, Low-Carbon Nickel-Chromium-Molybdenum-Copper, Low-Carbon Nickel-Chromium-Molybdenum-Tantalum, andLow-Carbon Nickel-Chromium-Molybdenum-Tungsten Alloy Plate, Sheet, and Strip.” West Conshohocken, Pennsylvania, American Society for Testing and Materials, 1999.
30. Hu, H., Turchi, P.E.A., Wong, F., “Computational Modeling of Phase Stability in Alloy 22 Over a Range of Chemical Compositions for the Yucca Mountain Project”, LLNL Internal Report, (May 2005).
31. Edgecumbe Summers, T.S., Rebak, R.B., Seeley, R.R., “Influence of Thermal Aging on the Mechanical and Corrosion Properties of C-22 Alloy Welds”, UCRL-JC-137727, June 15, 2000

32. Dunn, D.S., Daruwalla, D., Pan, Y.-M., “Effect of Fabrication Processes on Material Stability – Characterization and Corrosion,” Center for Nuclear Waste Regulatory Analyses Report No. CNWRA 2004-1, October 2003, pgs. 3-19, 3-26.
33. Torres, S.G., El-Dasher, B., Aging and Phase Stability of Alloy 22 Welds FY05 Summary Report, LLNL Report No. UCRL-TR-217339 (January 2006), 51pages.
34. Vander Voort, G.F. 2000. "Volume Fraction." *Metallography, Principles and Practice.* Pages 425-435. Materials Park, Ohio: ASM International.
35. P. Prevéy, N. Jayaraman and J. Cammett "Overview of Low Plasticity Burnishing for Mitigation of Fatigue Damage Mechanisms,"Proceedings of ICSP 9, Paris, Marne la Vallee, France, Sept. 6-9, 2005.
36. Lambda Research, “Effect of Low Plasticity Burnishing (LPB) on the HCF Life of IN718”, Cincinnati, OH, Diffraction Notes, No. 26, Spring 2000
37. Prevey, Paul S., “Burnishing Method and Apparatus for Providing a Layer of Compressive Residual Stress in the Surface of a Workpiece,” U.S. Patent #5,826,453, October 27, 1998, other patents pending.
38. Migala, T.S., Jacobs, T.L. (2002), "Low Plasticity Burnishing: An Affordable and Effective Means of Surface Enhancement", *Proceedings of 13th International Federation for Heat Treatment and Surface Engineering Congress*, October 2002.
39. Hackel, L. (1998, October). Blasts of Light to Strengthen Metals, *Science & Technology Review*, Lawrence Livermore National Laboratory.
40. “Haynes International, Inc..“ Corrosion-Resistant Alloys. (n.d.) Retrieved April 1, 2008, from Haynes International, Inc. Web site: http://www.haynesintl.com/CRAlloys.htm.

12. Appendices

12.1 Appendix A Phase Stability Studies Aging Log

Specimen Number	Furnace No./SN	TC/Readout ID	Aging Time (Hrs.)	Aging Temp. (C)	Testing Performed	Comments
ST184-D	5/999070	Y5536	1,100	550	None	
ST184-E	5/999070	Y5536	6,000	550	None	
ST184-F	1/999067	Y8120	1,100	650	None	
ST184-G	1/999067	Y8120	6,000	650	None	
ST184-H	4/999068	Y5537	1,100	500	None	
ST184-I	4/999068	Y5537	6,000	500	None	
ST184-K	5/999070	Y5536	500	550	None	
ST184-L	5/999070	Y5536	2,024	550	None	
ST184-M	5/999070	Y5536	3,010	550	None	SN-LLNL-SCI-434-V2
ST184-N	5/999070	Y5536	37,198	550	None	SN-LLNL-SCI-434-V2
ST184-O	1/999067	Y8120	500	650	None	
ST184-P	1/999067	Y8120	2,024	650	None	SN-LLNL-SCI-434-V2
ST184-Q	1/999067	Y8120	3,010	650	None	SN-LLNL-SCI-434-V2
ST184-R	1/999067	Y8120	37,169	650	None	SN-LLNL-SCI-434-V2
ST184-S	4/999068	Y5537	500	500	None	
ST184-T	4/999068	Y5537	2,024	500	None	SN-LLNL-SCI-434-V2
ST184-U	4/999068	Y5537	3,010	500	None	SN-LLNL-SCI-434-V2
ST184-V	4/999068	Y5537	37,194	500	None	SN-LLNL-SCI-434-V2
ST184-OO	5/999070	Y5536	8,000	550	None	
ST184-PP	5/999070	Y5536	10,024	550	None	
ST184-QQ	5/999070	Y5536	19,958	550	None	SN-LLNL-SCI-434-V2
ST184-RR	1/999067	Y8120	8,000	650	None	
ST184-SS	1/999067	Y8120	10,024	650	None	SN-LLNL-SCI-434-V2
ST184-TT	1/999067	Y8120	19,944	650	None	
ST184-UU	4/999068	Y5537	8,000	500	None	
ST184-VV	4/999068	Y5537	10,024	500	None	SN-LLNL-SCI-434-V2
ST184-WW	4/999068	Y5537	19,958	500	None	SN-LLNL-SCI-434-V2
ST185-C	5/999070	Y5536	6,000	550	None	
ST185-E	1/999067	Y8120	6,000	650	None	
ST185-G	4/999068	Y5537	6,000	500	None	
ST185-H	5/999070	Y5536	500	550	None	
ST185-I	5/999070	Y5536	2,024	550	None	
ST185-J	5/999070	Y5536	3,010	550	None	SN-LLNL-SCI-434-V2
ST185-K	5/999070	Y5536	37,198	550	None	SN-LLNL-SCI-434-V2
ST185-L	1/999067	Y8120	500	650	None	
ST185-M	1/999067	Y8120	2,024	650	None	SN-LLNL-SCI-434-V2
ST185-N	1/999067	Y8120	3,010	650	None	SN-LLNL-SCI-434-V2
ST185-O	1/999067	Y8120	37,169	650	None	SN-LLNL-SCI-434-V2
ST185-P	4/999068	Y5537	500	500	None	
ST185-Q	4/999068	Y5537	2,024	500	None	SN-LLNL-SCI-434-V2
ST185-R	4/999068	Y5537	3,010	500	None	SN-LLNL-SCI-434-V2
ST185-S	4/999068	Y5537	37,194	500	None	SN-LLNL-SCI-434-V2
ST185-U	5/999070	Y5536	8,000	550	None	
ST185-V	5/999070	Y5536	10,024	550	None	
ST185-W	5/999070	Y5536	19,958	550	None	SN-LLNL-SCI-434-V2
ST185-X	1/999067	Y8120	8,000	650	None	
ST185Y	1/999067	Y8120	10,024	650	None	SN-LLNL-SCI-434-V2
ST185-AA	4/999068	Y5537	8,000	500	None	
ST185-BB	4/999068	Y5537	10,024	500	None	SN-LLNL-SCI-434-V2
ST185-CC	4/999068	Y5537	19,958	500	None	SN-LLNL-SCI-434-V2
ST186-C	5/999070	Y5536	6,000	550	None	
ST186-E	1/999067	Y8120	6,000	650	None	
ST186-G	4/999068	Y5537	6,000	500	None	
ST186-H	5/999070	Y5536	500	550	None	
ST186-I	5/999070	Y5536	2,024	550	None	
ST186-J	5/999070	Y5536	3,010	550	None	SN-LLNL-SCI-434-V2
ST186-K	5/999070	Y5536	37,198	550	None	SN-LLNL-SCI-434-V2
ST186-L	1/999067	Y8120	500	650	None	
ST186-M	1/999067	Y8120	2,024	650	None	SN-LLNL-SCI-434-V2
ST186-N	1/999067	Y8120	3,010	650	None	SN-LLNL-SCI-434-V2
ST186-O	1/999067	Y8120	37,169	650	None	SN-LLNL-SCI-434-V2
ST186-P	4/999068	Y5537	500	500	None	
ST186-Q	4/999068	Y5537	2,024	500	None	SN-LLNL-SCI-434-V2
ST186-R	4/999068	Y5537	3,010	500	None	
ST186-S	4/999068	Y5537	37,194	500	None	SN-LLNL-SCI-434-V2
ST186-U	5/999070	Y5536	8,000	550	None	
ST186-V	5/999070	Y5536	10,024	550	None	
ST186-W	5/999070	Y5536	19,958	550	None	SN-LLNL-SCI-434-V2

Specimen Number	Furnace No./SN	TC/Readout ID	Aging Time (Hrs.)	Aging Temp. (C)	Testing Performed	Comments
ST186-X	1/999067	Y8120	8,000	650	None	
ST186-Y	1/999067	Y8120	10,024	650	None	SN-LLNL-SCI-434-V2
ST186-AA	4/999068	Y5537	8,000	500	None	
ST186-BB	4/999068	Y5537	10,024	500	None	SN-LLNL-SCI-434-V2
ST186-CC	4/999068	Y5537	19,958	500	None	SN-LLNL-SCI-434-V2
ST-434-B5C1	7/750950688858	AF8301/Y8124	1,000	550	TEM	SN-LLNL-SCI-434-V2
ST-434-B6C1	8/750960472556	AC7643/Y8124	500	700	EBSD	SN-LLNL-SCI-434-V2
ST-434-B6C2	6/750961033029	AD6790/Y8124	100	550	None	SN-LLNL-SCI-434-V2
ST-434-B7C1	8/750960472556	AC7643/Y8124	50	700	EBSD	SN-LLNL-SCI-434-V2
ST-434-D14Z1A2B1	8/750960472556	AE7717/AA2617	20 minutes	1075	EBSD, Corrosion	SN-LLNL-SCI-434-V2
ST-434-D14Z1A2B2	7/750950688858	AD6788/AA2617	20 minutes	1121	EBSD, Corrosion	SN-LLNL-SCI-434-V2
ST-434-D14Z1A2B3	8/750960472556	AE7717/AA2617	24	1075	EBSD, Corrosion	SN-LLNL-SCI-434-V2
ST-434-D14Z1A2B4	8/750960472556	AE7717/AA2617	72	1075	EBSD, Corrosion	SN-LLNL-SCI-434-V2
ST-434-D14Z1A2B5	8/750960472556	AE7717/AA2617	168	1075	EBSD, Corrosion	SN-LLNL-SCI-434-V2
ST-434-D14Z1A2B7	8/750960472556	AC7643/Y8124	24	1121	EBSD, Corrosion	SN-LLNL-SCI-434-V2
ST-434-D14Z1A2B8	8/750960472556	AC7643/Y8124	72	1121	EBSD, Corrosion	SN-LLNL-SCI-434-V2
ST-434-D14Z1A2B9	8/750960472556	AC7643/Y8124	168	1121	EBSD, Corrosion	SN-LLNL-SCI-434-V2
ST-434-D14Z1A2B10	13/U08N-500037-VN	002516/002474	20 minutes	1300	EBSD, Corrosion	SN-LLNL-SCI-434-V2
ST-434-D14Z1A2B11	13/U08N-500037-VN	002516/002474	20 minutes	1200	EBSD, Corrosion	SN-LLNL-SCI-434-V2
ST-434-D14Z1A2B12	13/U08N-500037-VN	002516/002474	24	1200	EBSD, Corrosion	SN-LLNL-SCI-434-V2
ST-434-D14Z1A2B13	13/U08N-500037-VN	002516/002474	72	1200	EBSD, Corrosion	SN-LLNL-SCI-434-V2
ST-434-D14Z1A2B14	13/U08N-500037-VN	002516/002474	168	1200	EBSD, Corrosion	SN-LLNL-SCI-434-V2
ST-434-D14Z1A2B15	13/U08N-500037-VN	002516/002474	24	1300	EBSD, Corrosion	SN-LLNL-SCI-434-V2
ST-434-D14Z1A2B16	13/U08N-500037-VN	002516/002474	72	1300	EBSD, Corrosion	SN-LLNL-SCI-434-V2
ST-434-D14Z1A2B17	13/U08N-500037-VN	002516/002474	168	1300	EBSD, Corrosion	SN-LLNL-SCI-434-V2
ST-434-D14Z1A2B18	11/170298-L	001494/010075	18,984	200	None	SN-LLNL-SCI-434-V2
ST-434-D14Z1A2B19	11/170298-L	001494/010075	18,984	200	None	SN-LLNL-SCI-434-V2
ST-434-D14Z1A2B20	11/170298-L	001494/010075	18,984	200	None	SN-LLNL-SCI-434-V2
ST-434-D14Z1A2B21	11/170298-L	001494/010075	18,984	200	None	SN-LLNL-SCI-434-V2
ST-434-D14Z1A2B22	11/170298-L	001494/010075	18,984	200	None	SN-LLNL-SCI-434-V2
ST-434-D14Z1A2B23	11/170298-L	001494/010075	18,984	200	None	SN-LLNL-SCI-434-V2
ST-434-D14Z1A2B24	11/170298-L	001494/010075	18,984	200	None	SN-LLNL-SCI-434-V2
ST-434-D14Z1A2B25	11/170298-L	001494/010075	18,984	200	None	SN-LLNL-SCI-434-V2
ST-434-D14Z1A2B26	12/170297-L	001669/010074	17,568	300	None	SN-LLNL-SCI-434-V2
ST-434-D14Z1A2B27	12/170297-L	001669/010074	17,568	300	None	SN-LLNL-SCI-434-V2
ST-434-D14Z1A2B28	12/170297-L	001669/010074	17,568	300	None	SN-LLNL-SCI-434-V2
ST-434-D14Z1A2B29	12/170297-L	001669/010074	17,568	300	None	SN-LLNL-SCI-434-V2
ST-434-D14Z1A2B30	12/170297-L	001669/010074	17,568	300	None	SN-LLNL-SCI-434-V2
ST-434-D14Z1A2B31	12/170297-L	001669/010074	17,568	300	None	SN-LLNL-SCI-434-V2
ST-434-D14Z1A2B32	12/170297-L	001669/010074	17,568	300	None	SN-LLNL-SCI-434-V2
ST-434-D14Z1A2B33	12/170297-L	001669/010074	17,568	300	None	SN-LLNL-SCI-434-V2
ST-434-D14Z1A2B34	3/999069	Y5538/AA2564	15,103	400	None	SN-LLNL-SCI-434-V2
ST-434-D14Z1A2B35	2/999066	Y8121	13,972	600	None	SN-LLNL-SCI-434-V2
ST-434-D14Z1A2B36	2/999066	Y8121	13,972	600	None	SN-LLNL-SCI-434-V2
ST-434-D14Z1A2B37	3/999069	Y5538/AA2564	13,975	400	None	SN-LLNL-SCI-434-V2
ST-434-D14Z1A2B38	3/999069	Y5538/AA2564	13,975	400	None	SN-LLNL-SCI-434-V2
ST-434-D14Z1A2B39	4/999068	Y5537	13,991	500	None	SN-LLNL-SCI-434-V2
ST-434-D14Z1B1	9/1057981147788	AD6788/Y8124	20 minutes	1075	EBSD, Corrosion	SN-LLNL-SCI-434-V2
ST-434-D14Z1B2	9/1057981147788	AD6788/Y8124	24	1075	EBSD, Corrosion	SN-LLNL-SCI-434-V2
ST-434-D14Z1B3	7/750950688858	AF8301/AA2617	72	1075	EBSD, Volume Fraction	SN-LLNL-SCI-434-V2
ST-434-D14Z1B4	6/750961033029	AD6790/Y8124	20 minutes	1121	EBSD, Volume Fraction	SN-LLNL-SCI-434-V2
ST-434-D14Z1B5	6/750961033029	AD6790/Y8124	24	1121	EBSD, Volume Fraction	SN-LLNL-SCI-434-V2
ST-434-D14Z1B6	7/750950688858	AF8301/Y8124	20 minutes	1200	EBSD, Volume Fraction	SN-LLNL-SCI-434-V2
ST-434-D14Z1B7	7/750950688858	AF8301/Y8124	24	1200	EBSD, Volume Fraction	SN-LLNL-SCI-434-V2
ST-434-D14Z1B8	6/750961033029	AD6790/AA2617	72	1121	EBSD, Volume Fraction	SN-LLNL-SCI-434-V2
ST-434-D14Z1B9	9/1057981147788	AD6788/AA2617	72	1200	EBSD, Volume Fraction	SN-LLNL-SCI-434-V2
ST-434-D14Z1B10	8/750960472556	AC7643/AA2617	168	1075	EBSD, Volume Fraction	SN-LLNL-SCI-434-V2
ST-434-D14Z1B11	7/750950688858	AF8301/Y2617	168	1200	EBSD, Volume Fraction	SN-LLNL-SCI-434-V2
ST-434-D14Z1B12	8/750960472556	AC7643/AA2617	168	1121	EBSD, Volume Fraction	SN-LLNL-SCI-434-V2
ST-434-D43B3	6/750961033029	002518/AA2617	100	750	None	SN-LLNL-SCI-434-V2
ST-434-D43B4	7/750950688858	AF8302/AA2617	100	700	None	SN-LLNL-SCI-434-V2
ST-434-D43B5	8/750960472556	AF8303/Y8124	100	650	None	SN-LLNL-SCI-434-V2
ST-434-D43B7	9/1057981147788	AA2563/Y8124	100	550	None	SN-LLNL-SCI-434-V2
ST-434-D43B8	10/1285040703970	AE7718/Y8124	5	550	None	SN-LLNL-SCI-434-V2
ST-434-D43B9	13/U08N-500037-VN	002516/002474	50	550	None	SN-LLNL-SCI-434-V2
ST-434-D43B10	10/1285040703970	AE7718/Y8124	1	750	None	SN-LLNL-SCI-434-V2
ST-434-D43B11	8/750960472556	AF8303/Y8124	20	650	None	SN-LLNL-SCI-434-V2
ST-434-D43B12	8/750960472556	AF8303/Y8124	1,012	650	None	SN-LLNL-SCI-434-V2
ST-434-D43B13	10/1285040703970	AE7718/Y8124	10	750	None	SN-LLNL-SCI-434-V2

Specimen Number	Furnace No./SN	TC/Readout ID	Aging Time (Hrs.)	Aging Temp. (C)	Testing Performed	Comments
ST-434-D43B14	9/1057981147788	AA2563/Y8124	1,000	750	None	SN-LLNL-SCI-434-V2
ST-434-D43B15	9/1057981147788	AA2563/AE6373/AC8305/Y8124/010821	17,593 (Extra)	750	None	SN-LLNL-SCI-434-V2
ST-434-D43B16	9/1057981147788	AA2563/AE6373/AC8305/Y8124/010821	17,593 (Extra)	750	None	SN-LLNL-SCI-434-V2
ST-434-D43B17	9/1057981147788	AA2563/Y8124	10	700	None	SN-LLNL-SCI-434-V2
ST-434-D43B18	13/U08N-500037-VN	002516/002474	10	550	None	SN-LLNL-SCI-434-V2
ST-434-D43B19	10/1285040703970	002525/Y8124	1,000	700	None	SN-LLNL-SCI-434-V2
ST-434-D43B20	10/1285040703970	002525/Y8124/AC8304/010822/AA2617/AE6372	17,568 (Extra)	700	None	SN-LLNL-SCI-434-V2
ST-434-D43B21	10/1285040703970	002525/Y8124/AC8304/010822/AA2617/AE6372	17,568 (Extra)	700	None	SN-LLNL-SCI-434-V2
ST-434-D43B22	2/999066	Y8121	1,000	600	None	SN-LLNL-SCI-434-V2
ST-434-D43B23	4/999068	Y5537	1,000	500	None	SN-LLNL-SCI-434-V2
ST-434-D43B24	4/999068	Y5537	24,015	500	None	SN-LLNL-SCI-434-V2
ST-434-D43B25	4/999068	Y5537	24,015	500	None	SN-LLNL-SCI-434-V2
ST-434-D43B26	5/999070	Y5536	1,000	550	None	SN-LLNL-SCI-434-V2
ST-434-D43B27	5/999070	Y5536	24,018	550	None	SN-LLNL-SCI-434-V2
ST-434-D43B28	5/999070	Y5536	24,018	550	None	SN-LLNL-SCI-434-V2
ST-434-D43C4	2/999066	Y8121	10,024	600	None	SN-LLNL-SCI-434-V2
ST-434-D43C5	4/999068	Y5537	10,024	500	None	SN-LLNL-SCI-434-V2
ST-434-D43C6	10/1285040703970	002525/Y8124/AC8304/010822	10,001	700	None	SN-LLNL-SCI-434-V2
ST-434-D43C7	1/999067	Y8120	10,025	650	None	SN-LLNL-SCI-434-V2
ST-434-D43C8	1/999067	Y8120	24,722	650	None	SN-LLNL-SCI-434-V2
ST-434-D43C9	1/999067	Y8120	24,722	650	None	SN-LLNL-SCI-434-V2
ST-434-D43C10	3/999069	Y5538/AA2564	23,863	400	None	SN-LLNL-SCI-434-V2
ST-434-D43C11	3/999069	Y5538/AA2564	23,863	400	None	SN-LLNL-SCI-434-V2
ST-434-D43C12	3/999069	Y5538/AA2564	23,863	400	None	SN-LLNL-SCI-434-V2
ST-434-D43C13	3/999069	Y5538/AA2564	23,863	400	None	SN-LLNL-SCI-434-V2
ST-434-D43C14	3/999069	Y5538/AA2564	8,760	400	None	SN-LLNL-SCI-434-V2
ST-434-D43C15	6/750961033029	002518/AA2617	5,000	450	None	SN-LLNL-SCI-434-V2
ST-434-D43C16	6/750961033029	010485/002518/AA2617/Y8124	9,880	450	None	SN-LLNL-SCI-434-V2
ST-434-D43C17	7/750950688858	AF8302/AE6362/002526/AA2617/Y8124	17,408 (Extra)	450	None	SN-LLNL-SCI-434-V2
ST-434-D43C18	7/750950688858	AF8302/AE6362/002526/AA2617/Y8124	17,408 (Extra)	450	None	SN-LLNL-SCI-434-V2
ST-434-D43C19	4/999068	Y5537	5,000	500	None	SN-LLNL-SCI-434-V2
ST-434-D43C20	2/999066	Y8121	22,995	600	None	SN-LLNL-SCI-434-V2
ST-434-D43C21	6/750961033029	AC8306/AE6374/002518/AA2617/Y8124	12,408 (TBD 6 mo. stagger)	450	None	SN-LLNL-SCI-434-V2 AC8306 aka 010483, AE6374 aka 010485
ST-434-D43C22	4/999068	Y5537	18,014	500	None	SN-LLNL-SCI-434-V2
ST-434-D43C23	3/999069	Y5538/AA2564	15,103	400	None	SN-LLNL-SCI-434-V2
ST-434-D44B2	11/170298-L	001494/010075	18,984	200	None	SN-LLNL-SCI-434-V2
ST-434-D44B3	11/170298-L	001494/010075	18,984	200	None	SN-LLNL-SCI-434-V2
ST-434-D44B4	11/170298-L	001494/010075	18,984	200	None	SN-LLNL-SCI-434-V2
ST-434-D44B5	11/170298-L	001494/010075	18,984	200	None	SN-LLNL-SCI-434-V2
ST-434-D44B6	11/170298-L	001494/010075	18,984	200	None	SN-LLNL-SCI-434-V2
ST-434-D44B7	11/170298-L	001494/010075	18,984	200	None	SN-LLNL-SCI-434-V2
ST-434-D44B8	11/170298-L	001494/010075	18,984	200	None	SN-LLNL-SCI-434-V2
ST-434-D44B9	11/170298-L	001494/010075	18,984	200	None	SN-LLNL-SCI-434-V2
ST-434-D44B10	11/170298-L	001494/010075	18,984	200	None	SN-LLNL-SCI-434-V2
ST-434-D44B11	11/170298-L	001494/010075	18,984	200	None	SN-LLNL-SCI-434-V2
ST-434-D44B12	11/170298-L	001494/010075	18,984	200	None	SN-LLNL-SCI-434-V2
ST-434-D44B13	11/170298-L	001494/010075	18,984	200	None	SN-LLNL-SCI-434-V2
ST-434-D44B14	11/170298-L	001494/010075	18,984	200	None	SN-LLNL-SCI-434-V2
ST-434-D44B15	11/170298-L	001494/010075	18,984	200	None	SN-LLNL-SCI-434-V2
ST-434-D44B16	11/170298-L	001494/010075	18,984	200	None	SN-LLNL-SCI-434-V2
ST-434-D44B17	11/170298-L	001494/010075	18,984	200	None	SN-LLNL-SCI-434-V2
ST-434-D44B18	11/170298-L	001494/010075	18,984	200	None	SN-LLNL-SCI-434-V2
ST-434-D44B19	11/170298-L	001494/010075	18,984	200	None	SN-LLNL-SCI-434-V2
ST-434-D44B20	11/170298-L	001494/010075	18,984	200	None	SN-LLNL-SCI-434-V2
ST-434-D44B21	11/170298-L	001494/010075	18,984	200	None	SN-LLNL-SCI-434-V2
ST-434-D44B22	11/170298-L	001494/010075	18,984	200	None	SN-LLNL-SCI-434-V2
ST-434-D44B23	11/170298-L	001494/010075	18,984	200	None	SN-LLNL-SCI-434-V2
ST-434-D44B24	11/170298-L	001494/010075	18,984	200	None	SN-LLNL-SCI-434-V2

Specimen Number	Furnace No./SN	TC/Readout ID	Aging Time (Hrs.)	Aging Temp. (C)	Testing Performed	Comments
ST-434-D44B25	11/170298-L	001494/010075	18,984	200	None	SN-LLNL-SCI-434-V2
ST-434-D44B26	12/170297-L	001669/010074	17,568	300	None	SN-LLNL-SCI-434-V2
ST-434-D44B27	12/170297-L	001669/010074	17,568	300	None	SN-LLNL-SCI-434-V2
ST-434-D44B28	12/170297-L	001669/010074	17,568	300	None	SN-LLNL-SCI-434-V2
ST-434-D44B29	12/170297-L	001669/010074	17,568	300	None	SN-LLNL-SCI-434-V2
ST-434-D44B30	12/170297-L	001669/010074	17,568	300	None	SN-LLNL-SCI-434-V2
ST-434-D44B31	12/170297-L	001669/010074	17,568	300	None	SN-LLNL-SCI-434-V2
ST-434-D44B32	12/170297-L	001669/010074	17,568	300	None	SN-LLNL-SCI-434-V2
ST-434-D44B33	12/170297-L	001669/010074	17,568	300	None	SN-LLNL-SCI-434-V2
ST-434-D44B34	12/170297-L	001669/010074	17,568	300	None	SN-LLNL-SCI-434-V2
ST-434-D44B35	12/170297-L	001669/010074	17,568	300	None	SN-LLNL-SCI-434-V2
ST-434-D44B36	12/170297-L	001669/010074	17,568	300	None	SN-LLNL-SCI-434-V2
ST-434-D44B37	12/170297-L	001669/010074	17,568	300	None	SN-LLNL-SCI-434-V2
ST-434-D44B38	12/170297-L	001669/010074	17,568	300	None	SN-LLNL-SCI-434-V2
ST-434-D45B2	12/170297-L	001669/010074	17,568	300	None	SN-LLNL-SCI-434-V2
ST-434-D45B3	12/170297-L	001669/010074	17,568	300	None	SN-LLNL-SCI-434-V2
ST-434-D45B4	12/170297-L	001669/010074	17,568	300	None	SN-LLNL-SCI-434-V2
ST-434-D45B5	12/170297-L	001669/010074	17,568	300	None	SN-LLNL-SCI-434-V2
ST-434-D45B6	12/170297-L	001669/010074	17,568	300	None	SN-LLNL-SCI-434-V2
ST-434-D45B7	12/170297-L	001669/010074	17,568	300	None	SN-LLNL-SCI-434-V2
ST-434-D45B8	12/170297-L	001669/010074	17,568	300	None	SN-LLNL-SCI-434-V2
ST-434-D45B9	12/170297-L	001669/010074	17,568	300	None	SN-LLNL-SCI-434-V2
ST-434-D45B10	12/170297-L	001669/010074	17,568	300	None	SN-LLNL-SCI-434-V2
ST-434-D45B11	12/170297-L	001669/010074	17,568	300	None	SN-LLNL-SCI-434-V2
ST-434-D45B12	12/170297-L	001669/010074	17,568	300	None	SN-LLNL-SCI-434-V2
ST-434-D45B13	13/U08N-500037-VN	002516/002474	50	550	None	SN-LLNL-SCI-434-V2
ST-434-D45B14	10/1285040703970	AE7718/Y8124	5	550	None	SN-LLNL-SCI-434-V2
ST-434-D45B15	10/1285040703970	AE7718/Y8124	5	550	None	SN-LLNL-SCI-434-V2
ST-434-D45B16	10/1285040703970	AE7718/Y8124	5	550	None	SN-LLNL-SCI-434-V2
ST-434-D45B17	13/U08N-500037-VN	002516/002474	50	550	None	SN-LLNL-SCI-434-V2
ST-434-D45B18	13/U08N-500037-VN	002516/002474	50	550	None	SN-LLNL-SCI-434-V2
ST-434-D45B19	13/U08N-500037-VN	002516/002474	10	550	None	SN-LLNL-SCI-434-V2
ST-434-D45B20	13/U08N-500037-VN	002516/002474	10	550	None	SN-LLNL-SCI-434-V2
ST-434-D45B21	13/U08N-500037-VN	002516/002474	10	550	None	SN-LLNL-SCI-434-V2
ST-434-D45B22	2/999066	Y8121	1,000	600	None	SN-LLNL-SCI-434-V2
ST-434-D45B23	2/999066	Y8121	1,000	600	None	SN-LLNL-SCI-434-V2
ST-434-D45B24	2/999066	Y8121	1,000	600	None	SN-LLNL-SCI-434-V2
ST-434-D45B25	4/999068	Y5537	1,000	500	None	SN-LLNL-SCI-434-V2
ST-434-D45B26	4/999068	Y5537	1,000	500	None	SN-LLNL-SCI-434-V2
ST-434-D45B27	4/999068	Y5537	1,000	500	None	SN-LLNL-SCI-434-V2
ST-434-D45B28	4/999068	Y5537	10,024	500	None	SN-LLNL-SCI-434-V2
ST-434-D45B29	4/999068	Y5537	10,024	500	None	SN-LLNL-SCI-434-V2
ST-434-D45B30	4/999068	Y5537	10,024	500	None	SN-LLNL-SCI-434-V2
ST-434-D45B31	3/999069	Y5538/AA2564	23,863	400	None	SN-LLNL-SCI-434-V2
ST-434-D45B32	3/999069	Y5538/AA2564	23,863	400	None	SN-LLNL-SCI-434-V2
ST-434-D45B33	3/999069	Y5538/AA2564	23,863	400	None	SN-LLNL-SCI-434-V2
ST-434-D45B34	3/999069	Y5538/AA2564	23,863	400	None	SN-LLNL-SCI-434-V2
ST-434-D45B35	3/999069	Y5538/AA2564	23,863	400	None	SN-LLNL-SCI-434-V2
ST-434-D45B36	3/999069	Y5538/AA2564	23,863	400	None	SN-LLNL-SCI-434-V2
ST-434-D45B37	3/999069	Y5538/AA2564	8,760	400	None	SN-LLNL-SCI-434-V2
ST-434-D45B38	3/999069	Y5538/AA2564	8,760	400	None	SN-LLNL-SCI-434-V2
ST-434-D46B2	3/999069	Y5538/AA2564	8,760	400	None	SN-LLNL-SCI-434-V2
ST-434-D46B3	3/999069	Y5538/AA2564	23,863	400	None	SN-LLNL-SCI-434-V2
ST-434-D46B4	3/999069	Y5538/AA2564	23,863	400	None	SN-LLNL-SCI-434-V2
ST-434-D46B5	3/999069	Y5538/AA2564	23,863	400	None	SN-LLNL-SCI-434-V2
ST-434-D46B6	3/999069	Y5538/AA2564	23,863	400	None	SN-LLNL-SCI-434-V2
ST-434-D46B7	3/999069	Y5538/AA2564	23,863	400	None	SN-LLNL-SCI-434-V2
ST-434-D46B8	3/999069	Y5538/AA2564	23,863	400	None	SN-LLNL-SCI-434-V2
ST-434-D46B9	6/750961033029	002518/AA2617	5,000	450	None	SN-LLNL-SCI-434-V2
ST-434-D46B10	6/750961033029	002518/AA2617	5,000	450	None	SN-LLNL-SCI-434-V2
ST-434-D46B11	6/750961033029	002518/AA2617	5,000	450	None	SN-LLNL-SCI-434-V2
ST-434-D46B12	6/750961033029	002518/AE6374/AA2617/Y8124	9,880	450	None	SN-LLNL-SCI-434-V2 AE6374 aka 010485
ST-434-D46B13	6/750961033029	002518/AE6374/AA2617/Y8124	9,880	450	None	SN-LLNL-SCI-434-V2 AE6374 aka 010485
ST-434-D46B14	6/750961033029	002518/AE6374/AA2617/Y8124	9,880	450	None	SN-LLNL-SCI-434-V2 AE6374 aka 010485
ST-434-D46B15	7/750950688858	AF8302/AE6362/002526/AA2617/Y8124	17,408 (Extra)	450	None	SN-LLNL-SCI-434-V2

Specimen Number	Furnace No./SN	TC/Readout ID	Aging Time (Hrs.)	Aging Temp. (C)	Testing Performed	Comments
ST-434-D46B16	7/750950688858	AF8302/AE6362/002 526/AA2617/Y8124	17,408 (Extra)	450	None	SN-LLNL-SCI-434-V2
ST-434-D46B17	7/750950688858	AF8302/AE6362/002 526/AA2617/Y8124	17,408 (Extra)	450	None	SN-LLNL-SCI-434-V2
ST-434-D46B18	7/750950688858	AF8302/AE6362/002 526/AA2617/Y8124	17,408 (Extra)	450	None	SN-LLNL-SCI-434-V2
ST-434-D46B19	7/750950688858	AF8302/AE6362/002 526/AA2617/Y8124	17,408 (Extra)	450	None	SN-LLNL-SCI-434-V2
ST-434-D46B20	7/750950688858	AF8302/AE6362/002 526/AA2617/Y8124	17,408 (Extra)	450	None	SN-LLNL-SCI-434-V2
ST-434-D46B21	4/999068	Y5537	5,000	500	None	SN-LLNL-SCI-434-V2
ST-434-D46B22	4/999068	Y5537	5,000	500	None	SN-LLNL-SCI-434-V2
ST-434-D46B23	4/999068	Y5537	5,000	500	None	SN-LLNL-SCI-434-V2
ST-434-D46B24	6/750961033029	AC8306/AE6374/002 518/AA2617/Y8124	12,408 (TBD 6 mo. stagger)	450	None	SN-LLNL-SCI-434-V2 AC8306 aka 010483, AE6374 aka 010485
ST-434-D46B25	6/750961033029	AC8306/AE6374/002 518/AA2617/Y8124	12,408 (TBD 6 mo. stagger)	450	None	SN-LLNL-SCI-434-V2 AC8306 aka 010483, AE6374 aka 010485
ST-434-D46B26	6/750961033029	AC8306/AE6374/002 518/AA2617/Y8124	12,408 (TBD 6 mo. stagger)	450	None	SN-LLNL-SCI-434-V2 AC8306 aka 010483, AE6374 aka 010485
ST-434-D46B27	4/999068	Y5537	18,014	500	None	SN-LLNL-SCI-434-V2
ST-434-D46B28	4/999068	Y5537	18,014	500	None	SN-LLNL-SCI-434-V2
ST-434-D46B29	4/999068	Y5537	18,014	500	None	SN-LLNL-SCI-434-V2
ST-434-D46B30	3/999069	Y5538/AA2564	15,103	400	None	SN-LLNL-SCI-434-V2
ST-434-D46B31	3/999069	Y5538/AA2564	15,103	400	None	SN-LLNL-SCI-434-V2
ST-434-D46B32	3/999069	Y5538/AA2564	15,103	400	None	SN-LLNL-SCI-434-V2
ST-434-D46B33	3/999069	Y5538/AA2564	15,103	400	None	SN-LLNL-SCI-434-V2
ST-434-D46B34	3/999069	Y5538/AA2564	15,103	400	None	SN-LLNL-SCI-434-V2
ST-434-D46B35	3/999069	Y5538/AA2564	15,103	400	None	SN-LLNL-SCI-434-V2
ST-434-D46B36	4/999068	Y5537	13,991	500	None	SN-LLNL-SCI-434-V2
ST-434-D47B7	4/999068	Y5537	13,991	500	None	SN-LLNL-SCI-434-V2
ST-434-D47B8	3/999069	Y5538/AA2564	13,975	400	None	SN-LLNL-SCI-434-V2
ST-434-D47B9	3/999069	Y5538/AA2564	13,975	400	None	SN-LLNL-SCI-434-V2
ST-434-D47B10	3/999069	Y5538/AA2564	13,975	400	None	SN-LLNL-SCI-434-V2
ST-434-D47B11	3/999069	Y5538/AA2564	13,975	400	None	SN-LLNL-SCI-434-V2
ST-434-D47B12	3/999069	Y5538/AA2564	13,975	400	None	SN-LLNL-SCI-434-V2
ST-434-D47B13	3/999069	Y5538/AA2564	13,975	400	None	SN-LLNL-SCI-434-V2
ST-434-D47B14	4/999068	Y5537	13,991	500	None	SN-LLNL-SCI-434-V2
ST-434-P9C2	7/750950688858	AF8301/Y8124	1,000	550	TEM	SN-LLNL-SCI-434-V2
ST-434-P10C1	8/750960472556	AC7643/Y8124	500	700	EBSD	SN-LLNL-SCI-434-V2
ST-434-P10C2	6/750961033029	AD6790/Y8124	100	550	None	SN-LLNL-SCI-434-V2
ST-434-P11C1	8/750960472556	AC7643/Y8124	50	700	EBSD	SN-LLNL-SCI-434-V2
ST-434-W9C1	7/750950688858	AF8301/Y8124	1,000	550	TEM	SN-LLNL-SCI-434-V2
ST-434-W10C1	8/750960472556	AC7643/Y8124	500	700	EBSD	SN-LLNL-SCI-434-V2
ST-434-W10C2	6/750961033029	AD6790/Y8124	100	550	None	SN-LLNL-SCI-434-V2
ST-434-W11C1	8/750960472556	AC7643/Y8124	500	700	EBSD	SN-LLNL-SCI-434-V2
TS-444-006A1	6/750961033029	Y5542	1	750	Mechanical	
TS-444-006A2	6/750961033029	Y5542	1	750	Mechanical	
TS-444-006A3	6/750961033029	Y5542	1	750	Mechanical	
TS-444-006B1	6/750961033029	Y5542	10	750	Mechanical	
TS-444-006B2	6/750961033029	Y5542	10	750	Mechanical	
TS-444-006B3	6/750961033029	Y5542	10	750	Mechanical	
TS-444-006C1	6/750961033029	Y5542	100	750	Mechanical	
TS-444-006C2	6/750961033029	Y5542	100	750	Mechanical	
TS-444-006C3	6/750961033029	Y5542	100	750	Mechanical	
TS-444-006D1	6/750961033029	Y5542	400	750	Mechanical	
TS-444-006D2	6/750961033029	Y5542	400	750	Mechanical	
TS-444-006D3	6/750961033029	Y5542	400	750	Mechanical	
TS-444-006E1	7/750950688858	Y5541	10	700	Mechanical	
TS-444-006E2	7/750950688858	Y5541	10	700	Mechanical	
TS-444-006E3	7/750950688858	Y5541	10	700	Mechanical	
TS-444-006F1	7/750950688858	Y5541	30	700	None	
TS-444-006F2	7/750950688858	Y5541	30	700	None	
TS-444-006F3	7/750950688858	Y5541	30	700	None	
TS-444-006G1	7/750950688858	Y5541	60	700	None	
TS-444-006G2	7/750950688858	Y5541	60	700	None	
TS-444-006G3	7/750950688858	Y5541	60	700	None	
TS-444-006H1	7/750950688858	Y5541	100	700	Mechanical	
TS-444-006H2	7/750950688858	Y5541	100	700	Mechanical	
TS-444-006H3	7/750950688858	Y5541	100	700	Mechanical	

Specimen Number	Furnace No./SN	TC/Readout ID	Aging Time (Hrs.)	Aging Temp. (C)	Testing Performed	Comments
TS-444-006I1	7/750950688858	Y5541	400	700	Mechanical	
TS-444-006I2	7/750950688858	Y5541	400	700	Mechanical	
TS-444-006I3	7/750950688858	Y5541	400	700	Mechanical	
TS-444-006J1	8/750960472556	Y8122	10	650	Mechanical	
TS-444-006J2	8/750960472556	Y8122	10	650	Mechanical	
TS-444-006J3	8/750960472556	Y8122	10	650	Mechanical	
TS-444-006K	5/999070	Y5536	1,000	550	None	
TS-444-006K1	5/999070	Y5536	1000	550	Mechanical	
TS-444-006K2	5/999070	Y5536	1000	550	Mechanical	
TS-444-006K3	5/999070	Y5536	1000	550	Mechanical	
TS-444-006L	5/999070	Y5536	67,393	550	None	SN-LLNL-SCI-434-V2
TS-444-006M	5/999070	Y5536	67,393	550	None	SN-LLNL-SCI-434-V2
TS-444-006N	4/999068	Y5537	4,500	550	None	
TS-444-006N1	4/999068	Y5537	4500	500	Mechanical	
TS-444-006N2	4/999068	Y5537	4500	500	Mechanical	
TS-444-006N3	4/999068	Y5537	4500	500	Mechanical	
TS-444-006O1	6/750961033029	Y5542	2	750	None	
TS-444-006O2	6/750961033029	Y5542	4	750	None	
TS-444-006O3	6/750961033029	Y5542	6	750	None	
TS-444-006O4	6/750961033029	Y5542	8	750	None	
TS-444-007A	5/999070	Y5536	67,393	550	None	SN-LLNL-SCI-434-V2
TS-444-007B	5/999070	Y5536	67,393	550	None	SN-LLNL-SCI-434-V2
TS-444-007C	3/999069	Y5538/AA2564	66,878	400	None	SN-LLNL-SCI-434-V2
TS-444-007D	3/999069	Y5538/AA2564	66,878	400	None	SN-LLNL-SCI-434-V2
TS-444-007E1	2/999066	Y5539	1000	750	Mechanical	
TS-444-007E2	2/999066	Y5539	1000	750	Mechanical	
TS-444-007E3	2/999066	Y5539	1000	750	Mechanical	
TS-444-007F1	2/999066	Y5539	4000	750	Mechanical	
TS-444-007F2	2/999066	Y5539	4000	750	Mechanical	
TS-444-007F3	2/999066	Y5539	4000	750	Mechanical	
TS-444-007G1A	2/999066	Y5539	10,076	750	None	
TS-444-007G1A1	2/999066	Y5539	10,076	750	None	
TS-444-007G1A1a	2/999066	Y5539	10,076	750	Bulk ppt. Vol. Frac. Data	00426LL Micrographs 2
TS-444-007G1A1b	2/999066	Y5539	10,076	750	None	
TS-444-007G1A2	2/999066	Y5539	10,076	750	Corrosion	
TS-444-007H	2/999066	Y5539	10,076	750	None	
TS-444-007I1	1/999067	Y5540	1000	700	Mechanical	
TS-444-007I2	1/999067	Y5540	1000	700	Mechanical	
TS-444-007I3	1/999067	Y5540	1000	700	Mechanical	
TS-444-007J1	1/999067	Y5540	4000	700	Mechanical	
TS-444-007J2	1/999067	Y5540	4000	700	Mechanical	
TS-444-007J3	1/999067	Y5540	4000	700	Mechanical	
TS-444-007K1	1/999067	Y5540	10,073	700	Bulk ppt. Vol. Frac. Data	00426LL Micrographs 2
TS-444-007K2	1/999067	Y5540	10,073	700	None	
TS-444-007L	1/999067	Y5540	10,073	700	None	
TS-444-007M1	6/750961033029	Y8117	100	650	Mechanical	
TS-444-007M2	6/750961033029	Y8117	100	650	Mechanical	
TS-444-007M3	6/750961033029	Y8117	100	650	Mechanical	
TS-444-007N1	6/750961033029	Y8117	300	650	Mechanical	
TS-444-007N2	6/750961033029	Y8117	300	650	Mechanical	
TS-444-007N3	6/750961033029	Y8117	300	650	Mechanical	
TS-444-007O1	6/750961033029	Y5542	10	750	None	
TS-444-007O2	6/750961033029	Y5542	30	750	None	
TS-444-007O3	6/750961033029	Y5542	60	750	None	
TS-444-007O4	6/750961033029	Y5542	100	750	None	
TS-444-008A1	8/750960472556	Y8122	600	650	Mechanical	
TS-444-008A2	8/750960472556	Y8122	600	650	Mechanical	
TS-444-008A3	8/750960472556	Y8122	600	650	Mechanical	
TS-444-008B	2/999066	Y8121	1000	600	None	
TS-444-008C	2/999066	Y8121	4000	600	None	
TS-444-008D	2/999066	Y8121	10,000	600	None	
TS-444-008E	1/999067	Y8120	1000	650	None	
TS-444-008F	1/999067	Y8120	4000	650	None	
TS-444-008G	1/999067	Y8120	51,170	650	None	SN-LLNL-SCI-434-V2
TS-444-008H	2/999066	Y8121	51,190	600	None	SN-LLNL-SCI-434-V2
TS-444-008I	2/999066	Y8121	51,190	600	None	SN-LLNL-SCI-434-V2
TS-444-008J	1/999067	Y8120	51,170	650	None	SN-LLNL-SCI-434-V2
TS-444-008K	1/999067	Y8120	51,170	650	None	SN-LLNL-SCI-434-V2
TS-444-008O1	6/750961033029	Y5542	400	750	None	

Specimen Number	Furnace No./SN	TC/Readout ID	Aging Time (Hrs.)	Aging Temp. (C)	Testing Performed	Comments
TS-444-008O2	7/750950688858	Y5541	1	700	None	
TS-444-008O3	7/750950688858	Y5541	4	700	None	
TS-444-008O4	7/750950688858	Y5541	10	700	None	
TS-444-009O1	7/750950688858	Y5541	20	700	None	
TS-444-009O2	7/750950688858	Y5541	40	700	None	
TS-444-009O3	7/750950688858	Y5541	60	700	None	
TS-444-009O4	7/750950688858	Y5541	80	700	None	
TS-444-010O1	7/750950688858	Y5541	100	700	None	
TS-444-010O2	7/750950688858	Y5541	300	700	None	
TS-444-010O3	7/750950688858	Y5541	400	700	None	
TS-444-010O4	7/750950688858	Y5541	600	700	None	
TS-444-011A	4/999068	Y5537	67,386	500	None	SN-LLNL-SCI-434-V2
TS-444-011B	4/999068	Y5537	67,386	500	None	SN-LLNL-SCI-434-V2
TS-444-011C	4/999068	Y5537	67,386	500	None	SN-LLNL-SCI-434-V2
TS-444-011D	4/999068	Y5537	67,386	500	None	SN-LLNL-SCI-434-V2
TS-444-011E	3/999069	Y5538/AA2564	66,878	400	None	SN-LLNL-SCI-434-V2
TS-444-011F	3/999069	Y5538/AA2564	66,878	400	None	SN-LLNL-SCI-434-V2
TS-444-011G	3/999069	Y5538/AA2564	66,878	400	None	SN-LLNL-SCI-434-V2
TS-444-012A1	5/999070	Y5536	1000	550	None	
TS-444-012A2	5/999070	Y5536	2000	550	None	
TS-444-012A3	5/999070	Y5536	4500	550	None	
TS-444-012A4	5/999070	Y5536	6000	550	None	
TS-444-012B1A1	5/999070	Y5536	8000	550	None	
TS-444-012B1A2	5/999070	Y5536	8000	550	Corrosion	SN-LLNL-SCI-465 (Supp 4)
TS-444-012B2	5/999070	Y5536	21053.5	550	None	
TS-444-012B3	5/999070	Y5536	67,393	550	None	SN-LLNL-SCI-434-V2
TS-444-012B4	5/999070	Y5536	30000	550	None	
TS-444-012C1	5/999070	Y5536	67,393	550	None	SN-LLNL-SCI-434-V2
TS-444-012C2	4/999068	Y5537	1000	500	TEM	
TS-444-012C3	4/999068	Y5537	2000	500	TEM	
TS-444-012C4	4/999068	Y5537	4500	500	None	
TS-444-012D1	4/999068	Y5537	6000	500	None	
TS-444-012D2	4/999068	Y5537	8000	500	None	
TS-444-012D3	4/999068	Y5537	21046.5	500	None	
TS-444-012D4	4/999068	Y5537	67,386	500	None	SN-LLNL-SCI-434-V2
TS-444-012E1	4/999068	Y5537	30000	500	None	
TS-444-012E2	4/999068	Y5537	67,386	500	None	SN-LLNL-SCI-434-V2
TS-444-012E3	3/999069	Y5538	1000	400	TEM	
TS-444-012E4	3/999069	Y5538	2000	400	TEM	
TS-444-012F1	3/999069	Y5538	4500	400	None	
TS-444-012F2	3/999069	Y5538	6000	400	None	
TS-444-012F3A1	3/999069	Y5538	8000	400	None	
TS-444-012F3A2	3/999069	Y5538	8000	400	Corrosion	
TS-444-012F4	3/999069	Y5538/AA2564	66,878	400	None	SN-LLNL-SCI-434-V2
TS-444-012G1	3/999069	Y5538/AA2564	66,878	400	None	SN-LLNL-SCI-434-V2
TS-444-012G2	3/999069	Y5538/AA2564	30000	400	None	
TS-444-012G3	3/999069	Y5538/AA2564	66,878	400	None	SN-LLNL-SCI-434-V2
TS-444-012G4	3/999069	Y5538/AA2564	66,878	400	None	SN-LLNL-SCI-434-V2
TS-444-012H1	3/999069	Y5538/AA2564	66,878	400	None	SN-LLNL-SCI-434-V2
TS-444-012H2	2/999066	Y5539	1000	750	TEM	
TS-444-012H3	2/999066	Y5539	4000	750	None	
TS-444-012H4	1/999067	Y5540	1000	700	TEM	
TS-444-012I1	1/999067	Y5540	4000	700	None	
TS-444-012I2	8/750960472556	Y8122	100	550	None	
TS-444-012I3	8/750960472556	Y8122	300	550	None	
TS-444-012I4	8/750960472556	Y8122	600	550	None	
TS-444-012J1	9/1057981147788	Y8123	100	500	None	
TS-444-012J2	9/1057981147788	Y8123	300	500	None	
TS-444-012J3	9/1057981147788	Y8123	600	500	None	
TS-444-012J4	6/750961033029	Y5542	1	750	None	
TS-444-013A	5/999070	Y5536	1000	550	Mechanical	
TS-444-013B	5/999070	Y5536	1000	550	Mechanical	
TS-444-013C	5/999070	Y5536	1000	550	Mechanical	
TS-444-013D	5/999070	Y5536	67,393	550	None	SN-LLNL-SCI-434-V2
TS-444-013E	5/999070	Y5536	67,393	550	None	SN-LLNL-SCI-434-V2
TS-444-013F	5/999070	Y5536	67,393	550	None	SN-LLNL-SCI-434-V2
TS-444-013G	5/999070	Y5536	67,393	550	None	SN-LLNL-SCI-434-V2
TS-444-013H	5/999070	Y5536	67,393	550	None	SN-LLNL-SCI-434-V2
TS-444-013I	5/999070	Y5536	67,393	550	None	SN-LLNL-SCI-434-V2

Specimen Number	Furnace No./SN	TC/Readout ID	Aging Time (Hrs.)	Aging Temp. (C)	Testing Performed	Comments
TS-444-013J	5/999070	Y5536	67,393	550	None	SN-LLNL-SCI-434-V2
TS-444-013K	5/999070	Y5536	67,393	550	None	SN-LLNL-SCI-434-V2
TS-444-013L	5/999070	Y5536	67,393	550	None	SN-LLNL-SCI-434-V2
TS-444-013M	5/999070	Y5536	67,393	550	None	SN-LLNL-SCI-434-V2
TS-444-013N	5/999070	Y5536	67,393	550	None	SN-LLNL-SCI-434-V2
TS-444-013O1	8/750960472556	Y8122	1	650	None	
TS-444-013O2	8/750960472556	Y8122	4	650	None	
TS-444-013P	5/999070	Y5536	67,393	550	None	SN-LLNL-SCI-434-V2
TS-444-013Q	4/999068	Y5537	4500	500	Mechanical	
TS-444-013R	4/999068	Y5537	4500	500	Mechanical	
TS-444-013S	4/999068	Y5537	4500	500	Mechanical	
TS-444-013T	4/999068	Y5537	67,386	500	None	SN-LLNL-SCI-434-V2
TS-444-013U	4/999068	Y5537	67,386	500	None	SN-LLNL-SCI-434-V2
TS-444-013V	4/999068	Y5537	67,386	500	None	SN-LLNL-SCI-434-V2
TS-444-013W	4/999068	Y5537	67,386	500	None	SN-LLNL-SCI-434-V2
TS-444-013X	4/999068	Y5537	67,386	500	None	SN-LLNL-SCI-434-V2
TS-444-013Y	4/999068	Y5537	67,386	500	None	SN-LLNL-SCI-434-V2
TS-444-013Z	4/999068	Y5537	67,386	500	None	SN-LLNL-SCI-434-V2
TS-444-013AA	4/999068	Y5537	67,386	500	None	SN-LLNL-SCI-434-V2
TS-444-013BB	4/999068	Y5537	67,386	500	None	SN-LLNL-SCI-434-V2
TS-444-013CC	4/999068	Y5537	67,386	500	None	SN-LLNL-SCI-434-V2
TS-444-013DD1	8/750960472556	Y8122	10	650	None	
TS-444-013DD2	8/750960472556	Y8122	40	650	None	
TS-444-014A1	6/750961033029	Y8117	100	650	None	
TS-444-014A2	6/750961033029	Y8117	200	650	None	
TS-444-014B	4/999068	Y5537	67,386	500	None	SN-LLNL-SCI-434-V2
TS-444-014C	4/999068	Y5537	67,386	500	None	SN-LLNL-SCI-434-V2
TS-444-014D	3/999069	Y5538/AA2564	66,878	400	None	SN-LLNL-SCI-434-V2
TS-444-014E	3/999069	Y5538/AA2564	66,878	400	None	SN-LLNL-SCI-434-V2
TS-444-014F	3/999069	Y5538/AA2564	66,878	400	None	SN-LLNL-SCI-434-V2
TS-444-014G	3/999069	Y5538/AA2564	66,878	400	None	SN-LLNL-SCI-434-V2
TS-444-014H	3/999069	Y5538/AA2564	66,878	400	None	SN-LLNL-SCI-434-V2
TS-444-014I	3/999069	Y5538/AA2564	66,878	400	None	SN-LLNL-SCI-434-V2
TS-444-014J	3/999069	Y5538/AA2564	66,878	400	None	SN-LLNL-SCI-434-V2
TS-444-014K	3/999069	Y5538/AA2564	66,878	400	None	SN-LLNL-SCI-434-V2
TS-444-014L	3/999069	Y5538/AA2564	66,878	400	None	SN-LLNL-SCI-434-V2
TS-444-014M	3/999069	Y5538/AA2564	66,878	400	None	SN-LLNL-SCI-434-V2
TS-444-014N	3/999069	Y5538/AA2564	66,878	400	None	SN-LLNL-SCI-434-V2
TS-444-014O1	9/1057981147788	Y8123	1	600	None	
TS-444-014O2	9/1057981147788	Y8123	4	600	None	
TS-444-014P1	9/1057981147788	Y8123	10	600	None	
TS-444-014P2	9/1057981147788	Y8123	40	600	None	
TS-444-014Q	3/999069	Y5538/AA2564	66,878	400	None	SN-LLNL-SCI-434-V2
TS-444-014R	3/999069	Y5538/AA2564	66,878	400	None	SN-LLNL-SCI-434-V2
TS-444-014S	3/999069	Y5538/AA2564	66,878	400	None	SN-LLNL-SCI-434-V2
TS-444-014T	3/999069	Y5538/AA2564	66,878	400	None	SN-LLNL-SCI-434-V2
TS-444-014U	2/999066	Y5539	1000	750	Mechanical	
TS-444-014V	2/999066	Y5539	1000	750	Mechanical	
TS-444-014W	2/999066	Y5539	1000	750	Mechanical	
TS-444-014X	2/999066	Y5539	4000	750	Mechanical	
TS-444-014Y	2/999066	Y5539	4000	750	Mechanical	
TS-444-014Z	2/999066	Y5539	4000	750	Mechanical	
TS-444-014AA	2/999066	Y5539	10,076	750	None	
TS-444-014BB	2/999066	Y5539	10,076	750	None	
TS-444-014CC	2/999066	Y5539	10,076	750	None	
TS-444-014DD1	8/750960472556	Y8122	400	650	None	
TS-444-014DD2a	8/750960472556	Y8122	600	650	Bulk ppt. Vol. Frac. Data	See 00426LL Micrographs 2
TS-444-014DD2b	8/750960472556	Y8122	600	650	None	
TS-444-015A1	7/750950688858	Y8119	100	600	None	
TS-444-015A2	7/750950688858	Y8119	200	600	None	
TS-444-015B	2/999066	Y5539	10,076	750	None	
TS-444-015C	2/999066	Y5539	10,076	750	None	
TS-444-015D	2/999066	Y5539	10,076	750	None	
TS-444-015E	1/999067	Y5540	1,000	700	Mechanical	
TS-444-015F	1/999067	Y5540	1000	700	Mechanical	
TS-444-015G	1/999067	Y5540	1000	700	Mechanical	
TS-444-015H	1/999067	Y5540	4000	700	Mechanical	
TS-444-015I	1/999067	Y5540	4000	700	Mechanical	
TS-444-015J	1/999067	Y5540	4000	700	Mechanical	

Specimen Number	Furnace No./SN	TC/Readout ID	Aging Time (Hrs.)	Aging Temp. (C)	Testing Performed	Comments
TS-444-015K	1/999067	Y5540	10,073	700	None	
TS-444-015L	1/999067	Y5540	10,073	700	None	
TS-444-015M	1/999067	Y5540	10,073	700	None	
TS-444-015N	1/999067	Y5540	10,073	700	None	
TS-444-015O1	8/750960472556	Y8122	800	650	None	
TS-444-015O2	9/1057981147788	Y8123	800	600	None	
TS-444-015Q	1/999067	Y5540	10,073	700	None	
TS-444-015R	1/999067	Y5540	10,073	700	None	
TS-444-015S	6/750961033029	Y5542	1	750	Mechanical	
TS-444-015T	6/750961033029	Y5542	1	750	Mechanical	
TS-444-015U	6/750961033029	Y5542	1	750	Mechanical	
TS-444-015V	6/750961033029	Y5542	10	750	Mechanical	
TS-444-015W	6/750961033029	Y5542	10	750	Mechanical	
TS-444-015X	6/750961033029	Y5542	10	750	Mechanical	
TS-444-015Y	6/750961033029	Y5542	100	750	Mechanical	
TS-444-015Z	6/750961033029	Y5542	100	750	Mechanical	
TS-444-015AA	6/750961033029	Y5542	100	750	Mechanical	
TS-444-015BB	6/750961033029	Y5542	400	750	Mechanical	
TS-444-015CC	6/750961033029	Y5542	400	750	Mechanical	
TS-444-015DD1	9/1057981147788	Y8123	400	600	None	
TS-444-015DD2	9/1057981147788	Y8123	600	600	None	
TS-444-016A	6/750961033029	Y5542	400	750	Mechanical	
TS-444-016B	7/750950688858	Y5541	10	700	Mechanical	
TS-444-016C	7/750950688858	Y5541	10	700	Mechanical	
TS-444-016D	7/750950688858	Y5541	10	700	Mechanical	
TS-444-016E	7/750950688858	Y5541	100	700	Mechanical	
TS-444-016F	7/750950688858	Y5541	100	700	Mechanical	
TS-444-016G	7/750950688858	Y5541	100	700	Mechanical	
TS-444-016H	7/750950688858	Y5541	400	700	Mechanical	
TS-444-016I	7/750950688858	Y5541	400	700	Mechanical	
TS-444-016J	7/750950688858	Y5541	400	700	Mechanical	
TS-444-016K	8/750960472556	Y8122	10	650	Mechanical	
TS-444-016L	8/750960472556	Y8122	10	650	Mechanical	
TS-444-016M	8/750960472556	Y8122	10	650	Mechanical	
TS-444-016N	6/750961033029	Y8117	100	650	Mechanical	
TS-444-016P	6/750961033029	Y8117	100	650	Mechanical	
TS-444-016Q	6/750961033029	Y8117	100	650	Mechanical	
TS-444-017G	2/999066	Y8121	51,190	600	None	SN-LLNL-SCI-434-V2
TS-444-017H	2/999066	Y8121	51,190	600	None	SN-LLNL-SCI-434-V2
TS-444-017I	2/999066	Y8121	51,190	600	None	SN-LLNL-SCI-434-V2
TS-444-017J	2/999066	Y8121	51,190	600	None	SN-LLNL-SCI-434-V2
TS-444-017K	2/999066	Y8121	51,190	600	None	SN-LLNL-SCI-434-V2
TS-444-017L	2/999066	Y8121	51,190	600	None	SN-LLNL-SCI-434-V2
TS-444-017M	1/999067	Y8120	9050	650	None	
TS-444-017N	1/999067	Y8120	51,170	650	None	SN-LLNL-SCI-434-V2
TS-444-017O1	2/999066	Y8121	4000	600	None	
TS-444-017O2	2/999066	Y8121	6000	600	None	
TS-444-017P	1/999067	Y8120	51,170	650	None	SN-LLNL-SCI-434-V2
TS-444-017Q	1/999067	Y8120	51,170	650	None	SN-LLNL-SCI-434-V2
TS-444-017R	1/999067	Y8120	51,170	650	None	SN-LLNL-SCI-434-V2
TS-444-017S	1/999067	Y8120	51,170	650	None	SN-LLNL-SCI-434-V2
TS-444-018O1	1/999067	Y8120	1000	650	None	
TS-444-018O2	1/999067	Y8120	3000	650	None	
TS-444-018DD2	1/999067	Y8120	6000	650	None	
TS-444-019O1	1/999067	Y8120	10,000	650	None	
TS-444-026	11/170298-L	001494/010075	18,984	200	None	SN-LLNL-SCI-434-V2
TS-444-027	12/170297-L	001669/010074	17,568	300	None	SN-LLNL-SCI-434-V2
TS-444-034	11/170298-L	001494/010075	18,984	200	None	SN-LLNL-SCI-434-V2
TS-444-035	12/170297-L	001669/010074	17,568	300	None	SN-LLNL-SCI-434-V2
TS-444-058A	5/999070	Y5536	1000	550	Mechanical	
TS-444-058B	5/999070	Y5536	1000	550	Mechanical	
TS-444-058C	5/999070	Y5536	1000	550	Mechanical	
TS-444-058D	5/999070	Y5536	67,393	550	None	SN-LLNL-SCI-434-V2 Alloy 59
TS-444-058E	5/999070	Y5536	67,393	550	None	SN-LLNL-SCI-434-V2 Alloy 59
TS-444-058F	5/999070	Y5536	67,393	550	None	SN-LLNL-SCI-434-V2 Alloy 59
TS-444-058G	5/999070	Y5536	67,393	550	None	SN-LLNL-SCI-434-V2 Alloy 59
TS-444-058H	5/999070	Y5536	67,393	550	None	SN-LLNL-SCI-434-V2 Alloy 59
TS-444-058I	5/999070	Y5536	67,393	550	None	SN-LLNL-SCI-434-V2 Alloy 59
TS-444-058J	5/999070	Y5536	67,393	550	None	SN-LLNL-SCI-434-V2 Alloy 59

Specimen Number	Furnace No./SN	TC/Readout ID	Aging Time (Hrs.)	Aging Temp. (C)	Testing Performed	Comments
TS-444-058K	5/999070	Y5536	67,393	550	None	SN-LLNL-SCI-434-V2 Alloy 59
TS-444-058L	5/999070	Y5536	67,393	550	None	SN-LLNL-SCI-434-V2 Alloy 59
TS-444-058M	5/999070	Y5536	67,393	550	None	SN-LLNL-SCI-434-V2 Alloy 59
TS-444-058N	5/999070	Y5536	67,393	550	None	SN-LLNL-SCI-434-V2 Alloy 59
TS-444-058O	5/999070	Y5536	67,393	550	None	SN-LLNL-SCI-434-V2 Alloy 59
TS-444-058P	4/999068	Y5537	4500	500	Mechanical	
TS-444-058Q	4/999068	Y5537	4500	500	Mechanical	
TS-444-058R	4/999068	Y5537	4500	500	Mechanical	
TS-444-058S	4/999068	Y5537	67,386	500	None	SN-LLNL-SCI-434-V2 Alloy 59
TS-444-058T	4/999068	Y5537	67,386	500	None	SN-LLNL-SCI-434-V2 Alloy 59
TS-444-058U	4/999068	Y5537	67,386	500	None	SN-LLNL-SCI-434-V2 Alloy 59
TS-444-058V	4/999068	Y5537	67,386	500	None	SN-LLNL-SCI-434-V2 Alloy 59
TS-444-058W	4/999068	Y5537	67,386	500	None	SN-LLNL-SCI-434-V2 Alloy 59
TS-444-058X	4/999068	Y5537	67,386	500	None	SN-LLNL-SCI-434-V2 Alloy 59
TS-444-058Y	4/999068	Y5537	67,386	500	None	SN-LLNL-SCI-434-V2 Alloy 59
TS-444-058Z	4/999068	Y5537	67,386	500	None	SN-LLNL-SCI-434-V2 Alloy 59
TS-444-058AA	4/999068	Y5537	67,386	500	None	SN-LLNL-SCI-434-V2 Alloy 59
TS-444-058BB	4/999068	Y5537	67,386	500	None	SN-LLNL-SCI-434-V2 Alloy 59
TS-444-058CC	4/999068	Y5537	67,386	500	None	SN-LLNL-SCI-434-V2 Alloy 59
TS-444-058DD	4/999068	Y5537	67,386	500	None	SN-LLNL-SCI-434-V2 Alloy 59
TS-444-058EE	3/999069	Y5538/AA2564	66,878	400	None	SN-LLNL-SCI-434-V2 Alloy 59
TS-444-058FF	3/999069	Y5538/AA2564	66,878	400	None	SN-LLNL-SCI-434-V2 Alloy 59
TS-444-058GG	3/999069	Y5538/AA2564	66,878	400	None	SN-LLNL-SCI-434-V2 Alloy 59
TS-444-058HH	3/999069	Y5538/AA2564	66,878	400	None	SN-LLNL-SCI-434-V2 Alloy 59
TS-444-058II	3/999069	Y5538/AA2564	66,878	400	None	SN-LLNL-SCI-434-V2 Alloy 59
TS-444-058JJ	3/999069	Y5538/AA2564	66,878	400	None	SN-LLNL-SCI-434-V2 Alloy 59
TS-444-058KK	3/999069	Y5538/AA2564	66,878	400	None	SN-LLNL-SCI-434-V2 Alloy 59
TS-444-058LL	3/999069	Y5538/AA2564	66,878	400	None	SN-LLNL-SCI-434-V2 Alloy 59
TS-444-058MM	3/999069	Y5538/AA2564	66,878	400	None	SN-LLNL-SCI-434-V2 Alloy 59
TS-444-058NN	3/999069	Y5538/AA2564	66,878	400	None	SN-LLNL-SCI-434-V2 Alloy 59
TS-444-058OO	3/999069	Y5538/AA2564	66,878	400	None	SN-LLNL-SCI-434-V2 Alloy 59
TS-444-058PP	3/999069	Y5538/AA2564	66,878	400	None	SN-LLNL-SCI-434-V2 Alloy 59
TS-444-058QQ	3/999069	Y5538/AA2564	66,878	400	None	SN-LLNL-SCI-434-V2 Alloy 59
TS-444-058RR	3/999069	Y5538/AA2564	66,878	400	None	SN-LLNL-SCI-434-V2 Alloy 59
TS-444-058SS	3/999069	Y5538/AA2564	66,878	400	None	SN-LLNL-SCI-434-V2 Alloy 59
TS-444-058TT	2/999066	Y5539	1000	750	Mechanical	
TS-444-058UU	2/999066	Y5539	1000	750	Mechanical	
TS-444-058VV	2/999066	Y5539	1000	750	Mechanical	
TS-444-058WW	2/999066	Y5539	4000	750	Mechanical	
TS-444-058XX	2/999066	Y5539	4000	750	Mechanical	
TS-444-058YY	2/999066	Y5539	4000	750	Mechanical	
TS-444-058ZZ	2/999066	Y5539	10,076	750	None	
TS-444-058AAA	2/999066	Y5539	10,076	750	None	
TS-444-058BBB	2/999066	Y5539	10,076	750	None	
TS-444-058CCC	2/999066	Y5539	10,076	750	None	
TS-444-058DDD	2/999066	Y5539	10,076	750	None	
TS-444-058EEE	2/999066	Y5539	10,076	750	None	
TS-444-058FFF	1/999067	Y5540	1000	700	Mechanical	
TS-444-058GGG	1/999067	Y5540	1000	700	Mechanical	
TS-444-058HHH	1/999067	Y5540	1000	700	Mechanical	
TS-444-058III	1/999067	Y5540	4000	700	Mechanical	
TS-444-058JJJ	1/999067	Y5540	4000	700	Mechanical	
TS-444-058KKK	1/999067	Y5540	4000	700	Mechanical	
TS-444-058LLL	1/999067	Y5540	10,073	700	None	
TS-444-058MMM	1/999067	Y5540	10,073	700	None	
TS-444-059A	1/999067	Y5540	10,073	700	None	
TS-444-059B	1/999067	Y5540	10,073	700	None	
TS-444-059C	1/999067	Y5540	10,073	700	None	
TS-444-059D	1/999067	Y5540	10,073	700	None	
TS-444-059E	6/750961033029	Y5542	1	750	Mechanical	
TS-444-059F	6/750961033029	Y5542	1	750	Mechanical	
TS-444-059G	6/750961033029	Y5542	1	750	Mechanical	
TS-444-059H	6/750961033029	Y5542	10	750	Mechanical	
TS-444-059I	6/750961033029	Y5542	10	750	Mechanical	
TS-444-059J	6/750961033029	Y5542	10	750	Mechanical	
TS-444-059K	6/750961033029	Y5542	100	750	Mechanical	
TS-444-059L	6/750961033029	Y5542	100	750	Mechanical	
TS-444-059M	6/750961033029	Y5542	100	750	Mechanical	
TS-444-059N	6/750961033029	Y5542	400	750	Mechanical	

Specimen Number	Furnace No./SN	TC/Readout ID	Aging Time (Hrs.)	Aging Temp. (C)	Testing Performed	Comments
TS-444-059O	6/750961033029	Y5542	400	750	Mechanical	
TS-444-059P	6/750961033029	Y5542	400	750	Mechanical	
TS-444-059Q	7/750950688858	Y5541	10	700	Mechanical	
TS-444-059R	7/750950688858	Y5541	10	700	Mechanical	
TS-444-059S	7/750950688858	Y5541	10	700	Mechanical	
TS-444-059T	7/750950688858	Y5541	30	700	None	
TS-444-059U	7/750950688858	Y5541	30	700	None	
TS-444-059V	7/750950688858	Y5541	30	700	None	
TS-444-059W	7/750950688858	Y5541	60	700	None	
TS-444-059X	7/750950688858	Y5541	60	700	None	
TS-444-059Y	7/750950688858	Y5541	60	700	None	
TS-444-059Z	7/750950688858	Y5541	100	700	Mechanical	
TS-444-059AA	7/750950688858	Y5541	100	700	Mechanical	
TS-444-059BB	7/750950688858	Y5541	100	700	Mechanical	
TS-444-059CC	5/999070	Y5536	1000	550	TEM	
TS-444-059DD	5/999070	Y5536	2000	550	TEM	
TS-444-059EE	5/999070	Y5536	4500	550	None	
TS-444-059FF	5/999070	Y5536	6000	550	None	
TS-444-059GG	5/999070	Y5536	8000	550	None	
TS-444-059HH	5/999070	Y5536	67,393	550	None	SN-LLNL-SCI-434-V2 Alloy 59
TS-444-059II	5/999070	Y5536	67,393	550	None	SN-LLNL-SCI-434-V2 Alloy 59
TS-444-059JJ	5/999070	Y5536	30000	550	None	
TS-444-059KK	5/999070	Y5536	67,393	550	None	SN-LLNL-SCI-434-V2 Alloy 59
TS-444-059LL	4/999068	Y5537	1000	500	TEM	
TS-444-059MM	4/999068	Y5537	2000	500	TEM	
TS-444-059NN	4/999068	Y5537	4500	500	None	
TS-444-059OO	4/999068	Y5537	6000	500	None	
TS-444-059PP	4/999068	Y5537	8000	500	None	
TS-444-059QQ	4/999068	Y5537	67,386	500	None	SN-LLNL-SCI-434-V2 Alloy 59
TS-444-059RR	4/999068	Y5537	67,386	500	None	SN-LLNL-SCI-434-V2 Alloy 59
TS-444-059SS	4/999068	Y5537	30000	500	None	
TS-444-059TT	4/999068	Y5537	67,386	500	None	SN-LLNL-SCI-434-V2 Alloy 59
TS-444-059UU	3/999069	Y5538	1000	400	TEM	
TS-444-059VV	5/999070	Y5536	1000	550	Mechanical	
TS-444-059WW	5/999070	Y5536	1000	550	Mechanical	
TS-444-059XX	5/999070	Y5536	1000	550	Mechanical	
TS-444-059YY	5/999070	Y5536	67,393	550	None	SN-LLNL-SCI-434-V2 Alloy 59
TS-444-059ZZ	5/999070	Y5536	67,393	550	None	SN-LLNL-SCI-434-V2 Alloy 59
TS-444-059AAA	5/999070	Y5536	67,393	550	None	SN-LLNL-SCI-434-V2 Alloy 59
TS-444-059BBB	5/999070	Y5536	67,393	550	None	SN-LLNL-SCI-434-V2 Alloy 59
TS-444-059CCC	5/999070	Y5536	67,393	550	None	SN-LLNL-SCI-434-V2 Alloy 59
TS-444-059DDD	5/999070	Y5536	67,393	550	None	SN-LLNL-SCI-434-V2 Alloy 59
TS-444-059EEE	5/999070	Y5536	67,393	550	None	SN-LLNL-SCI-434-V2 Alloy 59
TS-444-059FFF	5/999070	Y5536	67,393	550	None	SN-LLNL-SCI-434-V2 Alloy 59
TS-444-059GGG	5/999070	Y5536	67,393	550	None	SN-LLNL-SCI-434-V2 Alloy 59
TS-444-059HHH	5/999070	Y5536	67,393	550	None	SN-LLNL-SCI-434-V2 Alloy 59
TS-444-059III	5/999070	Y5536	67,393	550	None	SN-LLNL-SCI-434-V2 Alloy 59
TS-444-059JJJ	5/999070	Y5536	67,393	550	None	SN-LLNL-SCI-434-V2 Alloy 59
TS-444-059KKK	4/999068	Y5537	4500	500	Mechanical	
TS-444-059LLL	4/999068	Y5537	4500	500	Mechanical	
TS-444-059MMM	4/999068	Y5537	4500	500	Mechanical	
TS-444-059NNN	4/999068	Y5537	67,386	500	None	SN-LLNL-SCI-434-V2 Alloy 59
TS-444-060A	3/999069	Y5538	2000	400	TEM	
TS-444-060B	3/999069	Y5538	4500	400	None	
TS-444-060C	3/999069	Y5538	6000	400	None	
TS-444-060D	3/999069	Y5538	8000	400	None	
TS-444-060E	3/999069	Y5538/AA2564		400	None	
TS-444-060F	3/999069	Y5538/AA2564	66,878	400	None	SN-LLNL-SCI-434-V2 Alloy 59
TS-444-060G	3/999069	Y5538/AA2564	30000	400	None	
TS-444-060H	3/999069	Y5538/AA2564	66,878	400	None	SN-LLNL-SCI-434-V2 Alloy 59
TS-444-060I	3/999069	Y5538/AA2564	66,878	400	None	SN-LLNL-SCI-434-V2 Alloy 59
TS-444-060J	3/999069	Y5538/AA2564	66,878	400	None	SN-LLNL-SCI-434-V2 Alloy 59
TS-444-060K	2/999066	Y5539	1000	750	TEM	
TS-444-060L	2/999066	Y5539	4000	750	None	
TS-444-060M	1/999067	Y5540	1000	700	TEM	
TS-444-060N	1/999067	Y5540	4000	700	None	
TS-444-060O	8/750960472556	Y8122	100	550	None	
TS-444-060P	8/750960472556	Y8122	300	550	None	
TS-444-060Q	8/750960472556	Y8122	600	550	None	

Specimen Number	Furnace No./SN	TC/Readout ID	Aging Time (Hrs.)	Aging Temp. (C)	Testing Performed	Comments
TS-444-060R	9/1057981147788	Y8123	100	500	None	
TS-444-060S	9/1057981147788	Y8123	300	500	None	
TS-444-060T	9/1057981147788	Y8123	600	500	None	
TS-444-060U	6/750961033029	Y5542	1	750	None	
TS-444-060V	6/750961033029	Y5542	2	750	None	
TS-444-060W	6/750961033029	Y5542	4	750	None	
TS-444-060X	6/750961033029	Y5542	6	750	None	
TS-444-060Y	6/750961033029	Y5542	8	750	None	
TS-444-060Z	6/750961033029	Y5542	10	750	None	
TS-444-060AA	6/750961033029	Y5542	60	750	None	
TS-444-060BB	6/750961033029	Y5542	100	750	None	
TS-444-060CC	6/750961033029	Y5542	30	750	None	
TS-444-060DD	6/750961033029	Y5542	400	750	None	
TS-444-060EE	7/750950688858	Y5541	1	700	None	
TS-444-060FF	7/750950688858	Y5541	4	700	None	
TS-444-060GG	7/750950688858	Y5541	10	700	None	
TS-444-060HH	4/999068	Y5537	67,386	500		SN-LLNL-SCI-434-V2 Alloy 59
TS-444-060II	4/999068	Y5537	67,386	500	None	SN-LLNL-SCI-434-V2 Alloy 59
TS-444-060JJ	4/999068	Y5537	67,386	500	None	SN-LLNL-SCI-434-V2 Alloy 59
TS-444-060KK	4/999068	Y5537	67,386	500	None	SN-LLNL-SCI-434-V2 Alloy 59
TS-444-060LL	4/999068	Y5537	67,386	500	None	SN-LLNL-SCI-434-V2 Alloy 59
TS-444-060MM	4/999068	Y5537	67,386	500	None	SN-LLNL-SCI-434-V2 Alloy 59
TS-444-060NN	4/999068	Y5537	67,386	500	None	SN-LLNL-SCI-434-V2 Alloy 59
TS-444-060OO	4/999068	Y5537	67,386	500	None	SN-LLNL-SCI-434-V2 Alloy 59
TS-444-060PP	4/999068	Y5537	67,386	500	None	SN-LLNL-SCI-434-V2 Alloy 59
TS-444-060QQ	4/999068	Y5537	67,386	500	None	SN-LLNL-SCI-434-V2 Alloy 59
TS-444-060RR	4/999068	Y5537	67,386	500	None	SN-LLNL-SCI-434-V2 Alloy 59
TS-444-060SS	3/999069	Y5538/AA2564	66,878	400	None	SN-LLNL-SCI-434-V2 Alloy 59
TS-444-060TT	3/999069	Y5538/AA2564	66,878	400	None	SN-LLNL-SCI-434-V2 Alloy 59
TS-444-060UU	3/999069	Y5538/AA2564	66,878	400	None	SN-LLNL-SCI-434-V2 Alloy 59
TS-444-060VV	3/999069	Y5538/AA2564	66,878	400	None	SN-LLNL-SCI-434-V2 Alloy 59
TS-444-060WW	3/999069	Y5538/AA2564	66,878	400	None	SN-LLNL-SCI-434-V2 Alloy 59
TS-444-060XX	3/999069	Y5538/AA2564	66,878	400	None	SN-LLNL-SCI-434-V2 Alloy 59
TS-444-060YY	3/999069	Y5538/AA2564	66,878	400	None	SN-LLNL-SCI-434-V2 Alloy 59
TS-444-060ZZ	3/999069	Y5538/AA2564	66,878	400	None	SN-LLNL-SCI-434-V2 Alloy 59
TS-444-060AAA	3/999069	Y5538/AA2564	66,878	400	None	SN-LLNL-SCI-434-V2 Alloy 59
TS-444-060BBB	3/999069	Y5538/AA2564	66,878	400	None	SN-LLNL-SCI-434-V2 Alloy 59
TS-444-060CCC	3/999069	Y5538/AA2564	66,878	400	None	SN-LLNL-SCI-434-V2 Alloy 59
TS-444-060DDD	3/999069	Y5538/AA2564	66,878	400	None	SN-LLNL-SCI-434-V2 Alloy 59
TS-444-060EEE	3/999069	Y5538/AA2564	66,878	400	None	SN-LLNL-SCI-434-V2 Alloy 59
TS-444-060FFF	3/999069	Y5538/AA2564	66,878	400	None	SN-LLNL-SCI-434-V2 Alloy 59
TS-444-060GGG	3/999069	Y5538/AA2564	66,878	400	None	SN-LLNL-SCI-434-V2 Alloy 59
TS-444-060HHH	2/999066	Y5539	1000	750	Mechanical	
TS-444-060III	2/999066	Y5539	1000	750	Mechanical	
TS-444-060JJJ	2/999066	Y5539	1000	750	Mechanical	
TS-444-060KKK	2/999066	Y5539	4000	750	Mechanical	
TS-444-060LLL	2/999066	Y5539	4000	750	Mechanical	
TS-444-060MMM	2/999066	Y5539	4000	750	Mechanical	
TS-444-060NNN	2/999066	Y5539	10,037	750	None	
TS-444-061A	7/750950688858	Y5541	20	700	None	
TS-444-061B	7/750950688858	Y5541	40	700	None	
TS-444-061C	7/750950688858	Y5541	60	700	None	
TS-444-061D	7/750950688858	Y5541	80	700	None	
TS-444-061E	7/750950688858	Y5541	100	700	None	
TS-444-061F	7/750950688858	Y5541	300	700	None	
TS-444-061G	7/750950688858	Y5541	400	700	None	
TS-444-061H	7/750950688858	Y5541	600	700	None	
TS-444-061I	8/750960472556	Y8122	1	650	None	
TS-444-061J	8/750960472556	Y8122	4	650	None	
TS-444-061K	8/750960472556	Y8122	10	650	None	
TS-444-061L	8/750960472556	Y8122	40	650	None	
TS-444-061M	6/750961033029	Y8117	100	650	None	
TS-444-061N	6/750961033029	Y8117	200	650	None	
TS-444-061O	8/750960472556	Y8122	400	650	None	
TS-444-061P	8/750960472556	Y8122	600	650	None	
TS-444-061Q	9/1057981147788	Y8123	1	600	None	
TS-444-061R	9/1057981147788	Y8123	4	600	None	
TS-444-061S	9/1057981147788	Y8123	10	600	None	
TS-444-061T	9/1057981147788	Y8123	40	600	None	

Specimen Number	Furnace No./SN	TC/Readout ID	Aging Time (Hrs.)	Aging Temp. (C)	Testing Performed	Comments
TS-444-061U	7/750950688858	Y8119	100	600	None	
TS-444-061V	7/750950688858	Y8119	200	600	None	
TS-444-061W	9/1057981147788	Y8123	400	600	None	
TS-444-061X	9/1057981147788	Y8123	600	600	None	
TS-444-061Y	8/750960472556	Y8122	800	650	None	
TS-444-061Z	9/1057981147788	Y8123	800	600	None	
TS-444-061HH	2/999066	Y5539	10,073	750	None	
TS-444-061II	2/999066	Y5539	10,073	750	None	
TS-444-061JJ	2/999066	Y5539	10,073	750	None	
TS-444-061KK	2/999066	Y5539	10,073	750	None	
TS-444-061LL	2/999066	Y5539	10,073	750	None	
TS-444-061MM	1/999067	Y5540	1000	700	Mechanical	
TS-444-061NN	1/999067	Y5540	1000	700	None	
TS-444-061OO	1/999067	Y5540	1000	700	Mechanical	
TS-444-061PP	1/999067	Y5540	4000	700	Mechanical	
TS-444-061QQ	1/999067	Y5540	4000	700	Mechanical	
TS-444-061RR	1/999067	Y5540	4000	700	Mechanical	
TS-444-061SS	1/999067	Y5540	10,073	700	None	
TS-444-061TT	1/999067	Y5540	10,073	700	None	
TS-444-061UU	1/999067	Y5540	10,073	700	None	
TS-444-061VV	1/999067	Y5540	10,073	700	None	
TS-444-061WW	1/999067	Y5540	10,073	700	None	
TS-444-061XX	1/999067	Y5540	10,073	700	None	
TS-444-061YY	6/750961033029	Y5542	1	750	Mechanical	
TS-444-061ZZ	6/750961033029	Y5542	1	750	Mechanical	
TS-444-061AAA	6/750961033029	Y5542	1	750	Mechanical	
TS-444-061BBB	6/750961033029	Y5542	10	750	Mechanical	
TS-444-061CCC	6/750961033029	Y5542	10	750	Mechanical	
TS-444-061DDD	6/750961033029	Y5542	10	750	Mechanical	
TS-444-061EEE	6/750961033029	Y5542	100	750	Mechanical	
TS-444-061FFF	6/750961033029	Y5542	100	750	Mechanical	
TS-444-061GGG	6/750961033029	Y5542	100	750	Mechanical	
TS-444-061HHH	6/750961033029	Y5542	400	750	Mechanical	
TS-444-061III	6/750961033029	Y5542	400	750	Mechanical	
TS-444-061JJJ	6/750961033029	Y5542	400	750	Mechanical	
TS-444-061KKK	7/750950688858	Y5541	10	700	Mechanical	
TS-444-061LLL	7/750950688858	Y5541	10	700	Mechanical	
TS-444-061MMM	7/750950688858	Y5541	10	700	Mechanical	
TS-444-061NNN	7/750950688858	Y5541	100	700	Mechanical	
TS-444-062HH	7/750950688858	Y5541	100	700	Mechanical	
TS-444-062II	7/750950688858	Y5541	100	700	Mechanical	
TS-444-062JJ	7/750950688858	Y5541	400	700	Mechanical	
TS-444-062KK	7/750950688858	Y5541	400	700	Mechanical	
TS-444-062LL	7/750950688858	Y5541	400	700	Mechanical	
TS-444-062MM	8/750960472556	Y8122	10	650	Mechanical	
TS-444-062NN	8/750960472556	Y8122	10	650	Mechanical	
TS-444-062OO	8/750960472556	Y8122	10	650	Mechanical	
TS-444-062PP	6/750961033029	Y8117	100	650	Mechanical	
TS-444-062QQ	6/750961033029	Y8117	100	650	Mechanical	
TS-444-062RR	6/750961033029	Y8117	100	650	Mechanical	
TS-444-062KKK	2/999066	Y8121	51,190	600	None	SN-LLNL-SCI-434-V2 Alloy 59
TS-444-062LLL	2/999066	Y8121	51,190	600	None	SN-LLNL-SCI-434-V2 Alloy 59
TS-444-062MMM	2/999066	Y8121	51,190	600	None	SN-LLNL-SCI-434-V2 Alloy 59
TS-444-062NNN	2/999066	Y8121	51,190	600	None	SN-LLNL-SCI-434-V2 Alloy 59
TS-444-063EE	2/999066	Y8121	51,190	600	None	SN-LLNL-SCI-434-V2 Alloy 59
TS-444-063FF	2/999066	Y8121	51,190	600	None	SN-LLNL-SCI-434-V2 Alloy 59
TS-444-063GG	1/999067	Y8120	9050	650	None	
TS-444-063HH	1/999067	Y8120	51,170	650	None	SN-LLNL-SCI-434-V2 Alloy 59
TS-444-063II	1/999067	Y8120	51,170	650	None	SN-LLNL-SCI-434-V2 Alloy 59
TS-444-063JJ	1/999067	Y8120	51,170	650	None	SN-LLNL-SCI-434-V2 Alloy 59
TS-444-063KK	1/999067	Y8120	51,170	650	None	SN-LLNL-SCI-434-V2 Alloy 59
TS-444-063LL	1/999067	Y8120	51,170	650	None	SN-LLNL-SCI-434-V2 Alloy 59
TS-444-064A	7/750950688858	Y5541	400	700	Mechanical	
TS-444-064B	7/750950688858	Y5541	400	700	Mechanical	
TS-444-064C	7/750950688858	Y5541	400	700	Mechanical	
TS-444-064D	8/750960472556	Y8122	10	650	Mechanical	
TS-444-064E	8/750960472556	Y8122	10	650	Mechanical	
TS-444-064F	8/750960472556	Y8122	10	650	Mechanical	
TS-444-064G	6/750961033029	Y8117	100	650	Mechanical	

Specimen Number	Furnace No./SN	TC/Readout ID	Aging Time (Hrs.)	Aging Temp. (C)	Testing Performed	Comments
TS-444-064H	6/750961033029	Y8117	100	650	Mechanical	
TS-444-064I	6/750961033029	Y8117	100	650	Mechanical	
TS-444-064J	6/750961033029	Y8117	300	650	Mechanical	
TS-444-064K	6/750961033029	Y8117	300	650	Mechanical	
TS-444-064L	6/750961033029	Y8117	300	650	Mechanical	
TS-444-064M	8/750960472556	Y8122	600	650	Mechanical	
TS-444-064N	8/750960472556	Y8122	600	650	Mechanical	
TS-444-064O	8/750960472556	Y8122	600	650	Mechanical	
TS-444-064HH	2/999066	Y8122	51,190	600	None	SN-LLNL-SCI-434-V2 Alloy 59
TS-444-064II	2/999066	Y8122	51,190	600	None	SN-LLNL-SCI-434-V2 Alloy 59
TS-444-064JJ	2/999066	Y8122	51,190	600	None	SN-LLNL-SCI-434-V2 Alloy 59
TS-444-064KK	2/999066	Y8122	51,190	600	None	SN-LLNL-SCI-434-V2 Alloy 59
TS-444-064LL	2/999066	Y8122	51,190	600	None	SN-LLNL-SCI-434-V2 Alloy 59
TS-444-064MM	2/999066	Y8122	51,190	600	None	SN-LLNL-SCI-434-V2 Alloy 59
TS-444-064NN	1/999067	Y8120	51,170	650	None	SN-LLNL-SCI-434-V2 Alloy 59
TS-444-064OO	1/999067	Y8120	51,170	650	None	SN-LLNL-SCI-434-V2 Alloy 59
TS-444-064PP	1/999067	Y8120	51,170	650	None	SN-LLNL-SCI-434-V2 Alloy 59
TS-444-064QQ	1/999067	Y8120	51,170	650	None	SN-LLNL-SCI-434-V2 Alloy 59
TS-444-064RR	1/999067	Y8120	51,170	650	None	SN-LLNL-SCI-434-V2 Alloy 59
TS-444-064SS	1/999067	Y8120	51,170	650	None	SN-LLNL-SCI-434-V2 Alloy 59
DEA 113	750960472556	XCIB-2/8525309-1	10	700	Corrosion	SN-LLNL-SCI-426-V1
DEA 114	750960472556	XCIB-2/8525309-1	10	700	Corrosion	SN-LLNL-SCI-426-V1
DEA 115	750960472556	XCIB-2/8525309-1	10	700	Corrosion	SN-LLNL-SCI-426-V1
DEA 116	750960472556	XCIB-2/8525309-1	10	700	Corrosion	SN-LLNL-SCI-426-V1
DEA 117	750960472556	XCIB-2/8525309-1	10	700	Corrosion	SN-LLNL-SCI-426-V1
DEA 118	750960472556	XCIB-2/8525309-1	10	700	Corrosion	SN-LLNL-SCI-426-V1
DEA 119	750960472556	XCIB-2/8525309-1	10	700	Corrosion	SN-LLNL-SCI-426-V1
DEA 120	750960472556	XCIB-2/8525309-1	10	700	Corrosion	SN-LLNL-SCI-426-V1
DEA 121	750960472556	XCIB-2/8525309-1	10	700	Corrosion	SN-LLNL-SCI-426-V1
DEA 122	750960472556	XCIB-2/8525309-1	10	700	Corrosion	SN-LLNL-SCI-426-V1
DEA 123	750960472556	XCIB-2/8525309-1	10	700	Corrosion	SN-LLNL-SCI-426-V1
DEA 124	750960472556	XCIB-2/8525309-1	10	700	Corrosion	SN-LLNL-SCI-426-V1
DEA 125	750960472556	XCIB-2/8525309-1	10	700	Corrosion	SN-LLNL-SCI-426-V1
DEA 126	750960472556	XCIB-2/8525309-1	10	700	Corrosion	SN-LLNL-SCI-426-V1
DEA 127	750960472556	XCIB-2/8525309-1	10	700	Corrosion	SN-LLNL-SCI-426-V1
DEA 128	750960472556	XCIB-2/8525309-1	10	700	Corrosion	SN-LLNL-SCI-426-V1
DEA 129	750960472556	XCIB-2/8525309-1	10	700	Corrosion	SN-LLNL-SCI-426-V1
DEA 130	750960472556	XCIB-2/8525309-1	10	700	Corrosion	SN-LLNL-SCI-426-V1
DEA 131	750960472556	XCIB-2/8525309-1	10	700	Corrosion	SN-LLNL-SCI-426-V1
DEA 132	750960472556	XCIB-2/8525309-1	10	700	Corrosion	SN-LLNL-SCI-426-V1
DEA 133	750960472556	XCIB-2/8525309-1	10	700	Corrosion	SN-LLNL-SCI-426-V1
DEA 134	750960472556	XCIB-2/8525309-1	10	700	Corrosion	SN-LLNL-SCI-426-V1
DEA 135	750960472556	XCIB-2/8525309-1	10	700	Corrosion	SN-LLNL-SCI-426-V1
DEA 136	750960472556	XCIB-2/8525309-1	10	700	Corrosion	SN-LLNL-SCI-426-V1
DEA 137	750960472556	XCIB-2/8525309-1	10	700	Corrosion	SN-LLNL-SCI-426-V1
DEA 138	750960472556	XCIB-2/8525309-1	10	700	Corrosion	SN-LLNL-SCI-426-V1
DEA 139	750960472556	XCIB-2/8525309-1	10	700	Corrosion	SN-LLNL-SCI-426-V1
DEA 140	750960472556	XCIB-2/8525309-1	10	700	Corrosion	SN-LLNL-SCI-426-V1
DEA 141	750960472556	XCIB-2/8525309-1	10	700	Corrosion	SN-LLNL-SCI-426-V1
DEA 142	750960472556	XCIB-2/8525309-1	10	700	Corrosion	SN-LLNL-SCI-426-V1
DEA 143	750960472556	XCIB-2/8525309-1	10	700	Corrosion	SN-LLNL-SCI-426-V1
DEA 144	750960472556	XCIB-2/8525309-1	10	700	Corrosion	SN-LLNL-SCI-426-V1
DEA 145	750960472556	XCIB-2/8525309-1	10	700	Corrosion	SN-LLNL-SCI-426-V1
DEA 146	750960472556	XCIB-2/8525309-1	10	700	Corrosion	SN-LLNL-SCI-426-V1
DEA 147	750960472556	XCIB-2/8525309-1	10	700	Corrosion	SN-LLNL-SCI-426-V1
DEA 148	750960472556	XCIB-2/8525309-1	10	700	Corrosion	SN-LLNL-SCI-426-V1
DEA 149	750960472556	XCIB-2/8525309-1	10	700	Corrosion	SN-LLNL-SCI-426-V1
DEA 150	750960472556	XCIB-2/8525309-1	10	700	Corrosion	SN-LLNL-SCI-426-V1
DEA 151	750960472556	XCIB-2/8525309-1	10	700	Corrosion	SN-LLNL-SCI-426-V1
DEA 152	750960472556	XCIB-2/8525309-1	10	700	Corrosion	SN-LLNL-SCI-426-V1
DEA 153	750960472556	XCIB-2/8525309-1	10	700	Corrosion	SN-LLNL-SCI-426-V1
DEA 154	750960472556	XCIB-2/8525309-1	10	700	Corrosion	SN-LLNL-SCI-426-V1
DEA 155	750960472556	XCIB-2/8525309-1	10	700	Corrosion	SN-LLNL-SCI-426-V1
DEA 156	750960472556	XCIB-2/8525309-1	10	700	Corrosion	SN-LLNL-SCI-426-V1
DEA 157	750960472556	XCIB-2/8525309-1	10	700	Corrosion	SN-LLNL-SCI-426-V1
DEA 158	750960472556	XCIB-2/8525309-1	10	700	Corrosion	SN-LLNL-SCI-426-V1
DEA 159	750960472556	XCIB-2/8525309-1	10	700	Corrosion	SN-LLNL-SCI-426-V1
DEA 160	750960472556	XCIB-2/8525309-1	10	700	Corrosion	SN-LLNL-SCI-426-V1
DEA 161	750960472556	XCIB-2/8525309-1	10	700	Corrosion	SN-LLNL-SCI-426-V1

Specimen Number	Furnace No./SN	TC/Readout ID	Aging Time (Hrs.)	Aging Temp. (C)	Testing Performed	Comments
DEA 162	750960472556	XCIB-2/8525309-1	10	700	Corrosion	SN-LLNL-SCI-426-V1
DEA 163	750960472556	XCIB-2/8525309-1	10	700	Corrosion	SN-LLNL-SCI-426-V1
DEA 164	750960472556	XCIB-2/8525309-1	10	700	Corrosion	SN-LLNL-SCI-426-V1
DEA 165	750960472556	XCIB-2/8525309-1	10	700	Corrosion	SN-LLNL-SCI-426-V1
DEA 166	750960472556	XCIB-2/8525309-1	10	700	Corrosion	SN-LLNL-SCI-426-V1
DEA 167	750960472556	XCIB-2/8525309-1	10	700	Corrosion	SN-LLNL-SCI-426-V1
DEA 168	750960472556	XCIB-2/8525309-1	10	700	Corrosion	SN-LLNL-SCI-426-V1
DEA 169	750960472556	XCIB-2/8525309-1	10	700	Corrosion	SN-LLNL-SCI-426-V1
DEA 170	750960472556	XCIB-2/8525309-1	10	700	Corrosion	SN-LLNL-SCI-426-V1
DEA 171	750960472556	XCIB-2/8525309-1	10	700	Corrosion	SN-LLNL-SCI-426-V1
DEA 172	750960472556	XCIB-2/8525309-1	10	700	Corrosion	SN-LLNL-SCI-426-V1
DEA 173	750960472556	XCIB-1/8525309-1	173	700	Corrosion	SN-LLNL-SCI-426-V1
DEA 174	750960472556	XCIB-1/8525309-1	173	700	Corrosion	SN-LLNL-SCI-426-V1
DEA 175	750960472556	XCIB-1/8525309-1	173	700	Corrosion	SN-LLNL-SCI-426-V1
DEA 176	750960472556	XCIB-1/8525309-1	173	700	Corrosion	SN-LLNL-SCI-426-V1
DEA 177	750960472556	XCIB-1/8525309-1	173	700	Corrosion	SN-LLNL-SCI-426-V1
DEA 178	750960472556	XCIB-1/8525309-1	173	700	Corrosion	SN-LLNL-SCI-426-V1
DEA 179	750960472556	XCIB-1/8525309-1	173	700	Corrosion	SN-LLNL-SCI-426-V1
DEA 180	750960472556	XCIB-1/8525309-1	173	700	Corrosion	SN-LLNL-SCI-426-V1
DEA 181	750960472556	XCIB-1/8525309-1	173	700	Corrosion	SN-LLNL-SCI-426-V1
DEA 182	750960472556	XCIB-1/8525309-1	173	700	Corrosion	SN-LLNL-SCI-426-V1
DEA 183	750960472556	XCIB-1/8525309-1	173	700	Corrosion	SN-LLNL-SCI-426-V1
DEA 184	750960472556	XCIB-1/8525309-1	173	700	Corrosion	SN-LLNL-SCI-426-V1
DEA 185	750960472556	XCIB-1/8525309-1	173	700	Corrosion	SN-LLNL-SCI-426-V1
DEA 186	750960472556	XCIB-1/8525309-1	173	700	Corrosion	SN-LLNL-SCI-426-V1
DEA 187	750960472556	XCIB-1/8525309-1	173	700	Corrosion	SN-LLNL-SCI-426-V1
DEA 188	750960472556	XCIB-1/8525309-1	173	700	Corrosion	SN-LLNL-SCI-426-V1
DEA 189	750960472556	XCIB-1/8525309-1	173	700	Corrosion	SN-LLNL-SCI-426-V1
DEA 190	750960472556	XCIB-1/8525309-1	173	700	Corrosion	SN-LLNL-SCI-426-V1
DEA 191	750960472556	XCIB-1/8525309-1	173	700	Corrosion	SN-LLNL-SCI-426-V1
DEA 192	750960472556	XCIB-1/8525309-1	173	700	Corrosion	SN-LLNL-SCI-426-V1
DEA 193	750960472556	XCIB-1/8525309-1	173	700	Corrosion	SN-LLNL-SCI-426-V1
DEA 194	750960472556	XCIB-1/8525309-1	173	700	Corrosion	SN-LLNL-SCI-426-V1
DEA 195	750960472556	XCIB-1/8525309-1	173	700	Corrosion	SN-LLNL-SCI-426-V1
DEA 196	750960472556	XCIB-1/8525309-1	173	700	Corrosion	SN-LLNL-SCI-426-V1
DEA 197	750960472556	XCIB-1/8525309-1	173	700	Corrosion	SN-LLNL-SCI-426-V1
DEA 198	750960472556	XCIB-1/8525309-1	173	700	Corrosion	SN-LLNL-SCI-426-V1
DEA 199	750960472556	XCIB-1/8525309-1	173	700	Corrosion	SN-LLNL-SCI-426-V1
DEA 200	750960472556	XCIB-1/8525309-1	173	700	Corrosion	SN-LLNL-SCI-426-V1
DEA 201	750960472556	XCIB-1/8525309-1	173	700	Corrosion	SN-LLNL-SCI-426-V1
DEA 202	750960472556	XCIB-1/8525309-1	173	700	Corrosion	SN-LLNL-SCI-426-V1
DEA 203	750960472556	XCIB-1/8525309-1	173	700	Corrosion	SN-LLNL-SCI-426-V1
DEA 204	750960472556	XCIB-1/8525309-1	173	700	Corrosion	SN-LLNL-SCI-426-V1
DEA 205	750960472556	XCIB-1/8525309-1	173	700	Corrosion	SN-LLNL-SCI-426-V1
DEA 206	750960472556	XCIB-1/8525309-1	173	700	Corrosion	SN-LLNL-SCI-426-V1
DEA 207	750960472556	XCIB-1/8525309-1	173	700	Corrosion	SN-LLNL-SCI-426-V1
DEA 208	750960472556	XCIB-1/8525309-1	173	700	Corrosion	SN-LLNL-SCI-426-V1
DEA 209	750960472556	XCIB-1/8525309-1	173	700	Corrosion	SN-LLNL-SCI-426-V1
DEA 210	750960472556	XCIB-1/8525309-1	173	700	Corrosion	SN-LLNL-SCI-426-V1
DEA 211	750960472556	XCIB-1/8525309-1	173	700	Corrosion	SN-LLNL-SCI-426-V1
DEA 212	750960472556	XCIB-1/8525309-1	173	700	Corrosion	SN-LLNL-SCI-426-V1
DEA 213	750960472556	XCIB-1/8525309-1	173	700	Corrosion	SN-LLNL-SCI-426-V1
DEA 214	750960472556	XCIB-1/8525309-1	173	700	Corrosion	SN-LLNL-SCI-426-V1
DEA 215	750960472556	XCIB-1/8525309-1	173	700	Corrosion	SN-LLNL-SCI-426-V1
DEA 216	750960472556	XCIB-1/8525309-1	173	700	Corrosion	SN-LLNL-SCI-426-V1
DEA 217	750960472556	XCIB-1/8525309-1	173	700	Corrosion	SN-LLNL-SCI-426-V1
DEA 218	750960472556	XCIB-1/8525309-1	173	700	Corrosion	SN-LLNL-SCI-426-V1
DEA 219	750960472556	XCIB-1/8525309-1	173	700	Corrosion	SN-LLNL-SCI-426-V1
DEA 220	750960472556	XCIB-1/8525309-1	173	700	Corrosion	SN-LLNL-SCI-426-V1
DEA 221	750960472556	XCIB-1/8525309-1	173	700	Corrosion	SN-LLNL-SCI-426-V1
DEA 222	750960472556	XCIB-1/8525309-1	173	700	Corrosion	SN-LLNL-SCI-426-V1
DEA 223	750960472556	XCIB-1/8525309-1	173	700	Corrosion	SN-LLNL-SCI-426-V1
DEA 224	750960472556	XCIB-1/8525309-1	173	700	Corrosion	SN-LLNL-SCI-426-V1
DEA 225	750960472556	XCIB-1/8525309-1	173	700	Corrosion	SN-LLNL-SCI-426-V1
DEA 226	750960472556	XCIB-1/8525309-1	173	700	Corrosion	SN-LLNL-SCI-426-V1
DEA 227	750960472556	XCIB-1/8525309-1	173	700	Corrosion	SN-LLNL-SCI-426-V1
DEA 228	750960472556	XCIB-1/8525309-1	173	700	Corrosion	SN-LLNL-SCI-426-V1
DEA 229	750960472556	XCIB-1/8525309-1	173	700	Corrosion	SN-LLNL-SCI-426-V1
DEA 230	750960472556	XCIB-1/8525309-1	173	700	Corrosion	SN-LLNL-SCI-426-V1

Specimen Number	Furnace No./SN	TC/Readout ID	Aging Time (Hrs.)	Aging Temp. (C)	Testing Performed	Comments
DEA 231	750960472556	XCIB-1/8525309-1	173	700	Corrosion	SN-LLNL-SCI-426-V1
DEA 232	750960472556	XCIB-1/8525309-1	173	700	Corrosion	SN-LLNL-SCI-426-V1
DEA1591	5/999070	Y5536	67,393	550	None	SN-LLNL-SCI-434-V2
DEA1592	5/999070	Y5536	67,393	550	None	SN-LLNL-SCI-434-V2
DEA1593	5/999070	Y5536	67,393	550	None	SN-LLNL-SCI-434-V2
DEA1594	5/999070	Y5536	67,393	550	None	SN-LLNL-SCI-434-V2
DEA1595	5/999070	Y5536	67,393	550	None	SN-LLNL-SCI-434-V2
DEA1596	5/999070	Y5536	4500	550	None	
DEA1597	5/999070	Y5536	67,393	550	None	
DEA1598	5/999070	Y5536	67,393	550	None	
DEA1599	5/999070	Y5536	67,393	550	None	
DEA1600	5/999070	Y5536	67,393	550	None	
DEA1601	5/999070	Y5536	1000	550	TEM	
DEA1602	5/999070	Y5536	67,393	550	None	SN-LLNL-SCI-434-V2
DEA1603	5/999070	Y5536	67,393	550	None	SN-LLNL-SCI-434-V2
DEA1604	5/999070	Y5536	67,393	550	None	SN-LLNL-SCI-434-V2
DEA1605	5/999070	Y5536	4500	550	None	
DEA1606	5/999070	Y5536	4500	550	None	
DEA1607	5/999070	Y5536	67,393	550	None	SN-LLNL-SCI-434-V2
DEA1608	5/999070	Y5536	67,393	550	None	SN-LLNL-SCI-434-V2
DEA1609	5/999070	Y5536	4500	550	None	
DEA1610	5/999070	Y5536	67,393	550	None	SN-LLNL-SCI-434-V2
DEA1611	5/999070	Y5536	4500	550	None	
DEA1612	5/999070	Y5536	4500	550	None	
DEA1613	5/999070	Y5536	4500	550	None	
DEA1614	5/999070	Y5536	67,393	550	None	SN-LLNL-SCI-434-V2
DEA1615	5/999070	Y5536	67,393	550	None	SN-LLNL-SCI-434-V2
DEA1616	5/999070	Y5536	67,393	550	None	SN-LLNL-SCI-434-V2
DEA1617	5/999070	Y5536	67,393	550	None	SN-LLNL-SCI-434-V2
DEA1618	5/999070	Y5536	67,393	550	None	SN-LLNL-SCI-434-V2
DEA1619	5/999070	Y5536	1000	550	TEM	
DEA1620	5/999070	Y5536	1000	550	TEM	
DEA1621	5/999070	Y5536	4500	550	None	
DEA1622	5/999070	Y5536	4500	550	None	
DEA1623	5/999070	Y5536	1000	550	TEM	
DEA1624	5/999070	Y5536	67,393	550	None	SN-LLNL-SCI-434-V2
DEA1625	5/999070	Y5536	67,393	550	None	SN-LLNL-SCI-434-V2
DEA1626	5/999070	Y5536	67,393	550	None	SN-LLNL-SCI-434-V2
DEA1627	5/999070	Y5536	1000	550	TEM	
DEA1628	5/999070	Y5536	1000	550	TEM	
DEA1629	5/999070	Y5536	1000	550	TEM	
DEA1630	5/999070	Y5536	67,393	550	None	
DEA1631	5/999070	Y5536	67,393	550	None	
DEA1632	5/999070	Y5536	1000	550	TEM	
DEA1633	5/999070	Y5536	1000	550	TEM	
DEA1634	5/999070	Y5536	67,393	550	None	SN-LLNL-SCI-434-V2
DEA1635	5/999070	Y5536	67,393	550	None	SN-LLNL-SCI-434-V2
DEA1636	5/999070	Y5536	67,393	550	None	SN-LLNL-SCI-434-V2
DEA1637	5/999070	Y5536	67,393	550	None	SN-LLNL-SCI-434-V2
DEA1638	5/999070	Y5536	67,393	550	None	SN-LLNL-SCI-434-V2
DEA1639	5/999070	Y5536	67,393	550	None	SN-LLNL-SCI-434-V2
DEA1640	5/999070	Y5536	67,393	550	None	SN-LLNL-SCI-434-V2
DEA1641	5/999070	Y5536	67,393	550	None	SN-LLNL-SCI-434-V2
DEA1642	5/999070	Y5536	67,393	550	None	SN-LLNL-SCI-434-V2
DEA1643	5/999070	Y5536	67,393	550	None	SN-LLNL-SCI-434-V2
DEA1644	5/999070	Y5536	67,393	550	None	SN-LLNL-SCI-434-V2
DEA1645	5/999070	Y5536	67,393	550	None	SN-LLNL-SCI-434-V2
DEA1646	5/999070	Y5536	67,393	550	None	SN-LLNL-SCI-434-V2
DEA1647	5/999070	Y5536	67,393	550	None	SN-LLNL-SCI-434-V2
DEA1648	5/999070	Y5536	67,393	550	None	SN-LLNL-SCI-434-V2
DEA1649	5/999070	Y5536	67,393	550	None	SN-LLNL-SCI-434-V2
DEA1650	5/999070	Y5536	67,393	550	None	SN-LLNL-SCI-434-V2
DEA1651	5/999070	Y5536	67,393	550	None	SN-LLNL-SCI-434-V2
DEA1652	5/999070	Y5536	67,393	550	None	SN-LLNL-SCI-434-V2
DEA1653	5/999070	Y5536	67,393	550	None	SN-LLNL-SCI-434-V2
DEA1654	5/999070	Y5536	67,393	550	None	SN-LLNL-SCI-434-V2
DEA1655	5/999070	Y5536	67,393	550	None	SN-LLNL-SCI-434-V2
DEA1656	5/999070	Y5536	67,393	550	None	SN-LLNL-SCI-434-V2
DEA1657	5/999070	Y5536	67,393	550	None	SN-LLNL-SCI-434-V2

Specimen Number	Furnace No./SN	TC/Readout ID	Aging Time (Hrs.)	Aging Temp. (C)	Testing Performed	Comments
DEA1658	5/999070	Y5536	67,393	550	None	SN-LLNL-SCI-434-V2
DEA1659	5/999070	Y5536	67,393	550	None	SN-LLNL-SCI-434-V2
DEA1660	5/999070	Y5536	67,393	550	None	SN-LLNL-SCI-434-V2
DEA1661	5/999070	Y5536	67,393	550	None	SN-LLNL-SCI-434-V2
DEA1662	5/999070	Y5536	67,393	550	None	SN-LLNL-SCI-434-V2
DEA1663	5/999070	Y5536	67,393	550	None	SN-LLNL-SCI-434-V2
DEA1664	5/999070	Y5536	67,393	550	None	SN-LLNL-SCI-434-V2
DEA1665	5/999070	Y5536	67,393	550	None	SN-LLNL-SCI-434-V2
DEA1666	5/999070	Y5536	67,393	550	None	SN-LLNL-SCI-434-V2
DEA1667	5/999070	Y5536	67,393	550	None	SN-LLNL-SCI-434-V2
DEA1668	5/999070	Y5536	67,393	550	None	SN-LLNL-SCI-434-V2
DEA1669	5/999070	Y5536	67,393	550	None	SN-LLNL-SCI-434-V2
DEA1670	5/999070	Y5536	67,393	550	None	SN-LLNL-SCI-434-V2
DEA1671	5/999070	Y5536	67,393	550	None	SN-LLNL-SCI-434-V2
DEA1672	5/999070	Y5536	67,393	550	None	SN-LLNL-SCI-434-V2
DEA1673	5/999070	Y5536	67,393	550	None	SN-LLNL-SCI-434-V2
DEA1674	5/999070	Y5536	67,393	550	None	SN-LLNL-SCI-434-V2
DEA1675	5/999070	Y5536	67,393	550	None	SN-LLNL-SCI-434-V2
DEA1676	5/999070	Y5536	67,393	550	None	SN-LLNL-SCI-434-V2
DEA1677	5/999070	Y5536	67,393	550	None	SN-LLNL-SCI-434-V2
DEA1678	5/999070	Y5536	67,393	550	None	SN-LLNL-SCI-434-V2
DEA1679	5/999070	Y5536	67,393	550	None	SN-LLNL-SCI-434-V2
DEA1680	5/999070	Y5536	67,393	550	None	SN-LLNL-SCI-434-V2
DEA1681	5/999070	Y5536	67,393	550	None	SN-LLNL-SCI-434-V2
DEA1682	5/999070	Y5536	67,393	550	None	SN-LLNL-SCI-434-V2
DEA1683	5/999070	Y5536	67,393	550	None	SN-LLNL-SCI-434-V2
DEA1684	5/999070	Y5536	67,393	550	None	SN-LLNL-SCI-434-V2
DEA1685	5/999070	Y5536	67,393	550	None	SN-LLNL-SCI-434-V2
DEA1686	5/999070	Y5536	67,393	550	None	SN-LLNL-SCI-434-V2
DEA1687	5/999070	Y5536	67,393	550	None	SN-LLNL-SCI-434-V2
DEA1688	5/999070	Y5536	67,393	550	None	SN-LLNL-SCI-434-V2
DEA1689	5/999070	Y5536	67,393	550	None	SN-LLNL-SCI-434-V2
DEA1690	5/999070	Y5536	67,393	550	None	SN-LLNL-SCI-434-V2
DEA1691	5/999070	Y5536	67,393	550	None	SN-LLNL-SCI-434-V2
DEA1692	5/999070	Y5536	67,393	550	None	SN-LLNL-SCI-434-V2
DEA1693	4/999068	Y5537	1000	500	TEM	
DEA1694	4/999068	Y5537	1000	500	None	
DEA1695	4/999068	Y5537	1000	500	None	
DEA1696	4/999068	Y5537	1000	500	None	
DEA1697	4/999068	Y5537	1000	500	None	
DEA1698	4/999068	Y5537	1000	500	None	
DEA1699	4/999068	Y5537	1000	500	None	
DEA1700	4/999068	Y5537	1000	500	None	
DEA1701	4/999068	Y5537	1000	500	None	
DEA1702	4/999068	Y5537	4500	500	None	
DEA1703	4/999068	Y5537	4500	500	None	
DEA1704	4/999068	Y5537	4500	500	None	
DEA1705	4/999068	Y5537	4500	500	None	
DEA1706	4/999068	Y5537	4500	500	None	
DEA1707	4/999068	Y5537	4500	500	None	
DEA1708	4/999068	Y5537	4500	500	None	
DEA1709	4/999068	Y5537	4500	500	None	
DEA1710	4/999068	Y5537	4500	500	None	
DEA1711	4/999068	Y5537	67,386	500	None	SN-LLNL-SCI-434-V2
DEA1712	4/999068	Y5537	67,386	500	None	SN-LLNL-SCI-434-V2
DEA1713	4/999068	Y5537	67,386	500	None	SN-LLNL-SCI-434-V2
DEA1714	4/999068	Y5537	67,386	500	None	SN-LLNL-SCI-434-V2
DEA1715	4/999068	Y5537	67,386	500	None	SN-LLNL-SCI-434-V2
DEA1716	4/999068	Y5537	67,386	500	None	SN-LLNL-SCI-434-V2
DEA1717	4/999068	Y5537	67,386	500	None	SN-LLNL-SCI-434-V2
DEA1718	4/999068	Y5537	67,386	500	None	SN-LLNL-SCI-434-V2
DEA1719	4/999068	Y5537	67,386	500	None	SN-LLNL-SCI-434-V2
DEA1720	4/999068	Y5537	67,386	500	None	SN-LLNL-SCI-434-V2
DEA1721	4/999068	Y5537	67,386	500	None	SN-LLNL-SCI-434-V2
DEA1722	4/999068	Y5537	67,386	500	None	SN-LLNL-SCI-434-V2
DEA1723	4/999068	Y5537	67,386	500	None	SN-LLNL-SCI-434-V2
DEA1724	4/999068	Y5537	67,386	500	None	SN-LLNL-SCI-434-V2
DEA1725	4/999068	Y5537	67,386	500	None	SN-LLNL-SCI-434-V2
DEA1726	4/999068	Y5537	67,386	500	None	SN-LLNL-SCI-434-V2

Specimen Number	Furnace No./SN	TC/Readout ID	Aging Time (Hrs.)	Aging Temp. (C)	Testing Performed	Comments
DEA1727	4/999068	Y5537	67,386	500	None	SN-LLNL-SCI-434-V2
DEA1728	4/999068	Y5537	67,386	500	None	SN-LLNL-SCI-434-V2
DEA1729	4/999068	Y5537	67,386	500	None	SN-LLNL-SCI-434-V2
DEA1730	4/999068	Y5537	67,386	500	None	SN-LLNL-SCI-434-V2
DEA1731	4/999068	Y5537	67,386	500	None	SN-LLNL-SCI-434-V2
DEA1732	4/999068	Y5537	67,386	500	None	SN-LLNL-SCI-434-V2
DEA1733	4/999068	Y5537	67,386	500	None	SN-LLNL-SCI-434-V2
DEA1734	4/999068	Y5537	67,386	500	None	SN-LLNL-SCI-434-V2
DEA1735	4/999068	Y5537	67,386	500	None	SN-LLNL-SCI-434-V2
DEA1736	4/999068	Y5537	67,386	500	None	SN-LLNL-SCI-434-V2
DEA1737	4/999068	Y5537	67,386	500	None	SN-LLNL-SCI-434-V2
DEA1738	4/999068	Y5537	67,386	500	None	SN-LLNL-SCI-434-V2
DEA1739	4/999068	Y5537	67,386	500	None	SN-LLNL-SCI-434-V2
DEA1740	4/999068	Y5537	67,386	500	None	SN-LLNL-SCI-434-V2
DEA1741	4/999068	Y5537	67,386	500	None	SN-LLNL-SCI-434-V2
DEA1742	4/999068	Y5537	67,386	500	None	SN-LLNL-SCI-434-V2
DEA1743	4/999068	Y5537	67,386	500	None	SN-LLNL-SCI-434-V2
DEA1744	4/999068	Y5537	67,386	500	None	SN-LLNL-SCI-434-V2
DEA1745	4/999068	Y5537	67,386	500	None	SN-LLNL-SCI-434-V2
DEA1746	4/999068	Y5537	67,386	500	None	SN-LLNL-SCI-434-V2
DEA1747	4/999068	Y5537	67,386	500	None	SN-LLNL-SCI-434-V2
DEA1748	4/999068	Y5537	67,386	500	None	SN-LLNL-SCI-434-V2
DEA1749	4/999068	Y5537	67,386	500	None	SN-LLNL-SCI-434-V2
DEA1750	4/999068	Y5537	67,386	500	None	SN-LLNL-SCI-434-V2
DEA1751	4/999068	Y5537	67,386	500	None	SN-LLNL-SCI-434-V2
DEA1752	4/999068	Y5537	67,386	500	None	SN-LLNL-SCI-434-V2
DEA1753	4/999068	Y5537	67,386	500	None	SN-LLNL-SCI-434-V2
DEA1754	4/999068	Y5537	67,386	500	None	SN-LLNL-SCI-434-V2
DEA1755	4/999068	Y5537	67,386	500	None	SN-LLNL-SCI-434-V2
DEA1756	4/999068	Y5537	67,386	500	None	SN-LLNL-SCI-434-V2
DEA1757	4/999068	Y5537	67,386	500	None	SN-LLNL-SCI-434-V2
DEA1758	4/999068	Y5537	67,386	500	None	SN-LLNL-SCI-434-V2
DEA1759	4/999068	Y5537	67,386	500	None	SN-LLNL-SCI-434-V2
DEA1760	4/999068	Y5537	67,386	500	None	SN-LLNL-SCI-434-V2
DEA1761	4/999068	Y5537	67,386	500	None	SN-LLNL-SCI-434-V2
DEA1762	4/999068	Y5537	67,386	500	None	SN-LLNL-SCI-434-V2
DEA1763	4/999068	Y5537	67,386	500	None	SN-LLNL-SCI-434-V2
DEA1764	4/999068	Y5537	67,386	500	None	SN-LLNL-SCI-434-V2
DEA1765	4/999068	Y5537	67,386	500	None	SN-LLNL-SCI-434-V2
DEA1766	4/999068	Y5537	67,386	500	None	SN-LLNL-SCI-434-V2
DEA1767	4/999068	Y5537	67,386	500	None	SN-LLNL-SCI-434-V2
DEA1768	4/999068	Y5537	67,386	500	None	SN-LLNL-SCI-434-V2
DEA1769	4/999068	Y5537	67,386	500	None	SN-LLNL-SCI-434-V2
DEA1770	4/999068	Y5537	67,386	500	None	SN-LLNL-SCI-434-V2
DEA1771	4/999068	Y5537	67,386	500	None	SN-LLNL-SCI-434-V2
DEA1772	4/999068	Y5537	67,386	500	None	SN-LLNL-SCI-434-V2
DEA1773	4/999068	Y5537	67,386	500	None	SN-LLNL-SCI-434-V2
DEA1774	4/999068	Y5537	67,386	500	None	SN-LLNL-SCI-434-V2
DEA1775	4/999068	Y5537	67,386	500	None	SN-LLNL-SCI-434-V2
DEA1776	4/999068	Y5537	67,386	500	None	SN-LLNL-SCI-434-V2
DEA1777	4/999068	Y5537	67,386	500	None	SN-LLNL-SCI-434-V2
DEA1778	4/999068	Y5537	67,386	500	None	SN-LLNL-SCI-434-V2
DEA1779	4/999068	Y5537	67,386	500	None	SN-LLNL-SCI-434-V2
DEA1780	4/999068	Y5537	67,386	500	None	SN-LLNL-SCI-434-V2
DEA1781	4/999068	Y5537	67,386	500	None	SN-LLNL-SCI-434-V2
DEA1782	4/999068	Y5537	67,386	500	None	SN-LLNL-SCI-434-V2
DEA1783	4/999068	Y5537	67,386	500	None	SN-LLNL-SCI-434-V2
DEA1784	4/999068	Y5537	67,386	500	None	SN-LLNL-SCI-434-V2
DEA1785	4/999068	Y5537	67,386	500	None	SN-LLNL-SCI-434-V2
DEA1786	4/999068	Y5537	67,386	500	None	SN-LLNL-SCI-434-V2
DEA1787	4/999068	Y5537	67,386	500	None	SN-LLNL-SCI-434-V2
DEA1788	4/999068	Y5537	67,386	500	None	SN-LLNL-SCI-434-V2
DEA1789	4/999068	Y5537	67,386	500	None	SN-LLNL-SCI-434-V2
DEA1790	4/999068	Y5537	67,386	500	None	SN-LLNL-SCI-434-V2
DEA1791	4/999068	Y5537	67,386	500	None	SN-LLNL-SCI-434-V2
DEA1792	4/999068	Y5537	67,386	500	None	SN-LLNL-SCI-434-V2
DEA1793	4/999068	Y5537	67,386	500	None	SN-LLNL-SCI-434-V2
DEA1794	4/999068	Y5537	67,386	500	None	SN-LLNL-SCI-434-V2
DEA1795	3/999069	Y5538/AA2564	66,878	400	None	SN-LLNL-SCI-434-V2

Specimen Number	Furnace No./SN	TC/Readout ID	Aging Time (Hrs.)	Aging Temp. (C)	Testing Performed	Comments
DEA1796	3/999069	Y5538/AA2564	66,878	400	None	SN-LLNL-SCI-434-V2
DEA1797	3/999069	Y5538/AA2564	66,878	400	None	SN-LLNL-SCI-434-V2
DEA1798	3/999069	Y5538/AA2564	66,878	400	None	SN-LLNL-SCI-434-V2
DEA1799	3/999069	Y5538/AA2564	66,878	400	None	SN-LLNL-SCI-434-V2
DEA1800	3/999069	Y5538/AA2564	66,878	400	None	SN-LLNL-SCI-434-V2
DEA1801	3/999069	Y5538/AA2564	66,878	400	None	SN-LLNL-SCI-434-V2
DEA1802	3/999069	Y5538/AA2564	66,878	400	None	SN-LLNL-SCI-434-V2
DEA1803	3/999069	Y5538/AA2564	66,878	400	None	SN-LLNL-SCI-434-V2
DEA1804	3/999069	Y5538/AA2564	66,878	400	None	SN-LLNL-SCI-434-V2
DEA1805	3/999069	Y5538/AA2564	66,878	400	None	SN-LLNL-SCI-434-V2
DEA1806	3/999069	Y5538/AA2564	66,878	400	None	SN-LLNL-SCI-434-V2
DEA1807	3/999069	Y5538/AA2564	66,878	400	None	SN-LLNL-SCI-434-V2
DEA1808	3/999069	Y5538/AA2564	66,878	400	None	SN-LLNL-SCI-434-V2
DEA1809	3/999069	Y5538/AA2564	66,878	400	None	SN-LLNL-SCI-434-V2
DEA1810	3/999069	Y5538/AA2564	66,878	400	None	SN-LLNL-SCI-434-V2
DEA1811	3/999069	Y5538/AA2564	66,878	400	None	SN-LLNL-SCI-434-V2
DEA1812	3/999069	Y5538/AA2564	66,878	400	None	SN-LLNL-SCI-434-V2
DEA1813	3/999069	Y5538/AA2564	66,878	400	None	SN-LLNL-SCI-434-V2
DEA1814	3/999069	Y5538/AA2564	66,878	400	None	SN-LLNL-SCI-434-V2
DEA1815	3/999069	Y5538/AA2564	66,878	400	None	SN-LLNL-SCI-434-V2
DEA1816	3/999069	Y5538/AA2564	66,878	400	None	SN-LLNL-SCI-434-V2
DEA1817	3/999069	Y5538/AA2564	66,878	400	None	SN-LLNL-SCI-434-V2
DEA1818	3/999069	Y5538/AA2564	66,878	400	None	SN-LLNL-SCI-434-V2
DEA1819	3/999069	Y5538/AA2564	66,878	400	None	SN-LLNL-SCI-434-V2
DEA1820	3/999069	Y5538/AA2564	66,878	400	None	SN-LLNL-SCI-434-V2
DEA1821	3/999069	Y5538/AA2564	66,878	400	None	SN-LLNL-SCI-434-V2
DEA1822	3/999069	Y5538/AA2564	66,878	400	None	SN-LLNL-SCI-434-V2
DEA1823	3/999069	Y5538/AA2564	66,878	400	None	SN-LLNL-SCI-434-V2
DEA1824	3/999069	Y5538/AA2564	66,878	400	None	SN-LLNL-SCI-434-V2
DEA1825	3/999069	Y5538/AA2564	66,878	400	None	SN-LLNL-SCI-434-V2
DEA1826	3/999069	Y5538/AA2564	66,878	400	None	SN-LLNL-SCI-434-V2
DEA1827	3/999069	Y5538/AA2564	66,878	400	None	SN-LLNL-SCI-434-V2
DEA1828	3/999069	Y5538/AA2564	66,878	400	None	SN-LLNL-SCI-434-V2
DEA1829	3/999069	Y5538/AA2564	66,878	400	None	SN-LLNL-SCI-434-V2
DEA1830	3/999069	Y5538/AA2564	66,878	400	None	SN-LLNL-SCI-434-V2
DEA1831	3/999069	Y5538/AA2564	66,878	400	None	SN-LLNL-SCI-434-V2
DEA1832	3/999069	Y5538/AA2564	66,878	400	None	SN-LLNL-SCI-434-V2
DEA1833	3/999069	Y5538/AA2564	66,878	400	None	SN-LLNL-SCI-434-V2
DEA1834	3/999069	Y5538/AA2564	66,878	400	None	SN-LLNL-SCI-434-V2
DEA1835	3/999069	Y5538/AA2564	66,878	400	None	SN-LLNL-SCI-434-V2
DEA1836	3/999069	Y5538/AA2564	66,878	400	None	SN-LLNL-SCI-434-V2
DEA1837	3/999069	Y5538/AA2564	66,878	400	None	SN-LLNL-SCI-434-V2
DEA1838	3/999069	Y5538/AA2564	66,878	400	None	SN-LLNL-SCI-434-V2
DEA1839	3/999069	Y5538/AA2564	66,878	400	None	SN-LLNL-SCI-434-V2
DEA1840	3/999069	Y5538/AA2564	66,878	400	None	SN-LLNL-SCI-434-V2
DEA1841	3/999069	Y5538/AA2564	66,878	400	None	SN-LLNL-SCI-434-V2
DEA1842	3/999069	Y5538/AA2564	66,878	400	None	SN-LLNL-SCI-434-V2
DEA1843	3/999069	Y5538/AA2564	66,878	400	None	SN-LLNL-SCI-434-V2
DEA1844	3/999069	Y5538/AA2564	66,878	400	None	SN-LLNL-SCI-434-V2
DEA1845	3/999069	Y5538/AA2564	66,878	400	None	SN-LLNL-SCI-434-V2
DEA1846	3/999069	Y5538/AA2564	66,878	400	None	SN-LLNL-SCI-434-V2
DEA1847	3/999069	Y5538/AA2564	66,878	400	None	SN-LLNL-SCI-434-V2
DEA1848	3/999069	Y5538/AA2564	66,878	400	None	SN-LLNL-SCI-434-V2
DEA1849	3/999069	Y5538/AA2564	66,878	400	None	SN-LLNL-SCI-434-V2
DEA1850	3/999069	Y5538/AA2564	66,878	400	None	SN-LLNL-SCI-434-V2
DEA1851	3/999069	Y5538/AA2564	66,878	400	None	SN-LLNL-SCI-434-V2
DEA1852	3/999069	Y5538/AA2564	66,878	400	None	SN-LLNL-SCI-434-V2
DEA1853	3/999069	Y5538/AA2564	66,878	400	None	SN-LLNL-SCI-434-V2
DEA1854	3/999069	Y5538/AA2564	66,878	400	None	SN-LLNL-SCI-434-V2
DEA1855	3/999069	Y5538/AA2564	66,878	400	None	SN-LLNL-SCI-434-V2
DEA1856	3/999069	Y5538/AA2564	66,878	400	None	SN-LLNL-SCI-434-V2
DEA1857	3/999069	Y5538/AA2564	66,878	400	None	SN-LLNL-SCI-434-V2
DEA1858	3/999069	Y5538/AA2564	66,878	400	None	SN-LLNL-SCI-434-V2
DEA1859	3/999069	Y5538/AA2564	66,878	400	None	SN-LLNL-SCI-434-V2
DEA1860	3/999069	Y5538/AA2564	66,878	400	None	SN-LLNL-SCI-434-V2
DEA1861	3/999069	Y5538/AA2564	66,878	400	None	SN-LLNL-SCI-434-V2
DEA1862	3/999069	Y5538/AA2564	66,878	400	None	SN-LLNL-SCI-434-V2
DEA1863	3/999069	Y5538/AA2564	66,878	400	None	SN-LLNL-SCI-434-V2
DEA1864	3/999069	Y5538/AA2564	66,878	400	None	SN-LLNL-SCI-434-V2

Specimen Number	Furnace No./SN	TC/Readout ID	Aging Time (Hrs.)	Aging Temp. (C)	Testing Performed	Comments
DEA1865	3/999069	Y5538/AA2564	66,878	400	None	SN-LLNL-SCI-434-V2
DEA1866	3/999069	Y5538/AA2564	66,878	400	None	SN-LLNL-SCI-434-V2
DEA1867	3/999069	Y5538/AA2564	66,878	400	None	SN-LLNL-SCI-434-V2
DEA1868	3/999069	Y5538/AA2564	66,878	400	None	SN-LLNL-SCI-434-V2
DEA1869	3/999069	Y5538/AA2564	66,878	400	None	SN-LLNL-SCI-434-V2
DEA1870	3/999069	Y5538/AA2564	66,878	400	None	SN-LLNL-SCI-434-V2
DEA1871	3/999069	Y5538/AA2564	66,878	400	None	SN-LLNL-SCI-434-V2
DEA1872	3/999069	Y5538/AA2564	66,878	400	None	SN-LLNL-SCI-434-V2
DEA1873	3/999069	Y5538/AA2564	66,878	400	None	SN-LLNL-SCI-434-V2
DEA1874	3/999069	Y5538/AA2564	66,878	400	None	SN-LLNL-SCI-434-V2
DEA1875	3/999069	Y5538/AA2564	66,878	400	None	SN-LLNL-SCI-434-V2
DEA1876	3/999069	Y5538/AA2564	66,878	400	None	SN-LLNL-SCI-434-V2
DEA1877	3/999069	Y5538/AA2564	66,878	400	None	SN-LLNL-SCI-434-V2
DEA1878	3/999069	Y5538/AA2564	66,878	400	None	SN-LLNL-SCI-434-V2
DEA1879	3/999069	Y5538/AA2564	66,878	400	None	SN-LLNL-SCI-434-V2
DEA1880	3/999069	Y5538/AA2564	66,878	400	None	SN-LLNL-SCI-434-V2
DEA1881	3/999069	Y5538/AA2564	66,878	400	None	SN-LLNL-SCI-434-V2
DEA1882	3/999069	Y5538/AA2564	66,878	400	None	SN-LLNL-SCI-434-V2
DEA1883	3/999069	Y5538/AA2564	66,878	400	None	SN-LLNL-SCI-434-V2
DEA1884	3/999069	Y5538/AA2564	66,878	400	None	SN-LLNL-SCI-434-V2
DEA1885	3/999069	Y5538/AA2564	66,878	400	None	SN-LLNL-SCI-434-V2
DEA1886	3/999069	Y5538/AA2564	66,878	400	None	SN-LLNL-SCI-434-V2
DEA1887	3/999069	Y5538/AA2564	66,878	400	None	SN-LLNL-SCI-434-V2
DEA1888	1/999067	Y5540	1000	700	TEM	
DEA1889	1/999067	Y5540	1000	700	None	
DEA1890	1/999067	Y5540	1000	700	None	
DEA1891	1/999067	Y5540	1000	700	None	
DEA1892	1/999067	Y5540	1000	700	None	
DEA1893	1/999067	Y5540	1000	700	None	
DEA1894	1/999067	Y5540	1000	700	None	
DEA1895	1/999067	Y5540	1000	700	None	
DEA1896	1/999067	Y5540	1000	700	None	
DEA1897	1/999067	Y5540	1000	700	TEM	
DEA1898	1/999067	Y5540	1000	700	None	
DEA1899	1/999067	Y5540	1000	700	None	
DEA1900	1/999067	Y5540	1000	700	None	
DEA1901	1/999067	Y5540	1000	700	None	
DEA1902	1/999067	Y5540	1000	700	None	
DEA1903	1/999067	Y5540	1000	700	None	
DEA1904	1/999067	Y5540	1000	700	None	
DEA1905	1/999067	Y5540	1000	700	None	
DEA1906	1/999067	Y5540	1000	700	TEM	
DEA1907	1/999067	Y5540	1000	700	None	
DEA1908	1/999067	Y5540	1000	700	None	
DEA1909	1/999067	Y5540	1000	700	None	
DEA1910	1/999067	Y5540	1000	700	None	
DEA1911	1/999067	Y5540	1000	700	None	
DEA1912	1/999067	Y5540	1000	700	None	
DEA1913	1/999067	Y5540	1000	700	None	
DEA1914	1/999067	Y5540	1000	700	None	
DEA1915	1/999067	Y5540	1000	700	TEM	
DEA1916	1/999067	Y5540	1000	700	None	
DEA1917	1/999067	Y5540	1000	700	None	
DEA1918	1/999067	Y5540	1000	700	None	
DEA1919	1/999067	Y5540	1000	700	None	
DEA1920	1/999067	Y5540	1000	700	None	
DEA1921	1/999067	Y5540	10,073	700	None	
DEA1922	1/999067	Y5540	10,073	700	None	
DEA1923	1/999067	Y5540	10,073	700	None	
DEA1924	1/999067	Y5540	10,073	700	None	
DEA1925	1/999067	Y5540	10,073	700	None	
DEA1926	1/999067	Y5540	10,073	700	None	
DEA1927	1/999067	Y5540	10,073	700	None	
DEA1928	1/999067	Y5540	10,073	700	None	
DEA1929	1/999067	Y5540	10,073	700	None	
DEA1930	1/999067	Y5540	10,073	700	None	
DEA1931	1/999067	Y5540	10,073	700	None	
DEA1932	1/999067	Y5540	10,073	700	None	
DEA1933	1/999067	Y5540	10,073	700	None	

Specimen Number	Furnace No./SN	TC/Readout ID	Aging Time (Hrs.)	Aging Temp. (C)	Testing Performed	Comments
DEA1934	1/999067	Y5540	10,073	700	None	
DEA1935	1/999067	Y5540	10,073	700	None	
DEA1936	1/999067	Y5540	10,073	700	None	
DEA1937	1/999067	Y5540	10,073	700	None	
DEA1938	1/999067	Y5540	10,073	700	None	
DEA1939	6/750961033029	Y5542	1	750	None	
DEA1940	6/750961033029	Y5542	1	750	None	
DEA1941	6/750961033029	Y5542	1	750	None	
DEA1942	6/750961033029	Y5542	1	750	None	
DEA1943	6/750961033029	Y5542	1	750	None	
DEA1944	6/750961033029	Y5542	1	750	None	
DEA1945	6/750961033029	Y5542	1	750	None	
DEA1946	6/750961033029	Y5542	1	750	None	
DEA1947	6/750961033029	Y5542	1	750	None	
DEA1948	6/750961033029	Y5542	1	750	None	
DEA1949	6/750961033029	Y5542	1	750	None	
DEA1950	6/750961033029	Y5542	1	750	None	
DEA1951	6/750961033029	Y5542	1	750	None	
DEA1952	6/750961033029	Y5542	1	750	None	
DEA1953	6/750961033029	Y5542	1	750	None	
DEA1954	6/750961033029	Y5542	1	750	None	
DEA1955	6/750961033029	Y5542	1	750	None	
DEA1956	6/750961033029	Y5542	1	750	None	
DEA1957	6/750961033029	Y5542	1	750	None	
DEA1958	6/750961033029	Y5542	1	750	None	
DEA1959	6/750961033029	Y5542	1	750	None	
DEA1960	6/750961033029	Y5542	1	750	None	
DEA1961	6/750961033029	Y5542	1	750	None	
DEA1962	6/750961033029	Y5542	1	750	None	
DEA1963	6/750961033029	Y5542	1	750	None	
DEA1964	6/750961033029	Y5542	1	750	None	
DEA1965	6/750961033029	Y5542	1	750	None	
DEA1966	6/750961033029	Y5542	1	750	None	
DEA1967	6/750961033029	Y5542	1	750	None	
DEA1968	6/750961033029	Y5542	1	750	None	
DEA1969	6/750961033029	Y5542	1	750	None	
DEA1970	6/750961033029	Y5542	1	750	None	
DEA1971	6/750961033029	Y5542	1	750	None	
DEA1972	6/750961033029	Y5542	4	750	None	
DEA1973	6/750961033029	Y5542	4	750	None	
DEA1974	6/750961033029	Y5542	4	750	None	
DEA1975	6/750961033029	Y5542	4	750	None	
DEA1976	6/750961033029	Y5542	4	750	None	
DEA1977	6/750961033029	Y5542	4	750	None	
DEA1978	6/750961033029	Y5542	4	750	None	
DEA1979	6/750961033029	Y5542	4	750	None	
DEA1980	6/750961033029	Y5542	4	750	None	
DEA1981	6/750961033029	Y5542	10	750	None	
DEA1982	6/750961033029	Y5542	10	750	None	
DEA1983	6/750961033029	Y5542	10	750	None	
DEA1984	6/750961033029	Y5542	10	750	None	
DEA1985	6/750961033029	Y5542	10	750	None	
DEA1986	6/750961033029	Y5542	10	750	None	
DEA1987	6/750961033029	Y5542	10	750	None	
DEA1988	6/750961033029	Y5542	10	750	None	
DEA1989	6/750961033029	Y5542	10	750	None	
DEA1990	6/750961033029	Y5542	10	750	None	
DEA1991	6/750961033029	Y5542	10	750	None	
DEA1992	6/750961033029	Y5542	10	750	None	
DEA1993	6/750961033029	Y5542	10	750	None	
DEA1994	6/750961033029	Y5542	10	750	None	
DEA1995	6/750961033029	Y5542	10	750	None	
DEA1996	6/750961033029	Y5542	10	750	None	
DEA1997	6/750961033029	Y5542	10	750	None	
DEA1998	6/750961033029	Y5542	10	750	None	
DEA1999	6/750961033029	Y5542	10	750	None	
DEA2000	6/750961033029	Y5542	10	750	None	
DEA2001	6/750961033029	Y5542	10	750	None	
DEA2002	6/750961033029	Y5542	10	750	None	

Specimen Number	Furnace No./SN	TC/Readout ID	Aging Time (Hrs.)	Aging Temp. (C)	Testing Performed	Comments
DEA2003	6/750961033029	Y5542	10	750	None	
DEA2004	6/750961033029	Y5542	10	750	None	
DEA2005	6/750961033029	Y5542	10	750	None	
DEA2006	6/750961033029	Y5542	10	750	None	
DEA2007	6/750961033029	Y5542	10	750	None	
DEA2008	6/750961033029	Y5542	10	750	None	
DEA2009	6/750961033029	Y5542	10	750	None	
DEA2010	6/750961033029	Y5542	10	750	None	
DEA2011	6/750961033029	Y5542	10	750	None	
DEA2012	6/750961033029	Y5542	10	750	None	
DEA2013	6/750961033029	Y5542	10	750	None	
DEA2014	6/750961033029	Y5542	40	750	None	
DEA2015	6/750961033029	Y5542	40	750	None	
DEA2016	6/750961033029	Y5542	40	750	None	
DEA2017	6/750961033029	Y5542	40	750	None	
DEA2018	6/750961033029	Y5542	40	750	None	
DEA2019	6/750961033029	Y5542	40	750	None	
DEA2020	6/750961033029	Y5542	40	750	None	
DEA2021	6/750961033029	Y5542	40	750	None	
DEA2022	6/750961033029	Y5542	40	750	None	
DEA2023	6/750961033029	Y5542	100	750	None	
DEA2024	6/750961033029	Y5542	100	750	None	
DEA2025	6/750961033029	Y5542	100	750	None	
DEA2026	6/750961033029	Y5542	100	750	None	
DEA2027	6/750961033029	Y5542	100	750	None	
DEA2028	6/750961033029	Y5542	100	750	None	
DEA2029	6/750961033029	Y5542	100	750	None	
DEA2030	6/750961033029	Y5542	100	750	None	
DEA2031	6/750961033029	Y5542	100	750	None	
DEA2032	6/750961033029	Y5542	100	750	None	
DEA2033	6/750961033029	Y5542	100	750	None	
DEA2034	6/750961033029	Y5542	100	750	None	
DEA2035	6/750961033029	Y5542	100	750	None	
DEA2036	6/750961033029	Y5542	100	750	None	
DEA2037	6/750961033029	Y5542	100	750	None	
DEA2038	6/750961033029	Y5542	100	750	None	
DEA2039	6/750961033029	Y5542	100	750	None	
DEA2040	6/750961033029	Y5542	100	750	None	
DEA2041	6/750961033029	Y5542	100	750	None	
DEA2042	6/750961033029	Y5542	100	750	None	
DEA2043	6/750961033029	Y5542	100	750	None	
DEA2044	6/750961033029	Y5542	100	750	None	
DEA2045	6/750961033029	Y5542	100	750	None	
DEA2046	6/750961033029	Y5542	100	750	None	
DEA2047	6/750961033029	Y5542	100	750	None	
DEA2048	6/750961033029	Y5542	100	750	None	
DEA2049	6/750961033029	Y5542	100	750	None	
DEA2050	6/750961033029	Y5542	100	750	None	
DEA2051	6/750961033029	Y5542	100	750	None	
DEA2052	6/750961033029	Y5542	100	750	None	
DEA2053	6/750961033029	Y5542	100	750	None	
DEA2054	6/750961033029	Y5542	100	750	None	
DEA2055	6/750961033029	Y5542	100	750	None	
DEA2056	7/750950688858	Y5541	10	700	None	
DEA2057	7/750950688858	Y5541	10	700	None	
DEA2058	7/750950688858	Y5541	10	700	None	
DEA2059	7/750950688858	Y5541	10	700	None	
DEA2060	7/750950688858	Y5541	10	700	None	
DEA2061	7/750950688858	Y5541	10	700	None	
DEA2062	7/750950688858	Y5541	10	700	None	
DEA2063	7/750950688858	Y5541	10	700	None	
DEA2064	7/750950688858	Y5541	10	700	None	
DEA2065	7/750950688858	Y5541	10	700	None	
DEA2066	7/750950688858	Y5541	10	700	None	
DEA2067	7/750950688858	Y5541	10	700	None	
DEA2068	7/750950688858	Y5541	10	700	None	
DEA2069	7/750950688858	Y5541	10	700	None	
DEA2070	7/750950688858	Y5541	10	700	None	
DEA2071	7/750950688858	Y5541	10	700	None	

Specimen Number	Furnace No./SN	TC/Readout ID	Aging Time (Hrs.)	Aging Temp. (C)	Testing Performed	Comments
DEA2072	7/750950688858	Y5541	10	700	None	
DEA2073	7/750950688858	Y5541	10	700	None	
DEA2074	7/750950688858	Y5541	10	700	None	
DEA2075	7/750950688858	Y5541	10	700	None	
DEA2076	7/750950688858	Y5541	10	700	None	
DEA2077	7/750950688858	Y5541	10	700	None	
DEA2078	7/750950688858	Y5541	10	700	None	
DEA2079	7/750950688858	Y5541	10	700	None	
DEA2080	7/750950688858	Y5541	10	700	None	
DEA2081	7/750950688858	Y5541	10	700	None	
DEA2082	7/750950688858	Y5541	10	700	None	
DEA2083	7/750950688858	Y5541	10	700	None	
DEA2084	7/750950688858	Y5541	10	700	None	
DEA2085	7/750950688858	Y5541	10	700	None	
DEA2086	7/750950688858	Y5541	10	700	None	
DEA2087	7/750950688858	Y5541	10	700	None	
DEA2088	7/750950688858	Y5541	10	700	None	
DEA2089	7/750950688858	Y5541	40	700	None	
DEA2090	7/750950688858	Y5541	40	700	None	
DEA2091	7/750950688858	Y5541	40	700	None	
DEA2092	7/750950688858	Y5541	40	700	None	
DEA2093	7/750950688858	Y5541	40	700	None	
DEA2094	7/750950688858	Y5541	40	700	None	
DEA2095	7/750950688858	Y5541	40	700	None	
DEA2096	7/750950688858	Y5541	40	700	None	
DEA2097	7/750950688858	Y5541	40	700	None	
DEA2098	7/750950688858	Y5541	100	700	None	
DEA2099	7/750950688858	Y5541	100	700	None	
DEA2100	7/750950688858	Y5541	100	700	None	
DEA2101	7/750950688858	Y5541	100	700	None	
DEA2102	7/750950688858	Y5541	100	700	None	
DEA2103	7/750950688858	Y5541	100	700	None	
DEA2104	7/750950688858	Y5541	100	700	None	
DEA2105	7/750950688858	Y5541	100	700	None	
DEA2106	7/750950688858	Y5541	100	700	None	
DEA2107	7/750950688858	Y5541	100	700	None	
DEA2108	7/750950688858	Y5541	100	700	None	
DEA2109	7/750950688858	Y5541	100	700	None	
DEA2110	7/750950688858	Y5541	100	700	None	
DEA2111	7/750950688858	Y5541	100	700	None	
DEA2112	7/750950688858	Y5541	100	700	None	
DEA2113	7/750950688858	Y5541	100	700	None	
DEA2114	7/750950688858	Y5541	100	700	None	
DEA2115	7/750950688858	Y5541	100	700	None	
DEA2116	7/750950688858	Y5541	100	700	None	
DEA2117	7/750950688858	Y5541	100	700	None	
DEA2118	7/750950688858	Y5541	100	700	None	
DEA2119	7/750950688858	Y5541	100	700	None	
DEA2120	7/750950688858	Y5541	100	700	None	
DEA2121	7/750950688858	Y5541	100	700	None	
DEA2122	7/750950688858	Y5541	100	700	None	
DEA2123	7/750950688858	Y5541	100	700	None	
DEA2124	7/750950688858	Y5541	100	700	None	
DEA2125	7/750950688858	Y5541	100	700	None	
DEA2126	7/750950688858	Y5541	100	700	None	
DEA2127	7/750950688858	Y5541	100	700	None	
DEA2128	7/750950688858	Y5541	100	700	None	
DEA2129	7/750950688858	Y5541	100	700	None	
DEA2130	7/750950688858	Y5541	100	700	None	
DEA2131	7/750950688858	Y5541	400	700	None	
DEA2132	7/750950688858	Y5541	400	700	None	
DEA2133	7/750950688858	Y5541	400	700	None	
DEA2134	7/750950688858	Y5541	400	700	None	
DEA2135	7/750950688858	Y5541	400	700	None	
DEA2136	7/750950688858	Y5541	400	700	None	
DEA2137	7/750950688858	Y5541	400	700	None	
DEA2138	7/750950688858	Y5541	400	700	None	
DEA2139	7/750950688858	Y5541	400	700	None	
DEA2140	6/750961033029	Y8117	100	650	None	

Specimen Number	Furnace No./SN	TC/Readout ID	Aging Time (Hrs.)	Aging Temp. (C)	Testing Performed	Comments
DEA2141	6/750961033029	Y8117	100	650	None	
DEA2142	6/750961033029	Y8117	100	650	None	
DEA2143	6/750961033029	Y8117	100	650	None	
DEA2144	6/750961033029	Y8117	100	650	None	
DEA2145	6/750961033029	Y8117	100	650	None	
DEA2146	6/750961033029	Y8117	100	650	None	
DEA2147	6/750961033029	Y8117	100	650	None	
DEA2148	6/750961033029	Y8117	100	650	None	
DEA2149	6/750961033029	Y8117	100	650	None	
DEA2150	6/750961033029	Y8117	100	650	None	
DEA2151	6/750961033029	Y8117	100	650	None	
DEA2152	6/750961033029	Y8117	100	650	None	
DEA2153	6/750961033029	Y8117	100	650	None	
DEA2154	6/750961033029	Y8117	100	650	None	
DEA2155	6/750961033029	Y8117	100	650	None	
DEA2156	6/750961033029	Y8117	100	650	None	
DEA2157	6/750961033029	Y8117	100	650	None	
DEA2158	6/750961033029	Y8117	100	650	None	
DEA2159	6/750961033029	Y8117	100	650	None	
DEA2160	6/750961033029	Y8117	100	650	None	
DEA2162	6/750961033029	Y8117	100	650	None	
DEA2163	6/750961033029	Y8117	100	650	None	
DEA2164	6/750961033029	Y8117	100	650	None	
DEA2165	6/750961033029	Y8117	100	650	None	
DEA2166	6/750961033029	Y8117	100	650	None	
DEA2167	6/750961033029	Y8117	100	650	None	
DEA2168	6/750961033029	Y8117	100	650	None	
DEA2169	6/750961033029	Y8117	100	650	None	
DEA2170	6/750961033029	Y8117	100	650	None	
DEA2171	6/750961033029	Y8117	100	650	None	
DEA2172	6/750961033029	Y8117	100	650	None	
DEA2173	6/750961033029	Y8117	300	650	None	
DEA2174	6/750961033029	Y8117	300	650	None	
DEA2175	6/750961033029	Y8117	300	650	None	
DEA2176	6/750961033029	Y8117	300	650	None	
DEA2177	6/750961033029	Y8117	300	650	None	
DEA2178	6/750961033029	Y8117	300	650	None	
DEA2179	6/750961033029	Y8117	300	650	None	
DEA2180	6/750961033029	Y8117	300	650	None	
DEA2181	6/750961033029	Y8117	300	650	None	
DEA2182	8/750960472556	Y8122	600	650	None	
DEA2183	8/750960472556	Y8122	600	650	None	
DEA2184	8/750960472556	Y8122	600	650	None	
DEA2185	8/750960472556	Y8122	600	650	None	
DEA2186	8/750960472556	Y8122	600	650	None	
DEA2187	8/750960472556	Y8122	600	650	None	
DEA2188	8/750960472556	Y8122	600	650	None	
DEA2189	8/750960472556	Y8122	600	650	None	
DEA2190	8/750960472556	Y8122	600	650	None	
DEA2191	2/999066	Y8121	1000	600	None	
DEA2192	2/999066	Y8121	1000	600	None	
DEA2193	2/999066	Y8121	1000	600	None	
DEA2194	2/999066	Y8121	1000	600	None	
DEA2195	2/999066	Y8121	1000	600	None	
DEA2196	2/999066	Y8121	51,190	600	None	SN-LLNL-SCI-434-V2
DEA2197	2/999066	Y8121	1000	600	None	
DEA2198	2/999066	Y8121	1000	600	None	
DEA2199	2/999066	Y8121	1000	600	None	
DEA2200	2/999066	Y8121	1000	600	None	
DEA2201	2/999066	Y8121	1000	600	None	
DEA2202	2/999066	Y8121	1000	600	None	
DEA2203	2/999066	Y8121	1000	600	None	
DEA2204	2/999066	Y8121	1000	600	None	
DEA2205	2/999066	Y8121	1000	600	None	
DEA2206	2/999066	Y8121	1000	600	None	
DEA2207	2/999066	Y8121	1000	600	None	
DEA2208	2/999066	Y8121	1000	600	None	
DEA2209	2/999066	Y8121	1000	600	None	
DEA2210	2/999066	Y8121	1000	600	None	

Specimen Number	Furnace No./SN	TC/Readout ID	Aging Time (Hrs.)	Aging Temp. (C)	Testing Performed	Comments
DEA2211	2/999066	Y8121	1000	600	None	
DEA2212	2/999066	Y8121	1000	600	None	
DEA2213	2/999066	Y8121	1000	600	None	
DEA2214	2/999066	Y8121	1000	600	None	
DEA2215	2/999066	Y8121	1000	600	None	
DEA2216	2/999066	Y8121	1000	600	None	
DEA2217	2/999066	Y8121	1000	600	None	
DEA2218	2/999066	Y8121	1000	600	None	
DEA2219	2/999066	Y8121	1000	600	None	
DEA2220	2/999066	Y8121	1000	600	None	
DEA2221	2/999066	Y8121	1000	600	None	
DEA2222	2/999066	Y8121	1000	600	None	
DEA2223	2/999066	Y8121	1000	600	None	
DEA2224	2/999066	Y8121	4000	600	None	
DEA2225	2/999066	Y8121	4000	600	None	
DEA2226	2/999066	Y8121	4000	600	None	
DEA2227	2/999066	Y8121	4000	600	None	
DEA2228	2/999066	Y8121	4000	600	None	
DEA2229	2/999066	Y8121	4000	600	None	
DEA2230	2/999066	Y8121	4000	600	None	
DEA2231	2/999066	Y8121	4000	600	None	
DEA2232	2/999066	Y8121	4000	600	None	
DEA2233	2/999066	Y8121	10,000	600	None	
DEA2234	2/999066	Y8121	10,000	600	None	
DEA2235	2/999066	Y8121	10,000	600	None	
DEA2236	2/999066	Y8121	10,000	600	None	
DEA2237	2/999066	Y8121	10,000	600	None	
DEA2238	2/999066	Y8121	10,000	600	None	
DEA2239	2/999066	Y8121	10,000	600	None	
DEA2240	2/999066	Y8121	10,000	600	None	
DEA2241	2/999066	Y8121	10,000	600	None	
DEA2242	2/999066	Y8121	10,000	600	None	
DEA2243	2/999066	Y8121	10,000	600	None	
DEA2244	2/999066	Y8121	10,000	600	None	
DEA2245	2/999066	Y8121	10,000	600	None	
DEA2246	2/999066	Y8121	10,000	600	None	
DEA2247	2/999066	Y8121	10,000	600	None	
DEA2248	2/999066	Y8121	10,000	600	None	
DEA2249	2/999066	Y8121	10,000	600	None	
DEA2250	2/999066	Y8121	10,000	600	None	
DEA2251	2/999066	Y8121	10,000	600	None	
DEA2252	2/999066	Y8121	10,000	600	None	
DEA2253	2/999066	Y8121	10,000	600	None	
DEA2254	2/999066	Y8121	10,000	600	None	
DEA2255	2/999066	Y8121	10,000	600	None	
DEA2256	2/999066	Y8121	10,000	600	None	
DEA2257	2/999066	Y8121	10,000	600	None	
DEA2258	2/999066	Y8121	10,000	600	None	
DEA2259	2/999066	Y8121	10,000	600	None	
DEA2260	2/999066	Y8121	10,000	600	None	
DEA2261	2/999066	Y8121	10,000	600	None	
DEA2262	2/999066	Y8121	10,000	600	None	
DEA2263	2/999066	Y8121	10,000	600	None	
DEA2264	2/999066	Y8121	10,000	600	None	
DEA2265	2/999066	Y8121	10,000	600	None	
DEA2266	2/999066	Y8121	40,000	600	None	
DEA2267	2/999066	Y8121	40,000	600	None	
DEA2268	2/999066	Y8121	40,000	600	None	
DEA2269	2/999066	Y8121	40,000	600	None	
DEA2270	2/999066	Y8121	40,000	600	None	
DEA2271	2/999066	Y8121	40,000	600	None	
DEA2272	2/999066	Y8121	40,000	600	None	
DEA2273	2/999066	Y8121	40,000	600	None	
DEA2274	2/999066	Y8121	40,000	600	None	
DEA2275	1/99067	Y8120	1000	650	None	
DEA2276	1/99067	Y8120	1000	650	None	
DEA2277	1/99067	Y8120	1000	650	None	
DEA2278	1/99067	Y8120	1000	650	None	
DEA2279	1/99067	Y8120	1000	650	None	

Specimen Number	Furnace No./SN	TC/Readout ID	Aging Time (Hrs.)	Aging Temp. (C)	Testing Performed	Comments
DEA2280	1/99067	Y8120	1000	650	None	
DEA2281	1/99067	Y8120	1000	650	None	
DEA2282	1/99067	Y8120	1000	650	None	
DEA2283	1/99067	Y8120	1000	650	None	
DEA2284	1/99067	Y8120	1000	650	None	
DEA2285	1/99067	Y8120	1000	650	None	
DEA2286	1/99067	Y8120	1000	650	None	
DEA2287	1/99067	Y8120	1000	650	None	
DEA2288	1/99067	Y8120	1000	650	None	
DEA2289	1/99067	Y8120	1000	650	None	
DEA2290	1/99067	Y8120	1000	650	None	
DEA2291	1/99067	Y8120	1000	650	None	
DEA2292	1/99067	Y8120	1000	650	None	
DEA2293	1/99067	Y8120	1000	650	None	
DEA2294	1/99067	Y8120	1000	650	None	
DEA2295	1/99067	Y8120	1000	650	None	
DEA2296	1/99067	Y8120	1000	650	None	
DEA2297	1/99067	Y8120	1000	650	None	
DEA2298	1/99067	Y8120	1000	650	None	
DEA2299	1/99067	Y8120	1000	650	None	
DEA2300	1/99067	Y8120	1000	650	None	
DEA2301	1/99067	Y8120	1000	650	None	
DEA2302	1/99067	Y8120	1000	650	None	
DEA2303	1/99067	Y8120	1000	650	None	
DEA2304	1/99067	Y8120	1000	650	None	
DEA2305	1/99067	Y8120	1000	650	None	
DEA2306	1/99067	Y8120	1000	650	None	
DEA2307	1/99067	Y8120	1000	650	None	
DEA2308	1/99067	Y8120	51,170	650	None	SN-LLNL-SCI-434-V2
DEA2309	1/99067	Y8120	51,170	650	None	SN-LLNL-SCI-434-V2
DEA2310	1/99067	Y8120	51,170	650	None	SN-LLNL-SCI-434-V2
DEA2311	1/99067	Y8120	51,170	650	None	SN-LLNL-SCI-434-V2
DEA2312	1/99067	Y8120	51,170	650	None	SN-LLNL-SCI-434-V2
DEA2313	1/99067	Y8120	51,170	650	None	SN-LLNL-SCI-434-V2
DEA2314	1/99067	Y8120	51,170	650	None	SN-LLNL-SCI-434-V2
DEA2315	1/99067	Y8120	51,170	650	None	SN-LLNL-SCI-434-V2
DEA2316	1/99067	Y8120	51,170	650	None	SN-LLNL-SCI-434-V2
DEA2317	1/99067	Y8120	10,000	650	None	
DEA2318	1/99067	Y8120	10,000	650	None	
DEA2319	1/99067	Y8120	10,000	650	None	
DEA2320	1/99067	Y8120	10,000	650	None	
DEA2321	1/99067	Y8120	10,000	650	None	
DEA2322	1/99067	Y8120	10,000	650	None	
DEA2323	1/99067	Y8120	10,000	650	None	
DEA2324	1/99067	Y8120	10,000	650	None	
DEA2325	1/99067	Y8120	10,000	650	None	
DEA2326	1/99067	Y8120	10,000	650	None	
DEA2327	1/99067	Y8120	10,000	650	None	
DEA2328	1/99067	Y8120	10,000	650	None	
DEA2329	1/99067	Y8120	10,000	650	None	
DEA2330	1/99067	Y8120	10,000	650	None	
DEA2331	1/99067	Y8120	10,000	650	None	
DEA2332	1/99067	Y8120	10,000	650	None	
DEA2333	1/99067	Y8120	10,000	650	None	
DEA2334	1/99067	Y8120	10,000	650	None	
DEA2335	1/99067	Y8120	10,000	650	None	
DEA2336	1/99067	Y8120	10,000	650	None	
DEA2337	1/99067	Y8120	10,000	650	None	
DEA2338	1/99067	Y8120	10,000	650	None	
DEA2339	1/99067	Y8120	10,000	650	None	
DEA2340	1/99067	Y8120	10,000	650	None	
DEA2341	1/99067	Y8120	10,000	650	None	
DEA2342	1/99067	Y8120	10,000	650	None	
DEA2343	1/99067	Y8120	10,000	650	None	
DEA2344	1/99067	Y8120	10,000	650	None	
DEA2345	1/99067	Y8120	10,000	650	None	
DEA2346	1/99067	Y8120	10,000	650	None	
DEA2347	1/99067	Y8120	10,000	650	None	
DEA2348	1/99067	Y8120	10,000	650	None	

Specimen Number	Furnace No./SN	TC/Readout ID	Aging Time (Hrs.)	Aging Temp. (C)	Testing Performed	Comments
DEA2349	1/99067	Y8120	10,000	650	None	
DEA2350	2/999066	Y8121	51,190	600	None	SN-LLNL-SCI-434-V2
DEA2351	2/999066	Y8121	51,190	600	None	SN-LLNL-SCI-434-V2
DEA2352	2/999066	Y8121	51,190	600	None	SN-LLNL-SCI-434-V2
DEA2353	2/999066	Y8121	51,190	600	None	SN-LLNL-SCI-434-V2
DEA2354	2/999066	Y8121	51,190	600	None	SN-LLNL-SCI-434-V2
DEA2355	2/999066	Y8121	51,190	600	None	SN-LLNL-SCI-434-V2
DEA2356	2/999066	Y8121	51,190	600	None	SN-LLNL-SCI-434-V2
DEA2357	2/999066	Y8121	51,190	600	None	SN-LLNL-SCI-434-V2
DEA2358	2/999066	Y8121	51,190	600	None	SN-LLNL-SCI-434-V2
DEA2359	2/999066	Y8121	51,190	600	None	SN-LLNL-SCI-434-V2
DEA2360	2/999066	Y8121	51,190	600	None	SN-LLNL-SCI-434-V2
DEA2361	2/999066	Y8121	51,190	600	None	SN-LLNL-SCI-434-V2
DEA2362	2/999066	Y8121	51,190	600	None	SN-LLNL-SCI-434-V2
DEA2363	2/999066	Y8121	51,190	600	None	SN-LLNL-SCI-434-V2
DEA2364	2/999066	Y8121	51,190	600	None	SN-LLNL-SCI-434-V2
DEA2365	2/999066	Y8121	51,190	600	None	SN-LLNL-SCI-434-V2
DEA2366	2/999066	Y8121	51,190	600	None	SN-LLNL-SCI-434-V2
DEA2367	2/999066	Y8121	51,190	600	None	SN-LLNL-SCI-434-V2
DEA2368	1/999067	Y8120	51,170	650	None	SN-LLNL-SCI-434-V2
DEA2369	1/999067	Y8120	51,170	650	None	SN-LLNL-SCI-434-V2
DEA2370	1/999067	Y8120	51,170	650	None	SN-LLNL-SCI-434-V2
DEA2371	1/999067	Y8120	51,170	650	None	SN-LLNL-SCI-434-V2
DEA2372	1/999067	Y8120	51,170	650	None	SN-LLNL-SCI-434-V2
DEA2373	1/999067	Y8120	51,170	650	None	SN-LLNL-SCI-434-V2
DEA2374	1/999067	Y8120	51,170	650	None	SN-LLNL-SCI-434-V2
DEA2375	1/999067	Y8120	51,170	650	None	SN-LLNL-SCI-434-V2
DEA2376	1/999067	Y8120	51,170	650	None	SN-LLNL-SCI-434-V2
DEA2377	1/999067	Y8120	51,170	650	None	SN-LLNL-SCI-434-V2
DEA2378	1/999067	Y8120	51,170	650	None	SN-LLNL-SCI-434-V2
DEA2379	1/999067	Y8120	51,170	650	None	SN-LLNL-SCI-434-V2
DEA2380	1/999067	Y8120	51,170	650	None	SN-LLNL-SCI-434-V2
DEA2381	1/999067	Y8120	51,170	650	None	SN-LLNL-SCI-434-V2
DEA2382	1/999067	Y8120	51,170	650	None	SN-LLNL-SCI-434-V2
DEA2383	1/999067	Y8120	51,170	650	None	SN-LLNL-SCI-434-V2
DEA2384	1/999067	Y8120	51,170	650	None	SN-LLNL-SCI-434-V2
DEA2385	1/999067	Y8120	51,170	650	None	SN-LLNL-SCI-434-V2
KE0471	8/750960472556	AE7717/AA2617	20 minutes	1075	EBSD, Corrosion	SN-LLNL-SCI-434-V2
KE0472	8/750960472556	AE7717/AA2617	20 minutes	1075	EBSD, Corrosion	SN-LLNL-SCI-434-V2
KE0473	8/750960472556	AE7717/AA2617	20 minutes	1075	EBSD, Corrosion	SN-LLNL-SCI-434-V2
KE0474	8/750960472556	AE7717/AA2617	20 minutes	1075	EBSD, Corrosion	SN-LLNL-SCI-434-V2
KE0475	8/750960472556	AE7717/AA2617	20 minutes	1075	EBSD, Corrosion	SN-LLNL-SCI-434-V2
KE0476	8/750960472556	AE7717/AA2617	20 minutes	1075	EBSD, Corrosion	SN-LLNL-SCI-434-V2
KE0477	7/750950688858	AD6788/AA2617	20 minutes	1121	EBSD, Corrosion	SN-LLNL-SCI-434-V2
KE0478	7/750950688858	AD6788/AA2617	20 minutes	1121	EBSD, Corrosion	SN-LLNL-SCI-434-V2
KE0479	7/750950688858	AD6788/AA2617	20 minutes	1121	EBSD, Corrosion	SN-LLNL-SCI-434-V2
KE0480	7/750950688858	AD6788/AA2617	20 minutes	1121	EBSD, Corrosion	SN-LLNL-SCI-434-V2
KE0481	7/750950688858	AD6788/AA2617	20 minutes	1121	EBSD, Corrosion	SN-LLNL-SCI-434-V2
KE0482	7/750950688858	AD6788/AA2617	20 minutes	1121	EBSD, Corrosion	SN-LLNL-SCI-434-V2
KE0483	13/U08N-500037-VN	002516/002474	20 minutes	1200	EBSD, Corrosion	SN-LLNL-SCI-434-V2
KE0484	13/U08N-500037-VN	002516/002474	20 minutes	1200	EBSD, Corrosion	SN-LLNL-SCI-434-V2
KE0485	13/U08N-500037-VN	002516/002474	20 minutes	1200	EBSD, Corrosion	SN-LLNL-SCI-434-V2
KE0486	13/U08N-500037-VN	002516/002474	20 minutes	1200	EBSD, Corrosion	SN-LLNL-SCI-434-V2
KE0487	13/U08N-500037-VN	002516/002474	20 minutes	1200	EBSD, Corrosion	SN-LLNL-SCI-434-V2
KE0488	13/U08N-500037-VN	002516/002474	20 minutes	1200	EBSD, Corrosion	SN-LLNL-SCI-434-V2
KE0489	13/U08N-500037-VN	002516/002474	20 minutes	1300	EBSD, Corrosion	SN-LLNL-SCI-434-V2
KE0490	13/U08N-500037-VN	002516/002474	20 minutes	1300	EBSD, Corrosion	SN-LLNL-SCI-434-V2
KE0491	13/U08N-500037-VN	002516/002474	20 minutes	1300	EBSD, Corrosion	SN-LLNL-SCI-434-V2
KE0492	13/U08N-500037-VN	002516/002474	20 minutes	1300	EBSD, Corrosion	SN-LLNL-SCI-434-V2
KE0493	13/U08N-500037-VN	002516/002474	20 minutes	1300	EBSD, Corrosion	SN-LLNL-SCI-434-V2
KE0494	13/U08N-500037-VN	002516/002474	20 minutes	1300	EBSD, Corrosion	SN-LLNL-SCI-434-V2
PEA113	750961033029	XCIB-2/8310434	2,000	820	Corrosion	SN-LLNL-SCI-426-V1
PEA114	750961033029	XCIB-2/8310434	2,000	820	Corrosion	SN-LLNL-SCI-426-V1
PEA115	750961033029	XCIB-2/8310434	2,000	820	Corrosion	SN-LLNL-SCI-426-V1
PEA116	750961033029	XCIB-2/8310434	2,000	820	Corrosion	SN-LLNL-SCI-426-V1
PEA117	750961033029	XCIB-2/8310434	2,000	820	Corrosion	SN-LLNL-SCI-426-V1
PEA118	750961033029	XCIB-2/8310434	2,000	820	Corrosion	SN-LLNL-SCI-426-V1
PEA119	750961033029	XCIB-2/8310434	2,000	820	Corrosion	SN-LLNL-SCI-426-V1
PEA120	750961033029	XCIB-2/8310434	2,000	820	Corrosion	SN-LLNL-SCI-426-V1

Specimen Number	Furnace No./SN	TC/Readout ID	Aging Time (Hrs.)	Aging Temp. (C)	Testing Performed	Comments
PEA121	750961033029	XCIB-2/8310434	2,000	820	Corrosion	SN-LLNL-SCI-426-V1
PEA122	750961033029	XCIB-2/8310434	2,000	820	Corrosion	SN-LLNL-SCI-426-V1
PEA123	750961033029	XCIB-2/8310434	2,000	820	Corrosion	SN-LLNL-SCI-426-V1
PEA124	750961033029	XCIB-2/8310434	2,000	820	Corrosion	SN-LLNL-SCI-426-V1
PEA125	750961033029	XCIB-2/8310434	2,000	820	Corrosion	SN-LLNL-SCI-426-V1
PEA126	750961033029	XCIB-2/8310434	2,000	820	Corrosion	SN-LLNL-SCI-426-V1
PEA127	750961033029	XCIB-2/8310434	2,000	820	Corrosion	SN-LLNL-SCI-426-V1
PEA128	750961033029	XCIB-2/8310434	2,000	820	Corrosion	SN-LLNL-SCI-426-V1
PEA129	750961033029	XCIB-2/8310434	2,000	820	Corrosion	SN-LLNL-SCI-426-V1
PEA130	750961033029	XCIB-2/8310434	2,000	820	Corrosion	SN-LLNL-SCI-426-V1
PEA131	750961033029	XCIB-2/8310434	2,000	820	Corrosion	SN-LLNL-SCI-426-V1
PEA132	750961033029	XCIB-2/8310434	2,000	820	Corrosion	SN-LLNL-SCI-426-V1
PEA133	750961033029	XCIB-2/8310434	2,000	820	Corrosion	SN-LLNL-SCI-426-V1
PEA134	750961033029	XCIB-2/8310434	2,000	820	Corrosion	SN-LLNL-SCI-426-V1
PEA135	750961033029	XCIB-2/8310434	2,000	820	Corrosion	SN-LLNL-SCI-426-V1
PEA136	750961033029	XCIB-2/8310434	2,000	820	Corrosion	SN-LLNL-SCI-426-V1
PEA137	750961033029	XCIB-2/8310434	2,000	820	Corrosion	SN-LLNL-SCI-426-V1
PEA138	750961033029	XCIB-2/8310434	2,000	820	Corrosion	SN-LLNL-SCI-426-V1
PEA139	750961033029	XCIB-2/8310434	2,000	820	Corrosion	SN-LLNL-SCI-426-V1
PEA140	750961033029	XCIB-2/8310434	2,000	820	Corrosion	SN-LLNL-SCI-426-V1
PEA141	750961033029	XCIB-2/8310434	2,000	820	Corrosion	SN-LLNL-SCI-426-V1
PEA142	750961033029	XCIB-2/8310434	2,000	820	Corrosion	SN-LLNL-SCI-426-V1
PEA143	750961033029	XCIB-2/8310434	2,000	820	Corrosion	SN-LLNL-SCI-426-V1
PEA144	750961033029	XCIB-2/8310434	2,000	820	Corrosion	SN-LLNL-SCI-426-V1
PEA145	750961033029	XCIB-2/8310434	2,000	820	Corrosion	SN-LLNL-SCI-426-V1
PEA146	750961033029	XCIB-2/8310434	2,000	820	Corrosion	SN-LLNL-SCI-426-V1
PEA147	750961033029	XCIB-2/8310434	2,000	820	Corrosion	SN-LLNL-SCI-426-V1
PEA148	750961033029	XCIB-2/8310434	2,000	820	Corrosion	SN-LLNL-SCI-426-V1
PEA149	750961033029	XCIB-2/8310434	2,000	820	Corrosion	SN-LLNL-SCI-426-V1
PEA150	750961033029	XCIB-2/8310434	2,000	820	Corrosion	SN-LLNL-SCI-426-V1
PEA151	750961033029	XCIB-2/8310434	2,000	820	Corrosion	SN-LLNL-SCI-426-V1
PEA152	750961033029	XCIB-2/8310434	2,000	820	Corrosion	SN-LLNL-SCI-426-V1
PEA153	750961033029	XCIB-2/8310434	2,000	820	Corrosion	SN-LLNL-SCI-426-V1
PEA154	750961033029	XCIB-2/8310434	2,000	820	Corrosion	SN-LLNL-SCI-426-V1
PEA155	750961033029	XCIB-2/8310434	2,000	820	Corrosion	SN-LLNL-SCI-426-V1
PEA156	750961033029	XCIB-2/8310434	2,000	820	Corrosion	SN-LLNL-SCI-426-V1
PEA157	750961033029	XCIB-2/8310434	2,000	820	Corrosion	SN-LLNL-SCI-426-V1
PEA158	750961033029	XCIB-2/8310434	2,000	820	Corrosion	SN-LLNL-SCI-426-V1
PEA159	750961033029	XCIB-2/8310434	2,000	820	Corrosion	SN-LLNL-SCI-426-V1
PEA160	750961033029	XCIB-2/8310434	2,000	820	Corrosion	SN-LLNL-SCI-426-V1
PEA161	750961033029	XCIB-2/8310434	2,000	820	Corrosion	SN-LLNL-SCI-426-V1
PEA162	750961033029	XCIB-2/8310434	2,000	820	Corrosion	SN-LLNL-SCI-426-V1
PEA163	750961033029	XCIB-2/8310434	2,000	820	Corrosion	SN-LLNL-SCI-426-V1
PEA164	750961033029	XCIB-2/8310434	2,000	820	Corrosion	SN-LLNL-SCI-426-V1
PEA165	750961033029	XCIB-2/8310434	2,000	820	Corrosion	SN-LLNL-SCI-426-V1
PEA166	750961033029	XCIB-2/8310434	2,000	820	Corrosion	SN-LLNL-SCI-426-V1
PEA167	750961033029	XCIB-2/8310434	2,000	820	Corrosion	SN-LLNL-SCI-426-V1
PEA168	750961033029	XCIB-2/8310434	2,000	820	Corrosion	SN-LLNL-SCI-426-V1
PEA169	750961033029	XCIB-2/8310434	2,000	820	Corrosion	SN-LLNL-SCI-426-V1
PEA170	750961033029	XCIB-2/8310434	2,000	820	Corrosion	SN-LLNL-SCI-426-V1
PEA171	750961033029	XCIB-2/8310434	2,000	820	Corrosion	SN-LLNL-SCI-426-V1
PEA172	750961033029	XCIB-2/8310434	2,000	820	Corrosion	SN-LLNL-SCI-426-V1
PEA173	750961033029	XCIB3/8310434	200	820	Corrosion	SN-LLNL-SCI-426-V1
PEA174	750961033029	XCIB3/8310434	200	820	Corrosion	SN-LLNL-SCI-426-V1
PEA175	750961033029	XCIB3/8310434	200	820	Corrosion	SN-LLNL-SCI-426-V1
PEA176	750961033029	XCIB3/8310434	200	820	Corrosion	SN-LLNL-SCI-426-V1
PEA177	750961033029	XCIB3/8310434	200	820	Corrosion	SN-LLNL-SCI-426-V1
PEA178	750961033029	XCIB3/8310434	200	820	Corrosion	SN-LLNL-SCI-426-V1
PEA179	750961033029	XCIB3/8310434	200	820	Corrosion	SN-LLNL-SCI-426-V1
PEA180	750961033029	XCIB3/8310434	200	820	Corrosion	SN-LLNL-SCI-426-V1
PEA181	750961033029	XCIB3/8310434	200	820	Corrosion	SN-LLNL-SCI-426-V1
PEA182	750961033029	XCIB3/8310434	200	820	Corrosion	SN-LLNL-SCI-426-V1
PEA183	750961033029	XCIB3/8310434	200	820	Corrosion	SN-LLNL-SCI-426-V1
PEA184	750961033029	XCIB3/8310434	200	820	Corrosion	SN-LLNL-SCI-426-V1
PEA185	750961033029	XCIB3/8310434	200	820	Corrosion	SN-LLNL-SCI-426-V1
PEA186	750961033029	XCIB3/8310434	200	820	Corrosion	SN-LLNL-SCI-426-V1
PEA187	750961033029	XCIB3/8310434	200	820	Corrosion	SN-LLNL-SCI-426-V1
PEA188	750961033029	XCIB3/8310434	200	820	Corrosion	SN-LLNL-SCI-426-V1
PEA189	750961033029	XCIB3/8310434	200	820	Corrosion	SN-LLNL-SCI-426-V1

Specimen Number	Furnace No./SN	TC/Readout ID	Aging Time (Hrs.)	Aging Temp. (C)	Testing Performed	Comments
PEA190	750961033029	XCIB3/8310434	200	820	Corrosion	SN-LLNL-SCI-426-V1
PEA191	750961033029	XCIB3/8310434	200	820	Corrosion	SN-LLNL-SCI-426-V1
PEA192	750961033029	XCIB3/8310434	200	820	Corrosion	SN-LLNL-SCI-426-V1
PEA193	750961033029	XCIB3/8310434	200	820	Corrosion	SN-LLNL-SCI-426-V1
PEA194	750961033029	XCIB3/8310434	200	820	Corrosion	SN-LLNL-SCI-426-V1
PEA195	750961033029	XCIB3/8310434	200	820	Corrosion	SN-LLNL-SCI-426-V1
PEA196	750961033029	XCIB3/8310434	200	820	Corrosion	SN-LLNL-SCI-426-V1
PEA197	750961033029	XCIB3/8310434	200	820	Corrosion	SN-LLNL-SCI-426-V1
PEA198	750961033029	XCIB3/8310434	200	820	Corrosion	SN-LLNL-SCI-426-V1
PEA199	750961033029	XCIB3/8310434	200	820	Corrosion	SN-LLNL-SCI-426-V1
PEA200	750961033029	XCIB3/8310434	200	820	Corrosion	SN-LLNL-SCI-426-V1
PEA201	750961033029	XCIB3/8310434	200	820	Corrosion	SN-LLNL-SCI-426-V1
PEA202	750961033029	XCIB3/8310434	200	820	Corrosion	SN-LLNL-SCI-426-V1
PEA203	750961033029	XCIB3/8310434	200	820	Corrosion	SN-LLNL-SCI-426-V1
PEA204	750961033029	XCIB3/8310434	200	820	Corrosion	SN-LLNL-SCI-426-V1
PEA205	750961033029	XCIB3/8310434	200	820	Corrosion	SN-LLNL-SCI-426-V1
PEA206	750961033029	XCIB3/8310434	200	820	Corrosion	SN-LLNL-SCI-426-V1
PEA207	750961033029	XCIB3/8310434	200	820	Corrosion	SN-LLNL-SCI-426-V1
PEA208	750961033029	XCIB3/8310434	200	820	Corrosion	SN-LLNL-SCI-426-V1
PEA209	750961033029	XCIB3/8310434	200	820	Corrosion	SN-LLNL-SCI-426-V1
PEA210	750961033029	XCIB3/8310434	200	820	Corrosion	SN-LLNL-SCI-426-V1
PEA211	750961033029	XCIB3/8310434	200	820	Corrosion	SN-LLNL-SCI-426-V1
PEA212	750961033029	XCIB3/8310434	200	820	Corrosion	SN-LLNL-SCI-426-V1
PEA213	750961033029	XCIB3/8310434	200	820	Corrosion	SN-LLNL-SCI-426-V1
PEA214	750961033029	XCIB3/8310434	200	820	Corrosion	SN-LLNL-SCI-426-V1
PEA215	750961033029	XCIB3/8310434	200	820	Corrosion	SN-LLNL-SCI-426-V1
PEA216	750961033029	XCIB3/8310434	200	820	Corrosion	SN-LLNL-SCI-426-V1
PEA217	750961033029	XCIB3/8310434	200	820	Corrosion	SN-LLNL-SCI-426-V1
PEA218	750961033029	XCIB3/8310434	200	820	Corrosion	SN-LLNL-SCI-426-V1
PEA219	750961033029	XCIB3/8310434	200	820	Corrosion	SN-LLNL-SCI-426-V1
PEA220	750961033029	XCIB3/8310434	200	820	Corrosion	SN-LLNL-SCI-426-V1
PEA221	750961033029	XCIB3/8310434	200	820	Corrosion	SN-LLNL-SCI-426-V1
PEA222	750961033029	XCIB3/8310434	200	820	Corrosion	SN-LLNL-SCI-426-V1
PEA223	750961033029	XCIB3/8310434	200	820	Corrosion	SN-LLNL-SCI-426-V1
PEA224	750961033029	XCIB3/8310434	200	820	Corrosion	SN-LLNL-SCI-426-V1
PEA225	750961033029	XCIB3/8310434	200	820	Corrosion	SN-LLNL-SCI-426-V1
PEA226	750961033029	XCIB3/8310434	200	820	Corrosion	SN-LLNL-SCI-426-V1
PEA227	750961033029	XCIB3/8310434	200	820	Corrosion	SN-LLNL-SCI-426-V1
PEA228	750961033029	XCIB3/8310434	200	820	Corrosion	SN-LLNL-SCI-426-V1
PEA229	750961033029	XCIB3/8310434	200	820	Corrosion	SN-LLNL-SCI-426-V1
PEA230	750961033029	XCIB3/8310434	200	820	Corrosion	SN-LLNL-SCI-426-V1
PEA231	750961033029	XCIB3/8310434	200	820	Corrosion	SN-LLNL-SCI-426-V1
PEA232	750961033029	XCIB3/8310434	200	820	Corrosion	SN-LLNL-SCI-426-V1

12.2 Appendix B LLNL Alloy 22 Heats (Source: Documentation listed in Appendix D)

HEAT #	Al	C	Co	Cr	Cu	Fe	Mn	Mo	N	Ni	P	S	Si	V	W	0.2% YS (psi)
2277-0-3264	-	.004	1.14	21.30	-	4.40	0.29	13.40	-	BAL	0.010	.002	.047	0.17	2.90	57,000
2277-0-3270	-	.003	1.96	21.20	-	4.50	0.25	13.30	-	BAL	0.006	.003	.038	0.14	3.00	53,000
2277-8-3121	-	.003	0.48	21.24	-	3.82	0.30	13.43	-	BAL	0.006	.001	.035	0.17	2.85	
2277-8-3235	-	.003	1.31	21.40	-	3.94	0.24	13.47	-	BAL	0.008	.001	.023	0.17	2.87	
2277-9-3243	-	.002	1.04	21.28	-	3.60	0.28	13.29	-	BAL	0.007	.002	.036	0.14	2.80	
2277-0-3195		0.001	1.79	21.38		4.45	0.20	13.31		BAL	0.006	0.001	0.04	0.11	2.88	46,000 - 57,000
2277-1-3155		0.003	1.33	21.20		3.92	0.26	13.44		BAL	0.006	0.001	0.01	0.012	2.96	
2277-3-3223		0.002	1.68	21.77		3.86	0.24	13.44		BAL	0.006	0.001	0.06	0.13	2.99	49,000 - 64,000
2277-6-3181		0.003	1.35	21.94		3.52	0.26	13.51		BAL	0.005	0.001	0.03	0.17	3.02	
2277-6-5164		0.002	1.68	21.72		3.58	0.24	13.07		BAL	0.005	0.001	0.06	0.14	3.00	
2277-7-3131	0.29	0.003	2.01	21.40	0.06	4.30	0.26	14.00	0.04	55.41	0.010	0.002	0.02	0.16	3.00	42,000 - 59,000
2277-7-3145	0.22	0.003	1.23	21.10	0.08	4.20	0.25	13.80		BAL	0.130	0.002	0.02	0.15	3.30	54,000 - 63,000
2277-7-3145		0.003	1.17	22.31	0.08	3.89	0.26	13.25		BAL	0.004	0.001	0.03	0.14	2.83	
2277-7-3173	0.27	0.004	0.54	21.20	0.04	3.50	0.16	13.90	0.04	57.68	0.007	0.002	0.02	0.14	3.00	34,000 - 57,000
2277-7-3173		0.002	0.79	21.12		3.20	0.15	13.51		BAL	0.006	0.001	0.01	0.13	3.02	
2277-2-3239	0.27	0.003	1.49	21.30	0.05	4.80	0.20	13.20	0.03	55.56	0.003	0.004	0.031	0.14	2.90	47,000 - 77,000
2277-8-3121		0.002	0.50	21.80		3.80	0.34	13.00		BAL	0.010	0.010	0.08	0.18	3.00	58,700
2277-8-3230		0.002	1.45	21.88		3.76	0.29	13.23		BAL	0.005	0.001	0.03	0.14	3.25	
2277-8-3277		0.005	1.30	21.60		4.60	0.36	14.20		BAL	0.010	0.010	0.08	0.18	2.80	
2277-8-3281		0.005	1.40	21.90		4.50	0.36	14.00		BAL	0.010	0.010	0.07	0.17	2.80	
2277-9-3201		0.005	1.40	21.90		4.50	0.36	14.00		BAL	0.010	0.010	0.07	0.17	2.80	
8277-3-7281	0.21	0.003	0.21	21.49	0.04	3.13	0.18	13.38	0.035	57.97	0.008	0.002	0.06	0.15	3.00	30,000 - 70,000
059902LL1		0.005	0.01	20.38	0.01	2.85	0.16	13.82		BAL	0.008	0.0002	0.05	0.171	2.64	
ASTM B575	-	0.01	2.5	20 - 22.5	-	2.0 - 6.0	0.5	12.5 - 14.5	-	BAL	0.02	0.02	0.08	0.35	2.5 - 3.5	
Note: Variability in YS values may be due to varying test temperatures (room, 400, 600, and 800 F)																

12.3 Appendix C Haynes International Aging List

Specimen ID	Alloy	Aging Time (hrs.)	Aging Temp. (°C)	Type
ST434-A1	C-22	100,028	260	Plate
ST434-A2	C-22	100,028	260	Welded Plate
ST434-A3	C-276	100,028	260	Plate
ST434-A4	C-276	100,028	260	Welded Plate
ST434-A5	C-4	100,028	260	Plate
ST434-A6	C-4	100,028	260	Welded Plate
ST434-A7	Ultimet	90,028	260	Plate
ST434-A8	Ultimet	90,028	260	Welded Plate
ST434-A9	G-30	89,528	260	Plate
ST434-A10	G-30	89,528	260	Welded Plate
ST434-A11	C-22	59,528	260	Plate
ST434-A12	C-22	59,528	260	Welded Plate
ST434-A13	C-276	59,528	260	Plate
ST434-A14	C-276	59,528	260	Welded Plate
ST434-A15	C-4	59,528	260	Plate
ST434-A16	C-4	59,528	260	Welded Plate
ST434-A17	C-22	49,528	260	Plate
ST434-A18	C-22	49,528	260	Welded Plate
ST434-A19	C-276	49,528	260	Plate
ST434-A20	C-276	49,528	260	Welded Plate
ST434-A21	C-4	49,528	260	Plate
ST434-A22	C-4	49,528	260	Welded Plate
ST434-B1	C-22	100,028	260	Plate
ST434-B2	C-22	100,028	343	Welded Plate
ST434-B3	C-276	100,028	343	Plate
ST434-B4	C-276	100,028	343	Welded Plate
ST434-B5	C-4	100,028	343	Plate
ST434-B6	C-4	100,028	343	Welded Plate
ST434-B7	G-30	100,028	343	Plate
ST434-B8	G-30	100,028	343	Welded Plate
ST434-B9	Ultimet	90,028	343	Plate
ST434-B10	Ultimet	90,028	343	Plate
ST434-B11	Ultimet	90,028	343	Welded Plate
ST434-B12	Ultimet	90,028	343	Welded Plate
ST434-B13	C-22	59,528	343	Plate
ST434-B14	C-22	59,528	343	Welded Plate
ST434-B15	C-276	59,528	343	Plate
ST434-B16	C-276	59,528	343	Welded Plate
ST434-B17	C-4	59,528	343	Plate
ST434-B18	C-4	59,528	343	Welded Plate
ST434-B19	C-22	49,528	343	Plate
ST434-B20	C-22	49,528	343	Welded Plate
ST434-B21	C-276	49,528	343	Plate
ST434-B22	C-276	49,528	343	Welded Plate
ST434-B23	C-4	49,528	343	Plate
ST434-B24	C-4	49,528	343	Welded Plate
ST434-C1	C-22	100,004	427	Plate
ST434-C2	C-22	100,004	427	Welded Plate

Specimen ID	Alloy	Aging Time (hrs.)	Aging Temp. (°C)	Type
ST434-C3	C-276	100,004	427	Plate
ST434-C4	C-276	100,004	427	Welded Plate
ST434-C5	C-4	100,004	427	Plate
ST434-C6	C-4	100,004	427	Welded Plate
ST434-C7	Ultimet	90,004	427	Plate
ST434-C8	Ultimet	90,004	427	Welded Plate
ST434-C9	G-30	89,504	427	Plate
ST434-C10	G-30	89,504	427	Welded Plate
ST434-C11	C-22	59,504	427	Plate
ST434-C12	C-276	59,504	427	Plate
ST434-C13	C-4	59,504	427	Plate
ST434-C14	C-22	49,504	427	Plate
ST434-C15	C-276	49,504	427	Plate
ST434-C16	C-4	49,504	427	Plate

12.4 Appendix D Data Tracking Number (DTN) List, Software, Scientific Notebooks and Supplements for Analyses of Phase Stability Studies [33]

DTN and Notebook Numbers	Title of Data
LL000115905924.113	Micrographs Showing TCP Particles in Alloy 22 Welds
LL010107712251.012	Transmission Electron Microscopy Micrographs Used in Preliminary TCP and Carbide Phase Identification
LL021009912251.003 SN-LLNL-SCI-441-V2	Scanning Electron Microscope (SEM) Micrographs of Gas-Tungsten Arc-Welded (GTAW) Haynes Alloy 22 Specimens (As-Welded) and Aged at Various Times and Temperatures Used For Area Fraction Measurements of Topologically close-packed (TCP) Phases
LL030103612251.006	Precipitation Area-Fraction Measurements on Weld Metal
LL030103612251.010 SN-LLNL-SCI-426-V1	Grain Boundary Precipitation Measurements (Grain Boundary Coverage Fraction)
LL030103712251.007 SN-LLNL-SCI-426-V1	SEM Images of Base Metal Alloy 22 Specimens Aged at Various Times and Temperatures Used For Area Fraction Measurements of Topologically Close-Packed (TCP) Phases
LL030103812251.008 SN-LLNL-SCI-426-V1	Bulk Precipitation Area-Fraction Measurements (% Transformation)
LL030103912251.009 SN-LLNL-SCI-426-V1	Scanning Electron Microscope (SEM) Images of Base Metal Alloy 22 Specimens Aged at Various Times and Temperatures Used For Area Fraction Measurements of Topologically Close-Packed (TCP) Phases On Grain Boundaries
LL030104212251.012 SN-LLNL-SCI-426-V1	Scanning Electron Microscope (SEM) Images of Alloy 22 Base Metal and Welds Aged at Various Times and Temperatures For AMR ANL-EBS-MD-000002 Rev. 1.
LL030106312251.013	Property and Phase Kinetics Diagrams
LL030301612251.040 SN-LLNL-SCI 393-V1	Transmission Electron Microscopy (TEM), Scanning Electron Microscopy (SEM), and Optical Microscopy of Aged Alloy 22 Weld Metal Specimens
LL030606912251.020	Developed Data from Alloy 22 Volume Fraction Measurements
LL030607112251.021 SN-LLNL-SCI-426-V1	Long-Range Ordering (LRO) of Alloy 22 Base Metal Aged at Various Times and Temperatures Using Vickers Microhardness Measurements
LL050303112251.023 SN-LLNL-SCI-459-V1	High Magnification Scanning Electron Microscope (SEM) Images and Electron Backscatter Diffraction patterns (EBSDP) of Tetrahedrally close-packed (TCP) Phase Particles in As-welded, Low Plasticity Burnished and Laser Shock Peened Alloy 22 1.25”
LL050303212251.024 SN-LLNL-SCI-459-V1	Individual Tetrahedrally close-packed (TCP) Phase Type Volume Fraction Data of As-welded, Low Plasticity Burnished and Laser Shock Peened Alloy 22 1.25” Thick Welds Aged for Various Times at 700°C
LL050303312251.025 SN-LLNL-SCI-459-V1	Scanning Electron Microscope (SEM) Images of As-welded, Low Plasticity Burnished and Laser Shock Peened Alloy 22 1.25” Thick Welds Aged for Various Times at 700°C
LL050303412251.026 SN-LLNL-SCI-459-V1	Tetrahedrally close-packed (TCP) Phase Volume Fraction Data of As-welded, Low Plasticity Burnished and Laser Shock Peened Alloy 22 1.25” Thick Welds Aged for Various Times at 700°C

DTN and Notebook Numbers	Title of Data
LL050303512251.027 SN-LLNL-SCI-441-V2	Large Scale Electron Backscatter Diffraction Data of 1.5” Thick Double-U Alloy 22 Weld Specimens As-welded and Solution Annealed at 1075°C, 1121°C, 1200°C and 1300°C for Various Times and Conditions
LL050303612251.028 SN-LLNL-SCI-441-V2	Large Scale Electron Backscatter Diffraction Maps (EBSDM) of 1.5” Thick Double-U Alloy 22 Weld Specimens As-welded and Solution Annealed at 1075°C, 1121°C, 1200°C and 1300°C for Various Times and Conditions
LL050303712251.029 SN-LLNL-SCI-441-V2	Scanning Electron Microscope (SEM) Images of 1.5” Thick Double-U Alloy 22 Weld Specimens As-welded and Solution Annealed at 1075°C, 1121°C, 1200°C and 1300°C for Various Times and Conditions
LL050303812251.030 SN-LLNL-SCI-441-V2	Tetrahedrally Close Packed (TCP) Phase Volume Fraction Data of 1.5” Thick Double-U Alloy 22 Weld Specimens As-welded and Solution Annealed at 1075°C, 1121°C, 1200°C and 1300°C for Various Times and Conditions
LL050303912251.031 SN-LLNL-SCI-441-V2	Scanning Electron Microscope (SEM) Images of 1.5” Thick Double-U Alloy 22 Welds Used for Construction of Large-scale Weld Maps of Specimens in the As-welded and Solution Annealed (1121°C/20min) Conditions
LL050304012251.032 SN-LLNL-SCI-441-V2	Large-scale Collages of Analyzed Scanning Electron Microscope (SEM) Images of 1.5” Thick Double-U Alloy 22 Welds for Specimens in the As-welded and Solution Annealed (1121°C/20min) Conditions
LL050304112251.134 SN-LLNL-SCI-426-V1	Electron Backscatter Diffraction Data Obtained From the Top of the Trunnion Weld of a Specimen from a Solution Annealed, Quarter-scale, Alloy 22, Mockup Waste Package
LL050304412251.137 SN-LLNL-SCI-426-V1	Tetrahedrally Close Packed (TCP) Phase Volume Fraction Data from the Seam and Trunnion Welds of Specimens Prepared from a Solution Annealed, Quarter-scale, Alloy 22, Mockup Waste Package
LL050304212251.135 SN-LLNL-SCI-426-V1	Electron Backscatter Diffraction Maps (EBSDM) obtained at the Top of the Trunnion Weld of a Specimen from a Solution Annealed, Quarter-scale, Alloy 22, Mockup Waste Package
LL050304312251.136 SN-LLNL-SCI-426-V1	Scanning Electron Microscope (SEM) Images of the Cross-Section of the Seam and Trunnion Welds of Specimens Prepared from a Solution Annealed, Quarter-scale, Alloy 22, Mockup Waste Package
LL050304512251.138 SN-LLNL-SCI-441-V3	Scanning Electron Microscope (SEM) Images of Alloy 22 weld specimens aged at 650°C for 20 and 100 hours
LL050304612251.139 SN-LLNL-SCI-441-V3	Scanning Electron Microscope (SEM) Images of Alloy 22 weld specimens aged at 700°C for 10 and 100 hours
LL050304712251.140 SN-LLNL-SCI-441-V3	Scanning Electron Microscope (SEM) Images of Alloy 22 weld specimens aged at 750°C for 10 and 100 hours
LL050304912251.142 SN-LLNL-SCI-441-V3	Tetrahedrally close-packed (TCP) Phase Volume Fraction Data of Alloy 22 Thick Welds aged at 650°C for 20 and 100 hours, at 700°C for 10 and 100 hours, and 750°C for 10 and 100 hours
LL050803712251.036 SN-LLNL-SCI-463-V3	Effect of Solution Annealing Temperature on the Anodic Behavior of Alloy 22 Thick Welds
LL050803812251.037 SN-LLNL-SCI-463-V3	Repassivation Potentials of Alloy 22 Thick Welds Solution Annealed at Different Temperatures

DTN and Notebook Numbers	Title of Data
LL050901312251.038 SN-LLNL-SCI-459-V1	Transmission Electron Microscopy (TEM) Images of Aged Stress Mitigated Alloy 22 Welds
LL050901412251.039 SN-LLNL-SCI-442-V1	Transmission Electron Microscopy (TEM) Images of Haynes 11.4 Year Aged Alloy 22 Weld at 427°C
LL050901512251.040 SN-LLNL-SCI-442-V1	Scanning Electron Microscopy (SEM) Images of Haynes 11.4 Year Aged Alloy 22 Welds at 260°C and 343°C
LL050901612251.041 SN-LLNL-SCI-426-V2	Wavelength Dispersive Spectroscopy (WDS) Results of Hockey Puck Trunnion Longitudinal Seam Weld Specimen

12.4.1. Summary of Software Used in the Aging/Phase Stability Studies [22]

Software Name	Version Number	Software Tracking Number
Thermo-Calc	M	10170-M-00
DICTRA	20	10391-20-00
TexSem Lab OIM	Suite 4.0	Exempt
Image-Pro Plus	4.0, 4.1, and 4.5.1	Exempt
Excel	2000	Exempt

12.4.2 Summary of Notebooks and Associated Supplements for Phase Stability Studies

Notebook/Supplement ID	Contents
SN-LLNL-SCI-00369	TEM analyses
00369LL	Phase stability, miscellaneous documentation supporting analyses of TS369 specimens
00369LL Micrographs	SEM images of TS369 specimens
00369LL Micrographs 2	SEM images of TS369 specimens
00369LL Micrographs 3	SEM images of TS369 specimens
SN-LLNL-SCI-00393	TEM analyses of welds and base metal
00393LL	Misc. correspondence, cutting of C-22 plates
00393LL Micrographs 1	SEM weld images of TS393 specimens
00393LL Micrographs 2	SEM weld images of TS393 specimens
SN-LLNL-SCI-426-V1	Cold work, volume fraction development using EBSD, microhardness development for LRO
SN-LLNL-SCI-426-V2	Hockey puck analyses
426LL-V1-E1	EBSD scan data for TS369, TS393, and ST434 specimens
426LL-V1-M4 Micrographs 4	TCP volume fraction analyses of hockey pucks
00426LL-V2	Mock-up waste package/hockey pucks support documentation
SGT-00426LL-1	SEM images of TS441 welds, etching images
SGT-00426LL-2	Microhardness measurements
SGT-00426LL Micrographs 1	Etching development, SEM images of TS369 and TS393 specimens
SGT-00426LL Micrographs 2	SEM images for grain boundary volume fraction measurements of aged Alloy 22 base metal

Notebook/Supplement ID	Contents
SGT-00426LL Micrographs 3	SEM images for bulk volume fraction measurements of aged Alloy 22 base metal
SGT-00426LL-HP1	Hockey pucks, EBSD data
SGT-00426LL-EBSD	EBSD development data
SN-LLNL-SCI-434-V1	Continuation of work from 00393; DEA and PEA specimens; aging and testing plans; model validation; aging cold work specimens
SN-LLNL-SCI-434-V2	LLNL Aging Facilities decommissioning
00434LL-V1	TEM memos, misc. correspondence
00434LL-V2	Aging Facility heat treat logs
SN-LLNL-SCI-441-V1	Characterization of Haynes welds
SN-LLNL-SCI-441-V2	Characterization of Haynes welds
00441LL-V2-E1	EBSD data for solution anneal studies
00441LL-V1	SEM calibration studies, 441 sample logs
00441LL-V2	Characterization of Alloy 22 Haynes 0.5" welds by T. Palmer
00441LL-V2 Micrographs 1	Haynes 0.5" weld characterization data, SEM images
00441LL-V2-M2 Micrographs 2	Solution annealing study micrographs, collages, TCP volume fraction measurements for 1.25" aged Alloy 22 welds
00441LL-V3-M1 Micrographs 1	Images for volume fraction calculations of thick welds
SGT-00441LL-SA1	Solution annealing study, EBSD data
SGT-00441LL-SM1	Stress mitigation study, EBSD data
SN-LLNL-SCI-442-V1	TEM work by T. Shen for LRO; SNL work of 11.4 yr. aged specimens; documentation of procurement for Haynes closure of Aging Facility specimens
00442LL-V1	Haynes closure of Aging Facility specimens, TEM work by T. Shen
00444LL-V1	Aging sheets, TIP, cutting of Alloy 22 and Alloy 59 plates
00444LL-V2	Aging Sheets for TS444 specimens
SN-LLNL-SCI-459-V1	Study of the effect of laser peening process in Alloy 22 base metal and welds
00459LL	Study of effects of laser peening, Hao-Lin Chen work, microhardness data
00459LL-V1-E1	EBSD images/patterns, TCP phase ID for stress mitigated specimens
00459LL-V1-M1 Micrographs 1	Stress mitigation study, TCP volume fraction images and calculations
SN-LLNL-SCI-477-V1	Development of APS model